

THE REPUBLIC OF THE PHILIPPINES

METROPOLITAN WATERWORKS AND SEWERAGE SYSTEM

**The Republic of the Philippines**  
**The Study of Water Security Master Plan**  
**for Metro Manila and Its Adjoining Areas**

**Climate Change Impact Assessment**  
**and Hydrological Simulation**

**FINAL REPORT**

**June 2013**

**JAPAN INTERNATIONAL COOPERATION AGENCY**

**THE UNIVERSITY OF TOKYO**  
**NIPPON KOEI CO., LTD.**

GE
JR
13 - 143

THE REPUBLIC OF THE PHILIPPINES

METROPOLITAN WATERWORKS AND SEWERAGE SYSTEM

**The Republic of the Philippines**  
**The Study of Water Security Master Plan**  
**for Metro Manila and Its Adjoining Areas**

**Climate Change Impact Assessment**  
**and Hydrological Simulation**

**FINAL REPORT**

**June 2013**

**JAPAN INTERNATIONAL COOPERATION AGENCY**

**THE UNIVERSITY OF TOKYO**  
**NIPPON KOEI CO., LTD.**



METROPOLITAN WATERWORKS AND SEWAGE SYSTEM  
THE REPUBLIC OF THE PHILIPPINES

THE STUDY  
OF  
WATER SECURITY MASTER PLAN  
FOR  
METRO MANILA AND ITS ADJOINING AREAS

FINAL REPORT  
CLIMATE CHANGE IMPACT ASSESSMENT AND  
HYDROLOGICAL SIMULATION

**Table of Contents**

<b>CHAPTER 1 Introduction.....</b>	<b>1</b>
1.1 Background of the Study.....	1
1.2 Objectives.....	3
1.3 Study Area.....	3
1.4 Counterpart and Steering Committee.....	3
1.5 Implementation Strategy.....	3
<b>CHAPTER 2 Climate Change Impact Assessment Methodology and Results.....</b>	<b>5</b>
2.1 Overview of Methodology: GCM (Global Circulation Model) Selection, Bias-correction and Spatial downscaling.....	5
2.2 Evaluation of the Validity of the Simulations of the Current Status and GCM Selection for Assessment in the Targeted Areas.....	6
2.2.1 Selection of the Emission Scenario.....	6
2.2.2 GCM Selection.....	8
2.2.3 Other Parameters Considered for Projecting Future Trends in Climate Change...	15
2.3 Bias-Correction of the GCM Outputs.....	16
2.3.1 Three-Step Bias Correction Method.....	16
2.3.2 Bias Correction Results.....	19
2.4 Spatial Downscaling of Rainfall.....	36
2.5 Climate Change Impact Assessment in the Target Year of 2040.....	39
<b>CHAPTER 3 Hydrological Model Simulations.....</b>	<b>42</b>
3.1 Hydrological Model Development and River Runoff Simulations.....	42
3.2 Model Structure.....	43
3.3 Input Data.....	44
3.3.1 Static Parameters.....	44
3.3.2 Dynamic Parameters.....	50
3.3.2.1 Temporal Downscaling of Observed Rainfall Data.....	50
3.3.2.2 Temporal Downscaling of Observed Temperature Data.....	51
3.3.2.3 Photosynthetic Activity Considered with LAI and FPAR.....	53
3.4 Hydrological Model Development and Parameter Tuning.....	53

3.4.1 Angat River Basin.....	54
3.4.1.1 Angat River Basin Calibration (2003) and Validation.....	57
3.4.2 Kaliwa River Basin.....	60
3.4.2.1 Kaliwa River Basin Validation.....	62
3.4.3 Pampanga River Basin .....	69
3.4.3.1 Pampanga River Basin Calibration (2002) and Validation.....	71
3.5 Spatial Distribution of Soil Moisture.....	85
3.5.1 Introduction to LDAS-UT.....	85
3.6 Inter-Comparison of the Soil Moisture Products by WEB-DHM and LDAS-UT.....	87
<b>CHAPTER 4 Water Supply Analysis and Climate Change Impact Assessment.....</b>	<b>91</b>
4.1 Simulation of Stream Flow Under the Effects of Climate Change in the Future.....	91
4.1.1 Flood Trends.....	91
4.1.2 Low Flow Trends: Drought Discharge.....	91
4.1.3 Monthly Drought Frequency Trends.....	91
4.2 Angat River Basin.....	93
4.2.1 Changes in Overall Stream Regime.....	93
4.2.2 Base Flow Trends with Drought Discharge.....	95
4.2.3 Longer duration Droughts- and SA.....	102
4.3 Kaliwa River Basin.....	104
4.3.1 Changes in Overall Stream Regime.....	104
4.3.2 Base Flow Trends with Drought Discharge.....	106
4.3.3 Longer Duration Droughts-Using SA.....	114
4.4 Pampanga River Basin.....	115
4.4.1 Changes in Overall Stream Regime.....	115
4.4.2 Base Flow Trends with Drought Discharge.....	117
4.4.3 Longer Duration Droughts-Using SA.....	124
<b>CHAPTER 5 Examination of the Optimized Operation of Water-Use Facilities.....</b>	<b>126</b>
5.1 Recent Progress in Quantitative Precipitation Forecast (QPF).....	126
5.2 A Preliminary Study on In-advance Dam Release and its Potential Benefits.....	127
5.3 Angat Dam Specifications.....	128
5.3.1 Operational Water Levels in a Multi-Purpose Dam or Reservoir.....	129
5.3.2 Angat Dam Rule Curve.....	130
5.3.3 Upstream Water Storage Limitations in Angat Reservoir.....	131
5.3.4 Downstream Flood Control Limitations.....	132
5.4 Input Data Preparation.....	134
5.4.1 PAGASA WRF Forecast for Rainfall.....	134
5.4.2 Ensemble Rainfall Generation.....	136
5.4.3 Real-Time Data Management System.....	137
5.5 Introduction to Dam Optimization.....	138
5.5.1 Offline Dam Operation Optimization.....	138
5.6 Preliminary Dam Optimization Considering Water Storage and Flood (upstream case only).....	139
5.7 Finalized Dam Operation Optimization System.....	140
5.7.1 The DRESS System.....	141

5.7.2 Dam Operation Objective Functions for Water Storage and Flood (considering upstream and downstream).....	142
5.8 Possible Decision-Making issues: Laiban Dam Assumptions .....	144
5.9 Case Study 1: Typhoon Quiel at 214m Water Level Limit with Observed Dam Release and 50% Priority on Preventing Flood and 50% Priority on Water Storage ..	147
5.10 Case Study 2: Tropical Depression Ramon at 214m Water Level Limit with Observed Dam Release and 50% Priority on Flood and 50% Priority on Water Storage.....	152
5.11 Case Study 3: Typhoon Pedring at 214m Water Level Limit with Observed Dam Release, with 0% Priority on Flood and 100% Priority on Water Storage; 20% Priority on Flood and 80% Priority on Water Storage, 50% Priority on Flood and 50% Priority on Water Storage.....	157
5.11.1 Typhoon Pedring at 0% Priority on Flood 100% Priority on Water Storage.....	160
5.11.2 Typhoon Pedring with 20% Priority on Flood 80% Priority on Water Storage.....	165
5.11.3 Typhoon Pedring with 50% Priority on Flood 50% Priority on Water Storag.....	170
5.12 Case Study 4: Typhoon Pedring with a Different Initial Water Level at Sept. 26 (from 207m to 212m).....	175
5.13 Case Study 5: Typhoon Pedring at 212m Water Level Limit at 50%Priority on Flood-50% Priority on Water Storage.....	179
<b>CHAPTER 6 Conclusions and Recommendations.....</b>	<b>184</b>
<b>References.....</b>	<b>186</b>

## List of Figures

<b>Figure 1.5-1</b>	Overall Structure of the study.....	4
<b>Figure 2.1-1</b>	Framework for Climate Change Analysis.....	7
<b>Figure 2.2-1</b>	Area for local scale meteorological parameters.....	9
<b>Figure 2.2-2</b>	Area for large-scale circulations.....	9
<b>Figure 2.2-3</b>	GPCP climatological average precipitation from May to November (for 1981-2000).....	11
<b>Figure 2.2-4</b>	Climatological average precipitation from May to November for the 24 GCM models (small black box indicate local area considered for precipitation; models boxed in red indicate selected GCMs).....	11
<b>Figure 2.3-1</b>	Three-step bias correction dividing rainfall into extreme, normal and no rain days.....	17
<b>Figure 2.3-2</b>	Summary of the 3-step bias correction.....	19
<b>Figure 2.3-3</b>	Meteorological and synoptic gauges over Central and Southern Luzon with the 21 selected stations for bias correction.....	20
<b>Figure 2.3-4</b>	Bias Corrected Matulid station: frequency distribution and seasonality.....	21
<b>Figure 2.3-5</b>	Bias Corrected Matulid station: 10, 50 and 100-year probability of extreme rainfall.....	22
<b>Figure 2.3-6</b>	Bias Corrected Angat station: frequency distribution and seasonality.....	23
<b>Figure 2.3-7</b>	Bias Corrected Angat station: 10, 50 and 100-year probability of extreme rainfall.....	24
<b>Figure 2.3-8</b>	Bias Corrected Maputi station: frequency distribution and seasonality.....	25
<b>Figure 2.3-9</b>	Bias Corrected Maputi station: 10, 50 and 100-year probability of extreme rainfall.....	26
<b>Figure 2.3-10</b>	Bias Corrected Talaguio station: frequency distribution and seasonality.....	27
<b>Figure 2.3-11</b>	Bias Corrected Talaguio station: 10, 50 and 100-year probability of extreme rainfall.....	28
<b>Figure 2.3-12</b>	Bias Corrected past (1981-2000) and future (2046-2065) for Baguio station.....	29
<b>Figure 2.3-13</b>	Bias Corrected past (1981-2000) and future (2046-2065) for Angat station.....	29
<b>Figure 2.3-14</b>	Bias Corrected past (1981-2000) and future (2046-2065) for Talaguio station.....	29
<b>Figure 2.3-15</b>	Bias Corrected past (1981-2000) and future (2046-2065) for Maputi station.....	30
<b>Figure 2.3-16</b>	Bias Corrected past (1981-2000) and future (2046-2065) for Matulid station.....	30
<b>Figure 2.3-17</b>	Bias Corrected past (1981-2000) and future (2046-2065) for Ambulong station.....	30
<b>Figure 2.3-18</b>	Bias Corrected past (1981-2000) and future (2046-2065) for Bai Magalang station.....	31
<b>Figure 2.3-19</b>	Bias Corrected past (1981-2000) and future (2046-2065) for Baler station.....	31
<b>Figure 2.3-20</b>	Bias Corrected past (1981-2000) and future (2046-2065) for Balungao station.....	31
<b>Figure 2.3-21</b>	Bias Corrected past (1981-2000) and future (2046-2065) for Cabanatuan station.....	32
<b>Figure 2.3-22</b>	Bias Corrected past (1981-2000) and future (2046-2065) for CLSU station.....	32
<b>Figure 2.3-23</b>	Bias Corrected past (1981-2000) and future (2046-2065) for Cuyambay station.....	32
<b>Figure 2.3-24</b>	Bias Corrected past (1981-2000) and future (2046-2065) for Dagupan station.....	33

<b>Figure 2.3-25</b>	Bias Corrected past (1981-2000) and future (2046-2065) for Hacienda Luisita station.....	33
<b>Figure 2.3-26</b>	Bias Corrected past (1981-2000) and future (2046-2065) for Iba station.....	33
<b>Figure 2.3-27</b>	Bias Corrected past (1981-2000) and future (2046-2065) for Infanta station.....	34
<b>Figure 2.3-28</b>	Bias Corrected past (1981-2000) and future (2046-2065) for San Fernando station.....	34
<b>Figure 2.3-29</b>	Bias Corrected past (1981-2000) and future (2046-2065) for Science Garden station.....	34
<b>Figure 2.3-30</b>	Bias Corrected past (1981-2000) and future (2046-2065) for Sibul Spring station.....	35
<b>Figure 2.3-31</b>	Bias Corrected past (1981-2000) and future (2046-2065) for Tabak station.....	35
<b>Figure 2.3-32</b>	Bias Corrected past (1981-2000) and future (2046-2065) for Tayabas station.....	35
<b>Figure 2.4-1</b>	Sample spatial distribution for the average August rainfall in comparison with the average August rainfall from the corrected 6 GCMs.....	37
<b>Figure 2.4-2</b>	In-situ, Corrected GCM average, Future corrected GCM average and absolute change (future – past) for 10 year (upper figures) and 100 year (lower figures) return period.....	38
<b>Figure 2.5-1</b>	Availability of Daily Data Set on CMIP3 and the Target Year of This Study.....	40
<b>Figure 2.5-2</b>	Comparison of 2031-2050 versus 2046-2065 daily rainfall of csiro_mk3_5 in Angat Station.....	40
<b>Figure 2.5-3</b>	Comparison of 2031-2050 versus 2046-2065 daily rainfall of ncar_ccsm3_0 in Angat Station.....	41
<b>Figure 3.2-1</b>	The WEB-DHM. a.) division from a basin to sub-basins, b.) subdivision from a sub-basin to flow intervals comprising several model grids, c.) discretization from a model grid to a number of geometrically symmetrical hillslopes, d.) process descriptions of water moisture transfer from the atmosphere to river and e.) soil layers coupled with aquifer model in WEBDHM. (Wang et al., 2009a, 2009b).....	43
<b>Figure 3.3-1</b>	Local land use map reclassified to SiB2 land use classification.....	47
<b>Figure 3.3-2</b>	Local soil map (USDA 1975 classification) reclassified to FAO soil classification.....	49
<b>Figure 3.3-3</b>	Diurnal variation used for different intensities.....	51
<b>Figure 3.3-4</b>	Example of Hourly Temperature Calculation by the TM Model.....	51
<b>Figure 3.4-1</b>	River network, land use and calibrations in Pampanga, Angat and Kaliwa river basins.....	54
<b>Figure 3.4-2</b>	Static parameters of Angat River basin: a.) River Network, b.) Digital Elevation, c.) Local land use and d.) Local soil.....	55
<b>Figure 3.4-3</b>	The Umiray Angat conveyance tunnel.....	56
<b>Figure 3.4-4</b>	The flow in the Umiray-Angat conveyance tunnel ranged from 0 to 30 m <sup>3</sup> /s.....	56
<b>Figure 3.4-5</b>	Calibration of Angat dam inflow for 2003, a) normal scale, b) log-scale.....	57
<b>Figure 3.4-6</b>	Validation of Angat dam inflows from 2001-2009 .....	59
<b>Figure 3.4-7</b>	Kaliwa River Basin: a) River Network, b) Digital Elevation, c) Local land use and d) Local soil.....	61
<b>Figure 3.4-8</b>	Validation of Kaliwa River Basin from 1981-2009.....	63
<b>Figure 3.4-9</b>	Pampanga River basin: a) River Network, b) Digital Elevation, c) Local land use and d) Local soil..	70
<b>Figure 3.4-10</b>	The Casecanan trans-basin tunnel and the Aurora trans-basin channel upstream of Pantabangan dam and the Masiway dam outflows were considered for downstream calibration.....	71
<b>Figure 3.4-11</b>	2002 daily data calibration in a.) Pantabangan Dam, b.) Cabanatuan, c.) Zaragosa, d.) San Isidro and e.) Arayat stream gauges.....	72
<b>Figure 3.4-12</b>	Validation for Pampanga River Basin (2001-2009): Pantabangan Dam inflow.....	75



<b>Figure 3.4-13</b>	Validation for Pampanga River Basin (2001-2009): Cabanatuan.....	77
<b>Figure 3.4-14</b>	Validation for Pampanga River Basin (2001-2009): Zaragosa.....	79
<b>Figure 3.4-15</b>	Validation for Pampanga River Basin (2001-2009): San Isidro.....	81
<b>Figure 3.4-16</b>	Validation for Pampanga River Basin (2001-2009): Arayat.....	83
<b>Figure 3.5-1</b>	The Land Data Assimilation System (LDAS-UT).....	85
<b>Figure 3.6-1</b>	Comparison of surface soil moistures from LDAS-UT and WEBDHM in Zaragoza Station of Pampanga River Basin.....	87
<b>Figure 3.6-2</b>	January to December 2003 spatial patterns of surface soil moisture in the Pampanga River Basin simulated from WEB-DHM (lower figures) and assimilated from LDAS-UT(upper figures).....	88
<b>Figure 4.2-1</b>	Climate change trends on discharges for past and future in Angat River Basin in descending order.	93
<b>Figure 4.2-2</b>	Climate trends of the highest 20 peak discharges for past and future GCMs in Angat River Basin...	94
<b>Figure 4.2-3</b>	Discharge for the a.) past and b.) future 20 years of MIROC_3_2_MEDRES c.) average of the same rank discharge for past and future with past drought discharge at 355 <sup>th</sup> day rank=0.14m <sup>3</sup> /s for Angat Dam inflow .....	96
<b>Figure 4.2-4</b>	Discharge for the a.) past and b.) future 20 years of IPSL and c.) .) average of the same rank discharge for past and future with past drought discharge at 355 <sup>th</sup> day rank =1.85m <sup>3</sup> /s for Angat Dam inflow.....	97
<b>Figure 4.2-5</b>	Discharge for the a.) past and b.) future 20 years of INGV and c.) .) average of the same rank discharge for past and future with past drought discharge at 355 <sup>th</sup> day rank =0.17m <sup>3</sup> /s for Angat Dam inflow .....	98
<b>Figure 4.2-6</b>	Discharge for the a.) past and b.) future 20 years of GFDL_1 and c.) .) average of the same rank discharge for past and future with past drought discharge at 355 <sup>th</sup> day rank =0.16m <sup>3</sup> /s for Angat Dam inflow .....	99
<b>Figure 4.2-7</b>	Discharge for the a.) past and b.) future 20 years of GFDL_0 and c.) .) average of the same rank discharge for past and future with past drought discharge at 355 <sup>th</sup> day rank =0.17 m <sup>3</sup> /s for Angat Dam inflow .....	100
<b>Figure 4.2-8</b>	Discharge for the a.) past and b.) future 20 years of CSIRO and c.) .) average of the same rank discharge for past and future with past drought discharge at 355 <sup>th</sup> day rank =0.15 m <sup>3</sup> /s for Angat Dam inflow .....	101
<b>Figure 4.2-9</b>	SA indices for the 6 selected GCM models for Hydrological drought in Angat Dam (based on simulated monthly discharge).....	103
<b>Figure 4.3-1</b>	Climate change trends on discharges for past and future in Kaliwa River Basin in descending order..	104
<b>Figure 4.3-2</b>	Climate trends of the highest 20 peak discharges for past and future GCMs in Kaliwa River Basin...	105
<b>Figure 4.3-3</b>	Discharge for the a.) past and b.) future 20 years of CSIRO and c.) averaged for 365 days with drought discharge at 355 <sup>th</sup> day rank=0.05 m <sup>3</sup> /s for Kaliwa River Basin outlet.....	107
<b>Figure 4.3-4</b>	Discharge for the a.) past and b.) future 20 years of GFDL_CM2_0 and c.) average of the same rank discharge for past and future with past drought discharge at 355 <sup>th</sup> day rank =0.03365 m <sup>3</sup> /s for Kaliwa River Basin outlet.....	108
<b>Figure 4.3-5</b>	Discharge for the a.) past and b.) future 20 years of GFDL_CM2_1 and c.) average of the same rank discharge for past and future with past drought discharge at 355 <sup>th</sup> day rank =0.6802 m <sup>3</sup> /s for Kaliwa River Basin outlet .....	109
<b>Figure 4.3-6</b>	Discharge for the a.) past and b.) future 20 years of INGV and c.) average of the same rank discharge for past and future with past drought discharge at 355 <sup>th</sup> day rank =0.02775 m <sup>3</sup> /s for Kaliwa River Basin outlet .....	110
<b>Figure 4.3-7</b>	Discharge for the a.) past and b.) future 20 years of IPSL and c.) average of the same rank discharge for past and future with past drought discharge at 355 <sup>th</sup> day rank =2.4237 m <sup>3</sup> /s for Kaliwa River Basin outlet .....	111
<b>Figure 4.3-8</b>	Discharge for the a.) past and b.) future 20 years of MIROC and c.) average of the same rank discharge for past and future with past drought discharge at 355 <sup>th</sup> day rank =0.025 m <sup>3</sup> /s for Kaliwa River Basin outlet .....	112
<b>Figure 4.3-9</b>	SA indices for the 6 selected GCM models for Hydrological drought in Kaliwa River Basin outlet (based on simulated monthly discharge).....	114
<b>Figure 4.4-1</b>	Climate change trends on discharges for past and future in San Isidro gauge of the Pampanga River Basin (in descending order).....	115
<b>Figure 4.4-2</b>	Climate trends of the top 20 peak discharges for past and future GCMs in San Isidro gauge of Pampanga River Basin.....	116

<b>Figure 4.4-3</b>	Discharge for the <b>a.)</b> past and <b>b.)</b> future 20 years of CSIRO and <b>c.)</b> average of the same rank discharge for past and future with past drought discharge at 355 <sup>th</sup> day rank =12.66 m <sup>3</sup> /s for San Isidro, Pampanga River Basin .....	118
<b>Figure 4.4-4</b>	Discharge for the <b>a.)</b> past and <b>b.)</b> future 20 years of MIROC and <b>c.)</b> average of the same rank discharge for past and future with past drought discharge at 355 <sup>th</sup> day rank =3.84 m <sup>3</sup> /s for San Isidro, Pampanga River Basin.....	119
<b>Figure 4.4-5</b>	Discharge for the <b>a.)</b> past and <b>b.)</b> future 20 years of IPSL and <b>c.)</b> average of the same rank discharge for past and future with past drought discharge at 355 <sup>th</sup> day rank =11.78 m <sup>3</sup> /s for San Isidro, Pampanga River Basin.....	120
<b>Figure 4.4-6</b>	Discharge for the <b>a.)</b> past and <b>b.)</b> future 20 years of INGV and <b>c.)</b> average of the same rank discharge for past and future with past drought discharge at 355 <sup>th</sup> day rank =5.05m <sup>3</sup> /s for San Isidro, Pampanga River Basin.....	121
<b>Figure 4.4-7</b>	Discharge for the <b>a.)</b> past and <b>b.)</b> future 20 years of GFDL_1 and <b>c.)</b> average of the same rank discharge for past and future with past drought discharge at 355 <sup>th</sup> day rank =4.78m <sup>3</sup> /s for San Isidro, Pampanga River Basin .....	122
<b>Figure 4.4-8</b>	Discharge for the <b>a.)</b> past and <b>b.)</b> future 20 years of GFDL_0 and <b>c.)</b> average of the same rank discharge for past and future with past drought discharge at 355 <sup>th</sup> day rank =3.64 m <sup>3</sup> /s for San Isidro, Pampanga River Basin.....	123
<b>Figure 4.4-9</b>	SA indices for the 6 selected GCM models for Hydrological drought in San Isidro gauge,Pampanga River Basin.....	125
<b>Figure5.3-1</b>	Schematic diagram of various operational water levels for a hypothetical multipurpose dam/ Reservoir (Source: <a href="http://www.fao.org/docrep/005/AC675E/AC675E04.htm">http://www.fao.org/docrep/005/AC675E/AC675E04.htm</a> ).....	129
<b>Figure 5.3-2</b>	Rule Curve in Angat Dam.....	130
<b>Figure 5.3-3</b>	V-H curve in Angat Dam.....	131
<b>Figure 5.3-4</b>	Q-H Curve at Matictic gauge downstream.....	132
<b>Figure 5.3-5</b>	Current releases from Angat Dam to Ipo Dam and Bustos Dam.....	133
<b>Figure 5.4-1</b>	Dimensions of the forecasted WRF outputs from PAGASA.....	134
<b>Figure 5.4-2</b>	Typhoon Pedring affecting Luzon and Visayas (Source: PAGASA).....	135
<b>Figure 5.4-3</b>	Typhoon Quiel affecting Luzon (Source: PAGASA).....	136
<b>Figure 5.4-4</b>	Tropical Depression Ramon affecting Luzon (Source: PAGASA).....	136
<b>Figure 5.4-5</b>	Error Evaluation used 6 hours past information to create the QPF members.....	137
<b>Figure 5.4-6</b>	DIAS Real-time Data Management System.....	137
<b>Figure 5.5-1</b>	Overall framework of the Offline dam operation optimization system.....	138
<b>Figure 5.6-1</b>	Typhoon Winnie and Typhoon Yoyong Tracks for the preliminary study.....	139
<b>Figure 5.6-2</b>	Angat Dam reservoir optimization. Case 1: initial water level at 212m.....	140
<b>Figure 5.6-3</b>	Angat Dam reservoir optimization. Case 2: initial water level at 217m.....	140
<b>Figure 5.7-1</b>	Framework on how the DRESS system was used for the case of Angat Dam.....	141
<b>Figure 5.7-2</b>	Objective function of Dam Optimization for Angat.....	142
<b>Figure 5.7-3</b>	Optimization of Angat Dam Operation.....	143
<b>Figure 5.8-1</b>	Laiban Dam Hypothetical 2011 Drawdown curve from various initial conditions.....	144
<b>Figure 5.8-2</b>	Daily Rainfall for the 3 Typhoons: <b>a.)</b> Ramon, <b>b.)</b> Quiel and <b>c.)</b> Pedring.....	145

<b>Figure 5.8-3</b>	Inflows to Laiban Dam for a.) Pedring, b.) Quiel and c.) Ramon and d.) the hypothetical future location of Laiban dam in Kaliwa river basin hydrological simulation.....	146
<b>Figure 5.9-1</b>	Forecast water level (blue), dam inflow (orange) and optimized outflow (red) for Typhoon Quiel with 50% priority of water storage and 50% priority on flooding downstream with dam reservoir maximum limit at 214m. (Broken line shows 24 hours forecast; solid line shows simulated average for the previous time steps) .....	148
<b>Figure 5.9-2</b>	Typhoon Quiel 6-hourly average of discharge from a.) dam inflow and b.) dam release.....	150
<b>Figure 5.9-3</b>	Typhoon Quiel 6-hourly average of water level from a.) upstream and b.)downstream.....	151
<b>Figure 5.10-1</b>	Tropical Depression Ramon 6-hourly average of discharge a.) dam inflow and b.) dam release.....	152
<b>Figure 5.10-2</b>	Tropical Depression Ramon 6-hourly average of water level from a.) upstream and b.) downstream.....	153
<b>Figure 5.10-3</b>	Forecast water level (blue), dam inflow (orange) and optimized outflow (red) for Tropical Depression Ramon with 50% priority of water storage and 50% priority on flooding downstream with dam reservoir maximum limit at 214m.....	154
<b>Figure 5.11-1</b>	Typhoon Pedring 6-hourly average of a.) dam inflow and b.) dam outflows from the different priority schemes.....	157
<b>Figure 5.11-2</b>	Typhoon Pedring average water levels from a.) upstream with dam release, with no dam release and with actual observed daily release and b.) downstream actual water level with observed daily dam release.....	159
<b>Figure 5.11-3</b>	Typhoon Pedring 6-hourly average of dam release from daily observed and 0%-100% optimization scheme.....	160
<b>Figure 5.11-4</b>	Typhoon Pedring 6-hourly average of water level from a.) upstream and b.)downstream.....	161
<b>Figure 5.11-5</b>	Forecast water level (blue), dam inflow (orange) and optimized outflow (red) for typhoon Pedring with 0% priority on flood and 100% priority on water storage at dam reservoir maximum limit at 214m.....	162
<b>Figure 5.11-6</b>	Typhoon Pedring 6-hourly average of dam release from daily observed and 20%-80% optimization scheme.....	165
<b>Figure 5.11-7</b>	Typhoon Pedring 6-hourly average of water level from a.) upstream and b.)downstream.....	165
<b>Figure 5.11-8</b>	Forecast water level (blue), dam inflow (orange) and optimized outflow (red) for typhoon Pedring with 20% priority of water storage and 80% priority on flooding downstream with dam reservoir maximum limit at 214m.....	167
<b>Figure 5.11-9</b>	Typhoon Pedring 6-hourly average of dam release from daily observed and 50%-50% optimization scheme.....	170
<b>Figure 5.11-10</b>	Typhoon Pedring 6-hourly average of water level from a.) upstream and b.)downstream.....	170
<b>Figure 5.11-11</b>	Typhoon Pedring 6-hourly average of water level from a.) upstream and b.)downstream.....	171
<b>Figure 5.11-12</b>	Forecast water level (blue), dam inflow (orange) and optimized outflow (red) for typhoon Pedring with 50% priority of water storage and 50% priority on flooding downstream with dam reservoir maximum limit at 214m.....	172

<b>Figure 5.12-1</b>	Forecast water level (blue), dam inflow (orange) and optimized outflow (red) for typhoon Pedring with 50% priority of water storage and 50% priority on flooding downstream with dam reservoir maximum limit at 214m. Initial condition is increased from observed 207m to 212m (hypothetical).....	175
<b>Figure 5.12-2</b>	Pedring case assuming 207m initial condition and 212m initial condition.....	178
<b>Figure 5.12-3</b>	Typhoon Pedring 6-hourly average of dam release from daily observed and 50%-50% optimization scheme at initial water level changed from 207m to 212m.....	178
<b>Figure 5.13-1</b>	Typhoon Pedring 6-hourly average of dam release with different reservoir water level limits of 212m and 214m from 50%-50% optimization scheme.....	179
<b>Figure 5.13-2</b>	Typhoon Pedring 6-hourly average of water level from a.) upstream and b.)downstream for 50%-50% priority with different reservoir water level limits of 212m and 214m from 50%-50% optimization scheme.....	180
<b>Figure 5.13-3.</b>	Forecast water level (blue), dam inflow (orange) and optimized outflow (red) for typhoon Pedring with 50% priority of water storage and 50% priority on flooding downstream with dam reservoir maximum limit at 212m.....	181

## List of Tables

<b>Table 2.2-1</b>	The SRES Scenarios.....	7
<b>Table 2.2-2</b>	Ranking Scores and Selected GCMs for the wet season (June to November).....	12
<b>Table 2.2-3</b>	Ranking Scores and Selected GCMs for the dry season (December to May).....	13
<b>Table 2.2-4</b>	Ranking Scores and Selected GCMs for the entire year.....	14
<b>Table 2.2-5</b>	Global Circulation Models Developer Institutions.....	15
<b>Table 2.2-6</b>	Parameters used for the selected GCMs.....	15
<b>Table 2.5-1</b>	List of daily datasets available on CMIP3 SRESA1B GCMs.....	39
<b>Table 3.3-1</b>	Reclassification of Philippine local land use to SiB2 classification.....	46
<b>Table 3.3-2</b>	USDA 1975 Local soil classification reclassified to FAO soil classification.....	48
<b>Table 3.4-1</b>	Calibrated Soil Parameters for Angat River Basin .....	58
<b>Table 3.4-2</b>	Manning’s roughness for each sub-basin in Angat River Basin .....	58
<b>Table 3.4-3</b>	Soil anisotropy ratio for each land use type in Angat River Basin.....	58
<b>Table 3.4-4</b>	Calibrated Soil Parameters of Kaliwa River Basin .....	62
<b>Table 3.4-5</b>	Manning’s roughness for each sub-basin in Kaliwa River Basin.....	62
<b>Table 3.4-6</b>	Soil anisotropy ratio for each land use type in Kaliwa River Basin .....	62
<b>Table 3.4-7</b>	Calibrated Soil Parameters for Pampanga River Basin.....	74
<b>Table 3.4-8</b>	Manning’s roughness for each sub-basin for Pampanga River Basin.....	74
<b>Table 3.4-9</b>	Soil anisotropy ratio for each land use type for Pampanga River Basin.....	74
<b>Table 4.1-1</b>	Meteorological conditions considered for the range of SA values [UNL, available in <a href="http://www.drought.unl.edu/whatis/indices.htm#spi">http://www.drought.unl.edu/whatis/indices.htm#spi</a> , 2010]; [Mckee et al., 1993].....	92
<b>Table 4.2-1</b>	Summary of Flooding and drought trends in future GCMs for Angat dam Inflows.....	102
<b>Table 4.3-1</b>	Summary of drought trends from GCMs for Kaliwa river basin.....	113
<b>Table 4.4-1</b>	Summary of flooding and drought trends from GCMs in San Isidro gauge, Pampanga River Basin..	124
<b>Table 5.3-1</b>	Current Angat Reservoir Specifications: Upstream.....	131
<b>Table 5.3-2</b>	Assessment of flow and water level at Matictic gauging station.....	132
<b>Table 5.3-3</b>	Flood wave propagation time from Angat dam.....	133

## Abbreviations

Abbreviation	English
AMSL	Above Mean Sea Level
AR4	Fourth Assessment Report
BHU	Basic Hydrological Unit
CCSR	Center for Climate System Research
CGIAR-CSI	Consultative Group of International Agricultural Research Consortium for Spatial Information
CMIP3	The 3 <sup>rd</sup> phase of Coupled Model Inter-comparison Project
CSIRO	Commonwealth Scientific and Industrial Research Organization
DEM	Digital Elevation Model
DENR	Department of Environment and Natural Resources
DHM	Distributed Hydrological Model
DIAS	Data Integration and Analysis System
DPWH	Department of Public Works and Highways
DRESS	Dam Release Support System
ED	Extremely Dry
FAO	Food and Agriculture Organization of the United Nations
FPAR	Fraction of Photosynthetic Active Radiation
GBHM	Geomorphology-Based Hydrological Model
GCM	General Circulation Model
GEOSS	Global Earth Observation System of Systems
GFDL	Geophysical Fluid Dynamics Laboratory
GFS	Global Forecast System
GoP	Government of the Philippines
GPCP	Global Precipitation Climatology Project
GPD	General Parieto Distribution
GPV	Global Precipitation Dataset by JMA
IDW	Inverse Distance Weighing
INGV	National Institute of Geophysics and Volcanology
IPCC	Intergovernmental Panel on Climate Change
IPSL	Institut Pierre Simon Laplace, Paris, France
ITCZ	Inter-Tropical Convergence Zone
JAMSTEC	Japan Agency for Marine-Earth Science and Technology
JICA	Japan International Cooperation Agency
JRA25	25-year Japan Reanalysis Data
JMA	Japan Meteorological Agency
kW	Kilowatt
LAI	Leaf Area Index
LDAS-UT	Land Data Assimilation System by Coupling AMSR-E and SiB2
LGU	Local Government Unit
LSM	Land Surface Model
MCM	Million Cubic Meter
MD	Moderately Dry
MLIT	Ministry of Land Infrastructure and Transportation
MOM	Method of Moments
MMDA	Metropolitan Manila Development Authority
MWSS	Metropolitan Waterworks and Sewerage System
NEDA	National Economic Development Authority
NHWL	Normal High Water Level

Abbreviation	English
NIA	National Irrigation Authority
NIES	National Institute for Environmental Studies
NDRRMC	National Disaster Risk Reduction and Management Council
NPC	National Power Corporation
NS	Nash Coefficient
NWRB	National Water Resources Board
PAGASA	Philippine Atmospheric, Geophysical and Astronomical Services
PAR	Philippine Area of Responsibility
QPF	Quantitative Precipitation Forecast
RE	Relative Error
RMSE	Root Mean Squared Error
RTM	Radiative Transfer Model
R <sup>2</sup>	Correlation Coefficient
SiB2	Simple Biosphere 2
SPI	Standard Precipitation Index
SA	Standard Anomaly
SD	Severely Dry
SRES	Special Report on Emission Scenarios
SRTM	Shuttle Radar Topography Mission
SRESA1b	Special Report on Emission Scenarios A1b Scenario
SWI	Soil Wetness Index
TAR	Third Assessment Report
TGICA	Task Group on Data and Scenario Support for Impact and Climate Change Assessment
TRMM	Tropical Rainfall Measuring Mission
TS	Tropical Storm
UNL	University of Nebraska Lincoln
USDA	United States Department of Agriculture
USGS	United States Geological Survey
UTM	Universal Transverse Mercator
WEB-DHM	Water and Energy Budget based Distributed Hydrological Model
WRF	Weather Research and Forecasting. Model
WSP	Water Security Plan
WL	Water Level

## **CHAPTER 1 Introduction**

### **1.1 Background of the Study**

The Metropolitan Waterworks and Sewerage System (MWSS) is the sole organization directly responsible for managing water supply systems in Metro Manila, Philippines, serving a population of some 12 million. The MWSS entrusts its water supply operations to two water supply concessionaires, namely, the Manila Water Company, Inc. (MWCI) and Maynilad Water Services, Inc. (MWSI). The MWCI caters to the eastern part of Metro Manila and a part of Rizal Province, while the service area of MWSI is the western part of Metro Manila and a part of Cavite Province.

Local residents of the Manila Metropolitan area rely on the Angat dam in the Angat river basin for 97% of their water resources. However, they have been subject to serious water shortages as the population has grown. The Angat reservoir has undergone extreme drawdown due to climate fluctuations. Accordingly, it is critical to assess the possibility of developing other water resources in the Angat River Basin, as well as in the surrounding basins such as Kaliwa and Pampanga River Basin.

There is an urgent need for development of new water resources to ensure a stable water supply. To cope with this problem, the Government of the Philippines (GoP), through the leadership of President Benigno S. Aquino III, instructed the Metropolitan Waterworks and Sewerage System (MWSS) to establish several short term (one to two year) projects. The GoP adopted the principle that priority for water resource development should be vested in evaluating its conformity to the regional development plans in Metro Manila and its adjoining areas. This can be undertaken through a comprehensive study on the medium- and long-term projections of water demand and supply taking into account potential impacts of climate change in the future.

Under these policies, the MWSS suggested and designed the following Water Security Plans (WSP) to establish a new plan for mid and long range water resources development with consideration of the regional characteristics of Metro Manila and its adjoining areas.

- 1) Review of the MWSS (and Concessionaries) Business Plan
- 2) Water Efficiency Plan
- 3) Water Infrastructure Development Plan
- 4) Water Resources Management Plan
- 5) Disaster Risk Management and Mitigation Plan
- 6) Knowledge Management Plan
- 7) Stakeholder Engagement Plan

The MWSS requested the World Bank and Japan International Cooperation Agency (JICA) to support the formulation of the WSP (completed by the end of 2012). In response to the request by the MWSS, the World Bank has implemented the Metro Manila Water Security Study from July to



December 2011. JICA dispatched a study team to Metro Manila in June and November 2011 and had a series of discussions with officials from the MWSS to finalize the contents, scope, and implementation structure of the Study. JICA summarized the results of these discussions into the Minutes of Discussion and exchanged the memorandum with the MWSS in November 2011. In line with the Minutes of Discussion, the Study of Water Security Master Plan for Metro Manila and its Adjoining Areas (the Study) was initiated by JICA in February 2012

JICA has divided the Study into the following two components based on its technical complexity:

- 1.) Water Balance Study Component
- 2.) Climate Change Assessment and Runoff Simulation Component

To accomplish the objectives of the Study, the water balance of Metro Manila is needed to more accurately predict future water usage and validate the water-use project suggested in a previous study based on evaluation of the effects of climate change. Therefore, a detailed climate change analysis is essential for determination of the future climate and stream regime, especially for the Angat River Basin, Kaliwa River Basin, and Pampanga River Basin.

This Final Report describes the results of the Climate Change Assessment and Runoff Simulation Component of the Study and cases of dam optimization during typhoons in 2011.

## **1.2 Objectives**

There are two main objectives of the Climate Change Impact Analysis and Hydrological Simulation Component:

- To assess the effects of climate change on the water cycle in Metro Manila and its adjoining areas, including the Angat, Kaliwa and Pampanga river basins, as a basis of the water balance analysis and associated project assessment.
- To propose optimized operations of the water resources management facilities.

## **1.3 Study Area**

The study area covers Metro Manila and its adjoining areas, including the:

- Angat River Basin (1,085 km<sup>2</sup>);
- Kaliwa River Basin (including the Agos River Basin; 280 km<sup>2</sup>) and
- Pampanga River Basin (10,981 km<sup>2</sup>).

In this report, the adjoining areas are also referred to as the “river basins”. The location of the study area is given in the location map.

## **1.4 Counterpart and Steering Committee**

The counterpart agency of the Study, the MWSS, set up a steering committee to provide guidance and approve the outputs of the Study under the chairmanship of the MWSS. The committee consists of the following representatives of the relevant organizations:

- Metropolitan Waterworks and Sewerage System (MWSS)
- Department of Public Works and Highways (DPWH)
- Department of Environment and Natural Resources (DENR)
- National Irrigation Administration (NIA)
- National Water Resources Board (NWRB)
- National Economic Development Authority (NEDA)
- National Power Corporation (NPC)
- Metropolitan Manila Development Authority (MMDA)
- Department of Interior and Local Government (DILG)
- Local Government Unit (LGU)

## **1.5 Implementation Strategy**

It has been acknowledged that the water supply balance in Metro Manila should be analyzed in a comprehensive manner, and that a comprehensive development project for the surrounding regional development was needed to prioritize the individual issues unique to each project with respect to the water resources development. Under climate change with frequent heavy rainfall events, larger

drought-affected areas and severe typhoons as pointed in the IPCC Fourth Assessment Report (2007), it is important to evaluate the vulnerability of long-term water resources and the merits of employing multiple water-use facilities. An integrated water cycle analysis during both the low-water and high-water periods is needed, and such analyses should be conducted quantitatively, continuously, and comprehensively. Furthermore, optimized operation of multiple water-use facilities should be examined as a part of climate change adaptation.

To accomplish these targets, this study includes:

- Water supply analysis and climate change impact assessment;
  - Collection of climate prediction simulation results in Metro Manila and its adjoining river basins
  - Evaluation of the effects of climate change in Angat River Basin, Kaliwa River Basin, and Pampanga River Basin
  - Hydrological model development and river runoff simulation
  - Simulation and evaluation of stream flow under the effects of climate change in the future
- Examination of the optimized operation for multiple water-use facilities.
  - Using Angat Dam operation as a case study for optimization of 2 objective functions (water storage upstream and flood control downstream)
  - Utilizing the 2011 typhoon events as sub-cases in the usability of the optimization scheme for decision making.

Figure 1.5-1 shows the overall study structure.

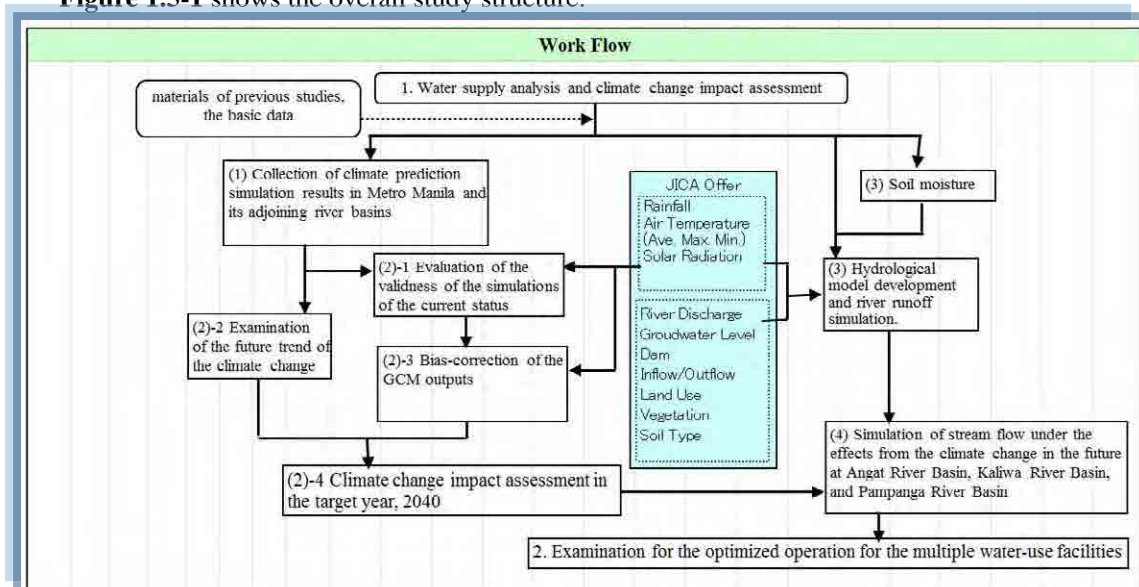


Figure 1.5-1. Overall Structure of the study.

## **CHAPTER 2 Climate Change Impact Assessment Methodology and Results**

### **2.1 Overview of Methodology: GCM (Global Circulation Model) Selection, Bias-correction and Spatial Downscaling**

Weather is the day to day condition of the atmosphere in terms of heat, pressure, wind and moisture (Lehr, et al., 1987). The stability of climate, the long-term averages, totals and extremes of the weather in a particular region, is the premise for planning and design in past hydrological studies. Design parameters for projecting extreme events have been established using statistical studies of past observed records. Findings from the Intergovernmental Panel on Climate Change (IPCC) show that the rate of changes in climate has accelerated significantly due to anthropogenic (human) activities in the past. The target year of the Water Security Plan (WSP) for Metro Manila is set to account for changes by the year 2040. Since it is difficult to assume that future climate conditions will be similar with the current conditions, projected climate changes have to be considered.

The General Circulation Models (GCMs) are some of the most current tools in understanding current climate and projecting future climate conditions. The GCMs have been developed by various research teams and introduced in the assessment report (AR2, AR3, AR4, etc), conducted by the IPCC, and most of those data are archived in Phase 3 of Coupled Model Inter-comparison Project (CMIP3). In this study, the effects of climate change on Metro Manila and its adjoining area were studied using GCM projections.

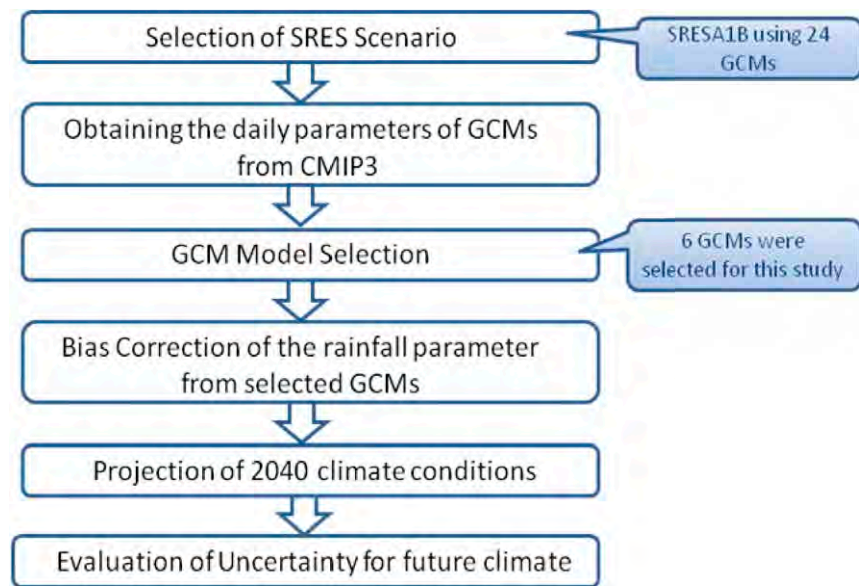
Generally, coupled GCMs are most widely applied to climate change impact assessments. However, there are large uncertainties associated with the outputs of these models. Particularly, the bias of precipitation projected by GCMs is too large. To reduce such uncertainties, it is necessary to conduct more analyses based on multi-model and multi-projection ensembles instead of single model analyses. In addition, there is a large gap in the grid resolution of GCMs and catchment-scale hydrology models. To address this mismatch, downscaling of GCMs data is essential for regional and local impact studies. There are two main types of downscaling, *dynamic* and *statistical*. *Dynamic downscaling* refers to nesting to the fine scale resolution in the large-scale resolution while preserving some spatial correlation. However, this method is computationally expensive and impossible for multi-decade simulations of different GCMs. *Statistical downscaling* is based on the relationship between large-scale circulation and local-scale phenomena. This method can be implemented with reasonable computational costs.

Although the GCMs are accepted widely as the best physically-based tool for projecting future climate scenarios, there is considerable gap (bias) between the local climate condition and the simulation results. This bias should be corrected prior to using parameters in the GCM outputs. Rainfall is the parameter with the most pronounced bias in terms of the rainfall extremes, normal rain, and the absence of no rain days rainfall is the parameter that is bias corrected in this study.

There are 24 GCMs of CMIP3 with daily data sets archived in the Data Integration and Analysis System (DIAS) Japan. The daily data sets were provided to JICA from DIAS as part of the cooperation between the University of Tokyo and JICA.

There is a large uncertainty involved in the future projections from the GCMs. This should be considered in the evaluation of results. A multi-model ensemble analysis was carried out to evaluate future climate.

The framework of the climate change analysis is shown in **Figure 2.2-1**. This begins with selection of appropriate GCMs from 24 models in the SRESA1b scenario (Special Report on Emission Scenarios A1b scenario). Secondly, daily hydrometeorological parameters are obtained from the selected models. Thirdly, bias correction of the rainfall parameter is considered using the 3-step bias correction method. This is followed by projection of 2040 conditions and lastly, evaluation of uncertainty for future climate.



**Figure 2.1-1.** Framework for Climate Change Analysis

## 2.2 Evaluation of the Validity of the Simulations of the Current Status and GCM Selection for Assessment in the Targeted Areas

### 2. 2.1 Selection of the Emission Scenario

To study the impact of climate change in the future, the concentrations of greenhouse gases and other pollutants in the atmosphere should be given as the boundary conditions for the numerical simulation models, to which climate is sensitive.

The Special Report on Emission Scenarios (SRES), published by the IPCC in 2000, describes the emissions scenarios that have been used to make projections of possible future climate change, for the IPCC Third Assessment Report (TAR) and in the IPCC Fourth Assessment Report (AR4). Emission scenarios describe future releases of greenhouse gases, aerosols, and the other pollutants into the atmosphere, along with information on land use and land cover. A set of four scenario families (A1, A2, B1, B2) have been developed. Each of these scenarios describes one possible demographic, socio-economic, political and technological future. The SRES scenario families are described in **Table 2.2-1**.

**Table 2.2-1. The SRES Scenarios**

Scenario family	SRES Emissions Scenarios	CO <sub>2</sub> Stabilization
A1	A future world of very rapid economic growth, global population that peaks in mid-century and declines thereafter, and rapid introduction of new and more efficient technologies. The A1 scenario family develops into three groups that describe alternative directions of technological change in the energy system. -A1F1: fossil-intensive -A1T: non-fossil energy sources -A1B: balance across all sources	A1F1: Not stabilized A1T:650 ppm A1B:750 ppm
A2	A very heterogeneous world with continuously increasing global population and regionally oriented economic growth that is more fragmented and slower than in other Scenario family.	Not stabilized
B1	A convergent world with the same global population as in the A1 storyline but with rapid changes in economic structures toward a service and information economy, with reductions in materials intensity, and the introduction of clean and resource-efficient technologies.	550 ppm
B2	A world in which the emphasis is on local solutions to economic, social, and environmental sustainability, with continuously increasing population (lower than A2) and intermediate economic development.	650 ppm

Source: Task Group on Data and Scenario Support for Impact and Climate Assessment (TGICA), IPCC

The SRESa1b scenario is the GCM scenario used for this study. This is under the A1 storyline and scenario family describing a future world of very rapid economic growth, global population that peaks in mid-century and declines thereafter, and the rapid introduction of new and more efficient technologies. The major underlying themes are convergence among regions, capacity building and increased cultural and social interactions, with substantial reduction in regional differences in per capita income. The A1B scenario considers a balance across all sources (where balanced is defined as not relying too heavily on one particular energy source, on the assumption that similar improvement rates apply to all energy supply and end-user technologies). This scenario is characterized by low population growth, very high GDP growth, very high energy use changes, medium resource availability and rapid but balanced pace and direction of technological change (IPCC SRES, 2000).

### 2.2.2 GCM Selection

Selection of proper GCMs is crucial for multi-model analysis. Such selection is conducted based on the performance of the GCMs that joined the Coupled Model Inter-comparison Project 3 (CMIP3).

Selection is based on the ability of the GCM to represent the regional climate of the area under investigation. Asian summer monsoons, the ITCZ (Inter-Tropical Convergence Zone) are some but a few of the regional phenomena that should be used. If a GCM is not able to reproduce the climatology of the region under study; then it should not be used for further consideration. The selection of the domain is based on these broad synoptic scale phenomena. The climate systems unique to the basins as well as the spatial coverage should be accounted for.

At the basin scale, the selected GCMs should be able to reproduce the seasonal pattern of precipitation. Spatial correlation and the root mean square error was used to identify similarities and differences between the models versus current observed global datasets. The Global Precipitation Climatology Project (GPCP) dataset was used for comparing similarities in average monthly precipitations while the Japan Reanalysis data (JRA25) output was used to compare other meteorological variables.

$$Scorr = r_{xy} = \frac{\sum_{i=1}^N (x_i - \bar{x})(y_i - \bar{y})}{(n-1)S_x S_y} = \frac{\sum_{i=1}^N (x_i - \bar{x})(y_i - \bar{y})}{\sqrt{\sum_{i=1}^N (x_i - \bar{x})^2 \sum_{i=1}^N (y_i - \bar{y})^2}} \quad (\text{eq.1})$$

$$RMSE = \sqrt{\frac{1}{N} \sum_{i=1}^N (R_{st} - R_{obs})^2} \quad (\text{eq.2})$$

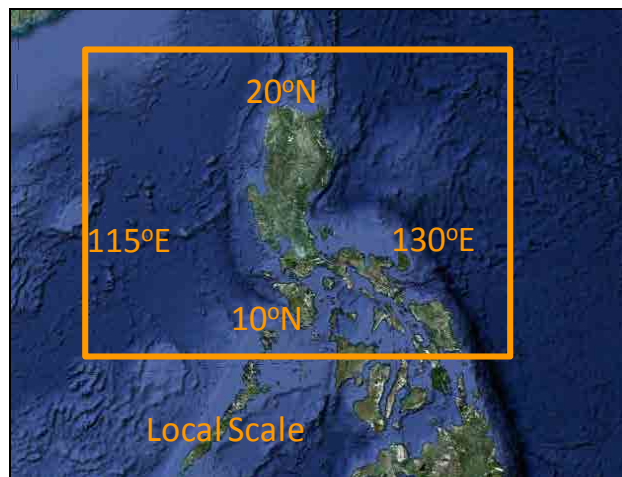
To evaluate the GCMs' ability to represent the small-scale precipitation, additional screening should be done to eliminate the worst performing GCMs. Three additional criteria should be used to achieve this:

- 1) The long term basin observed rainfall average (climatology) should be compared to the GCMs. If a GCM is not able to represent the seasonal variability, then it should be eliminated.
- 2) If the GCM produces too little rainfall such that after the no-rain correction unreasonably dry days exist; then that model too should be eliminated.
- 3) Lastly, if the observed rainfall distribution within the basin is not uniformly distributed, consideration on basin subdivision climatological average (based on areas with high rainfall, medium rainfall, small rainfall –usually related to elevation and land use) should be considered in the model selection comparison.

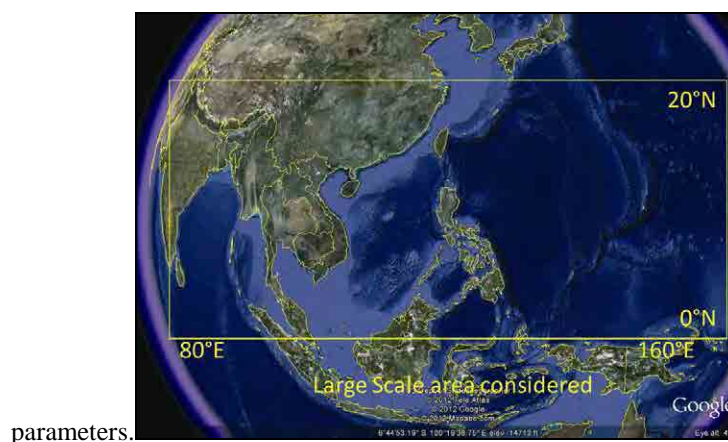
Selection of GCMs among available models in the Coupled Model Inter-comparison Project 3 (CMIP3) is crucial for this multi-model analysis. Most GCMs have problems with low rainfall

intensity during heavy rainfall, low seasonal representation and low intensity but long rainy days (drizzle). There are 7 parameters considered in selecting the appropriate Global circulation models that comprises the ensemble. These parameters are precipitation, outgoing longwave radiation, sea surface temperature, seal level pressure, air temperature, meridional wind and zonal wind. The area considered for local scale meteorological parameter (precipitation) is: 115°E to 130°E, 10°N to 20°N (**Figure 2.2-1**).

For large scale circulations and surrounding oceans, the area considered is: 80°E to 160°E; 0°N to 20°N (**Figure 2.2-2**). This includes the Bay of Bengal, Indian Ocean, Philippine Sea and Java Sea. The parameters considered are: sea level pressure, air temperature, meridional wind, zonal wind, outgoing longwave radiation and sea surface temperature. This area was selected to consider effects of the Asian Summer Monsoon: Southeast Asian Summer Monsoon (0°N to 10°N; 90°E to 130°E) and the Indian Summer Monsoon (5°N to 20°N; 40°E to 80°E).



**Figure 2.2-1.** Area for local scale meteorological



**Figure 2.2-2.** Area for large-scale circulations.



In the study area, both the wet and dry seasons are very important for water management so the spatial correlation (scorr) and root mean square error (RMSE) for each month was considered while prioritizing the models that showed high spatial correlation and low root mean square error during the wet season (May to November). A simple index counter was used for identifying the models which had RMSE and scorr values above the average RMSE and scorr (if above average, index = 1, else index = 0). Priority is given to models that were selected for precipitation and seasonality of these models were checked and compared with observed rainfall gauges. **Figure 2.2-3** shows the climatological average of the GPCP precipitation from May to November (1981-2000). The scoring of the 7 meteorological parameters for the wet season (**Table 2.2-2**), dry season (**Table 2.2-3**) and for the whole year (**Table 2.2-4**) are given in the tables. Primarily, models that had very high scores (grand total scores above 1) during the wet season are given priority. However, to ensure that the rainfall patterns are exhibited, only those models with a +1 score for precipitation were selected (gfdl\_cm2\_0, gfdl\_cm2\_1, ipsl\_cm4, ingv\_echam4, and miroc3\_2\_medres). Other models that were selected but had missing (miub\_echo\_g, ncar\_ccsm3\_0) or incomplete data were rejected. In addition, seasonality and ability of the model to exhibit extreme events were considered in the selection, models that did not show similar climatology of extremes were rejected (giss\_aom, giss\_model\_e\_r). Second priority was given to models (in addition to those already selected for the wet season, miroc3\_2\_medres, csiro\_mk3\_0) that showed high scores and +1 for precipitation when selected for the entire year (**Table 2.2-4**). For this study, 6 models were finally selected to study projected changes in climate over Metro Manila and its surrounding areas. These are: gfdl\_cm2\_0, gfdl\_cm2\_1, ipsl\_cm4, ingv\_echam4, csiro\_mk3\_0, miroc\_3\_2\_medres (see **Table 2.2-5** for the model developer institutions). **Figure 2.2-4** shows how the spatial distribution of rainfall over the region for these selected models shows similar patterns as those of GPCP (**Figure 2.2-3**) for the wet season. The figure covers 100°E to 160°E, 0°N to 30°N for expressing the regional characteristics of rainfall distribution clearly, while the selection was done by checking the climatological parameters within 80°E to 160°E and 0°N to 20°N as shown in **Figure 2.2-2**.

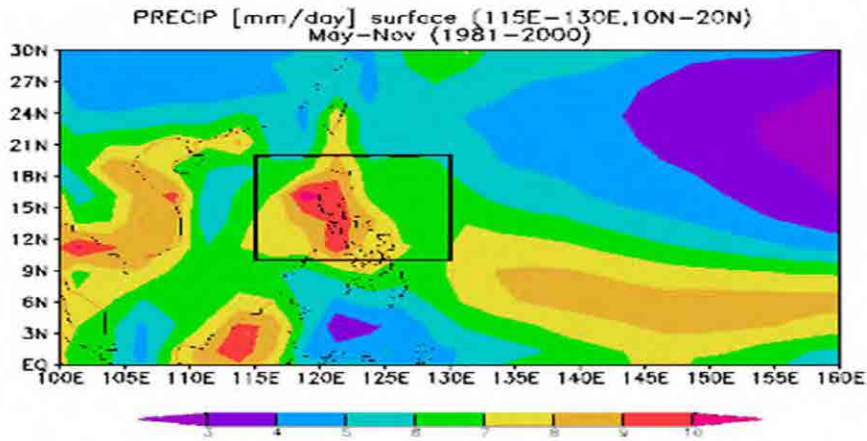


Figure 2.2-3. GPCP climatological average precipitation from May to November (for 1981-2000).

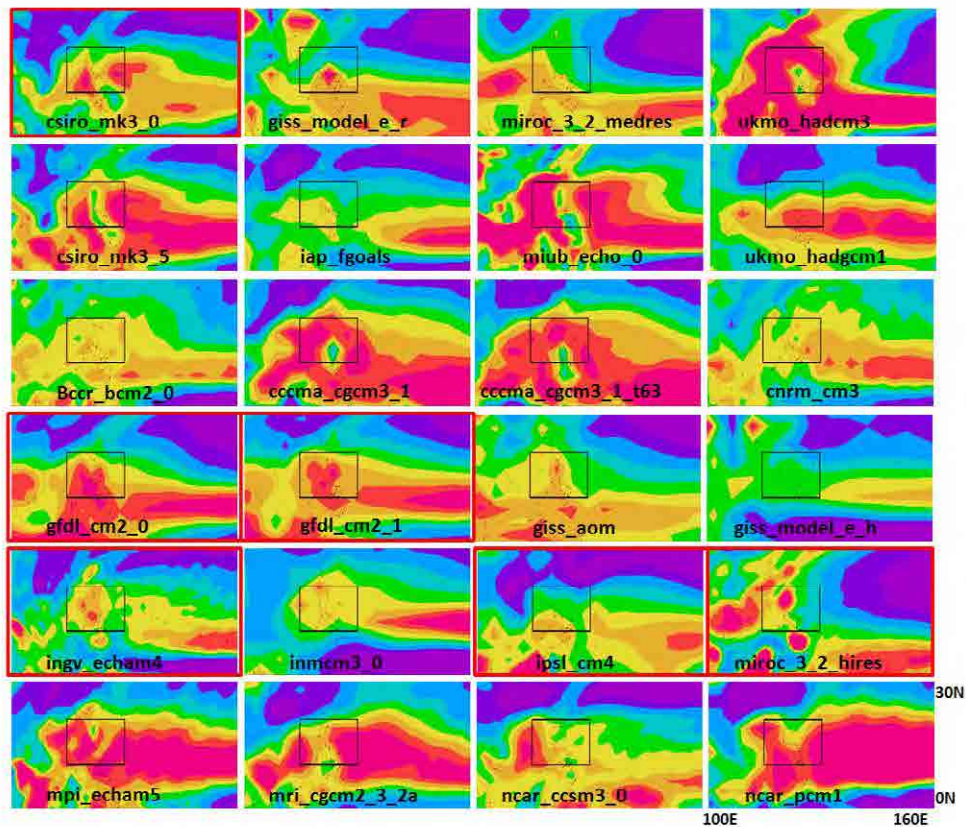


Figure 2.2-4. Climatological average precipitation from May to November for the 24 GCM models (small black box indicate local area considered for precipitation; models boxed in red indicate selected GCMs).

**Table 2.2-2.** Ranking Scores and Selected GCMs for the wet season (June to November).

RANK	Models	Precipitation	T air	OLR	U Wind	V Wind	SLP	SST	Grand Total
			80°E	80°E-	80°E-	80°E-	80°E-	80°E-	
		115°E to 130°E; 10°N to 20°N	-160°E 0°N-20°N	160°E 0°N-20°N	160°E 0°N-20°N	160°E; 0°N-20°N	160°E 0°N-20°N	160°E 0°N-20°N	
1	gfdl_cm2_0	1	1	1	1	1	1	1	7
2	gfdl_cm2_1	1	1	1	1	1	1	1	7
3	cccma_cgcm3_1	0	1	0	1	1	1	1	5
4	ipsl_cm4	1	1	-1	1	1	1	1	5
5	near_ccsm3_0	1	1	1	0	0	1	1	5
6	ukmo_hadgcm1	0	1	1	1	0	1	1	5
7	bccr_bcm2_0	0	0	1	1	1	1	0	4
8	cccma_cgcm3_1_t63	-1	1	0	1	1	1	1	4
9	giss_aom	1	0	1	-1	1	1	1	4
10	ingv_echam4	1	0	1	1	1	0	0	4
11	csiro_mk3_0	0	1	-1	1	1	1	0	3
12	miub_echo_g	1	**	0	**	**	1	1	3
13	mpi_echam5	-1	1	0	1	1	0	1	3
14	cnrm_cm3	0	1	1	0	0	0	0	2
15	csiro_mk3_5	0	0	-1	1	1	1	0	2
16	miroc3_2_medres	1	0	1	0	0	0	0	2
17	mri_cgcm2_3_2a	-1	0	0	1	1	0	1	2
18	miroc3_2_hires	0	1	0	0	0	-1	0	0
19	giss_model_e_r	1	0	-1	0	0	-1	0	-1
20	ukmo_hadcm3	-1	0	0	0	0	0	-1	-2
21	iap_fgoals1_0_g	0	-1	0	-1	0	-1	-1	-4
22	inmcm3_0	0	-1	-1	-1	-1	0	-1	-5
23	giss_model_e_h	0	-1	-1	-1	-1	-1	-1	-6
24	near_pcm1	-1	0	-1	-1	-1	-1	-1	-6

**Table 2.2-3** Ranking Scores and Selected GCMs for the dry season (December to May).

RANK	Models	Precipitation	T air	OLR	U Wind	V Wind	SLP	SST	Grand Total
			80°E-1 115°E to 130°E	80°E- 160°E	80°E- 160°E	80°E- 160°E	80°E- 160°E	80°E- 160°E	
			0°N- 10°N to 20°N	0°N- 20°N	0°N- 20°N	0°N- 20°N	0°N- 20°N	0°N- 20°N	
1	mpi_echam5	1	1	1	1	1	1	1	7
2	cccma_cgcm3_1_t63	0	1	1	1	1	1	1	6
3	gfdl_cm2_1	1	1	1	1	1	1	0	6
4	cccma_cgcm3_1	0	1	1	1	1	0	1	5
5	gfdl_cm2_0	1	0	1	1	1	1	0	5
6	ipsl_cm4	1	1	-1	1	1	1	1	5
7	mri_cgcm2_3_2a	1	1	0	1	0	1	1	5
8	ingv_echam4	0	0	1	1	1	0	1	4
9	miroc3_2_hires	0	1	0	1	0	0	1	3
10	miub_echo_g	1	**	1	**	**	0	1	3
11	miroc3_2_medres	0	0	1	0	0	0	1	2
12	ncar_ccsm3_0	1	0	1	0	0	0	0	2
13	giss_model_e_r	0	1	0	0	0	-1	1	1
14	iap_fggoals1_0_g	0	0	0	1	0	0	0	1
15	bccr_bcm2_0	-1	0	1	1	0	0	-1	0
16	csiro_mk3_5	1	-1	-1	1	0	0	0	0
17	giss_aom	-1	-1	1	0	0	1	0	0
18	ukmo_hadcm3	-1	0	0	-1	1	0	-1	-2
19	cnrm_cm3	0	-1	0	0	0	-1	-1	-3
20	csiro_mk3_0	1	-1	-1	0	0	0	-1	-3
21	inmcm3_0	0	-1	-1	0	0	0	-1	-3
22	ncar_pcm1	0	0	-1	-1	0	0	-1	-3
23	ukmo_hadgem1	-1	0	0	-1	0	0	-1	-3
24	giss_model_e_h	-1	-1	-1	-1	0	-1	0	-5

**Table 2.2-4.** Ranking Scores and Selected GCMs for the entire year.

RANK	Models	Precipitation	T air	OLR	U Wind	V Wind	SST	SLP	Grand Total
		115°E to 130°E;	80°E-1 60°E	80°E-1 60°E	80°E- 160°E	80°E- 160°E	80°E-1 60°E	80°E- 160°E	
		10°N to 20°N	0°N-20° N	0°N-20° N	0°N-20° N	0°N-20° N	0°N-20° N	0°N-20° N	
1	gfdl_cm2_1	1	1	1	1	1	1	1	7
2	gfdl_cm2_0	1	1	1	1	1	0	1	6
3	mpi_echam5	0	1	1	1	1	1	1	6
4	cccma_cgcm3_1	0	1	0	1	1	1	1	5
5	cccma_cgcm3_1_t63	0	1	0	1	1	1	1	5
6	ingv_echam4	1	0	1	1	1	1	0	5
7	ipsl_cm4	1	1	-1	1	1	1	1	5
8	ncar_ccsm3_0	1	0	1	0	0	1	1	4
9	bccr_bcm2_0	0	0	1	1	1	-1	1	3
10	giss_aom	-1	0	1	1	-1	1	1	2
11	miub_echo_g	1	**	0	**	**	1	0	2
12	mri_cgcm2_3_2a	-1	0	0	1	1	1	0	2
13	csiro_mk3_0	1	0	-1	1	-1	0	1	1
14	csiro_mk3_5	0	0	-1	1	0	0	1	1
15	miroc3_2_medres	1	0	1	0	-1	0	0	1
16	ukmo_hadgcm1	0	1	0	0	0	-1	1	1
17	miroc3_2_hires	0	1	0	0	-1	0	-1	0
18	giss_model_e_r	1	0	0	0	1	0	-1	-1
19	ukmo_hadcm3	-1	0	0	0	-1	-1	0	-1
20	cnrm_cm3	-1	0	1	0	-1	-1	0	-2
21	iap_fgoals1_0_g	0	-1	0	0	1	-1	0	-3
22	inmcm3_0	0	-1	0	-1	-1	-1	0	-4
23	giss_model_e_h	0	-1	-1	-1	-1	0	-1	-5
24	ncar_pcm1	-1	0	-1	-1	-1	-1	-1	-6

**Table 2.2-5** Global Circulation Models Developer Institutions.

<b>Model</b>	<b>Institution</b>	<b>Country</b>
gfdl_cm2_0	US Dept of Commerce / NOAA / Geophysical Fluid Dynamics Laboratory, Princeton, NJ, USA	USA
Gfdl_cm2_1	US Dept of Commerce / NOAA / Geophysical Fluid Dynamics Laboratory, Princeton, NJ, USA	USA
Ingv_echam4	National Institute of Geophysics and Volcanology, Bologna, Italy	Italy
ipsl_cm4	Institut Pierre Simon Laplace, Paris, France	France
csiro_mk3_0	Commonwealth Scientific and Industrial Research Organisation, Australia	Australia
miroc3_2_medres	CCSR (Center for Climate System Research, University of Tokyo)/NIES (National Institute for Environmental Studies) /FGCGC (Frontier Research Center for Global Change, Japan Agency for Marine-Earth Science and Technology (JAMSTEC), Japan	Japan

### 2.2.3 Other Parameters Considered for Projecting Future Trends in Climate Change

**Table 2.2-6.** Parameters used for the selected GCMs.

<b>Model</b>	<b>Parameters used</b>
gfdl_cm2_0	Rainfall, minimum and maximum temperatures, short wave radiation, long wave radiation
gfdl_cm2_1	Rainfall, minimum and maximum temperatures, short wave radiation, long wave radiation
ipsl_cm4	Rainfall, minimum and maximum temperatures
ingv_echam4	Rainfall, minimum and maximum temperatures, short wave radiation, long wave radiation
csiro_mk3_0	Rainfall, minimum and maximum temperatures short wave radiation
miroc3_2_medres	Rainfall, minimum and maximum temperatures, short wave radiation, long wave radiation

Aside from rainfall, future trends in climate change were projected by using other meteorological parameters from the general circulation models. However, these parameters were

used directly and were not bias corrected since these parameters have more periodicity and have similar behaviors as in the past observed data. Depending on availability of the dataset, a single value was considered for every time step of each parameter for the entire basin. **Table 2.2-6** lists the parameters used for each of the 6 selected models.

### **2.3 Bias-Correction of the GCM Outputs**

Most of the precipitation data in the GCMs show three main problems, including underestimation of heavy rainfall intensity, low seasonal representation and too many rainy days with very weak rainfall referred to as drizzle. In the Study, we focus on bias-correction of GCM to reduce these problems. To accomplish this, annual maximum rainfall, normal rainfall and numbers of no rain days are bias-corrected statistically (Nyunt, et al., 2012).

#### **2.3.1 Three-Step Bias Correction Method**

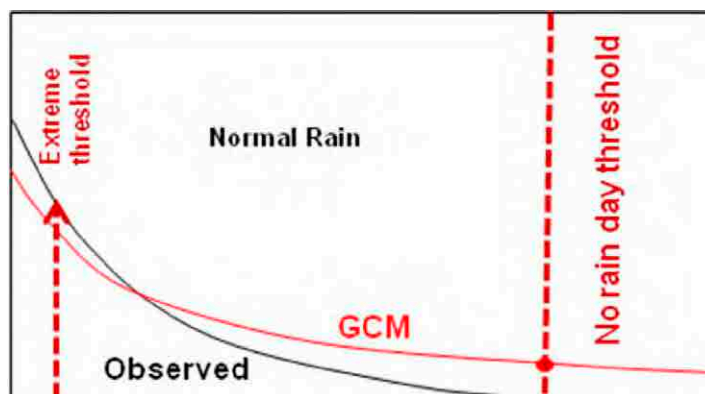
Precipitation outputs from the GCMs cannot be directly used to force hydrological or other impact assessment models without some form of prior bias correction if realistic output is sought (Ines and Hansen, 2006; Feddersen and Andersen, 2005; Sharma et al., 2007). If used directly, it may magnify the errors resulting from these biases. Hence, it is necessary to correct the biases prior to utilization of model outputs. And since there are differences between models, the use of a model ensemble especially precipitation (most sensitive dynamic parameter affecting moisture fluctuations), on the water supply in the basin was investigated. A variety of tools for evaluation, selection and downloading of GCM data have been developed by the DIAS system and disseminated via the data access system.

To utilize GCM scenario outputs in a hydrological study, appropriate downscaling is needed. Two downscaling approaches are typically available; statistical downscaling and dynamical downscaling. Dynamic downscaling involves the use of finer resolution numerical weather prediction models with GCM output as initial and boundary conditions. Statistical downscaling involves the use of statistical relationships to convert the large-scale projections from a GCM to higher spatial resolutions. This part of the report presents steps necessary to achieve a simplified statistical approach based on statistics.

To achieve reasonable bias correction of precipitation, there is a need to separate no-rain days, normal rain days and extreme rain days. Due to their failure to incorporate parameterization schemes in their simulations; GCM outputs are characterized by many wet days (with plenty of drizzle) and its inability to represent extreme events. This necessitates the separation of these three types of rainfall events. To account for basins with extremely distinct seasons (e.g very dry and wet seasons), bias correction should be performed separately for these seasons. This should be done at monthly or

bi-monthly scales depending on the basin climatology.

Bias correction using this approach is a three step process: 1.) for dry days, 2.) normal days and 3.) extreme rain days. **Figure 2.3-1** illustrates how the 3 categories of rainfall are considered (Nyunt, et al., 2012).



**Figure 2.3-1.** Three-step bias correction dividing rainfall into extreme, normal and no rain days.

#### **STEP 1: No-rain day correction**

A common characteristic of all GCMs is unrealistically high number of wet days. Most of this is represented as drizzle and it can be attributed to lack of parameterization in GCMs. To correct for this, the method below is employed.

- 1) Both past observations and GCM extracted values are ranked in descending order.
- 2) A threshold of 0 mm/day was considered for no-rain day in the observations. The rank of this threshold is then used to determine the corresponding value of no rain day in the GCMs
- 3) All values equal or below this rank in the GCM is equated to zero
- 4) No-rain day correction for the future GCM is based on the threshold for past GCMs

#### **STEP 2: Extreme rainfall correction**

Most of the GCMs underestimate extreme rainfall compared to observations. To account for this, appropriate correction should be applied to adjust these values to match the distribution of the observations.

Annual maxima rainfall was selected for each year in the observed dataset. The lowest value of the annual maxima was selected as the threshold of the extreme events for observed rainfall. Values above this threshold are defined as extreme events. The number of extreme events are determined from observed stations and set with the same number of extreme events in past GCMs by ranking. Above this threshold the General Pareto Distribution (GPD) was fitted into the data.



The GPD fitting parameter for GCM corrected extremes were determined (shape, scale and location) using the Methods of Moments (MOM) used for parameterization using the MOM equations below (Hosking and Wallis, 1987; Madsen et al., 1997). The best fitting GPD of GCM extreme events was determined by the minimum root mean squared error (RMSE) between inversed GPD of extreme and observed station (checked using trial and error with different thresholds). The same checking (past GCM) and fitting procedure was applied to all extremes. GCM extremes for future projections were extracted and the transfer function of the past GCM extremes correction was applied.

All values greater than a threshold  $u$ ,

the distribution of excess  $x$  over  $u$  is defined by

$$F_u(y) = \Pr\{X - u \leq x | X > u\} = \frac{F(x) - F(u)}{1 - F(u)} \quad (\text{eq.3})$$

Generalized Pareto distribution (GPD) is given by :

$$G(x; K, \alpha, u) = 1 - \left(1 - K \frac{x - \mu}{\alpha}\right)^{1/\xi} \quad \xi \neq 0$$

$$1 - e^{-(x-\mu)/\alpha} \quad \xi = 0$$

$K = 0 \Rightarrow$  exponential distribution (medium - size tail)

$K < 0 \Rightarrow$  Pareto distribution (long - tailed)

$K > 0 \Rightarrow$  Pareto II type distribution (short tailed)

$$\alpha = \frac{1}{2} \mu \left( \frac{\mu^2}{\sigma^2} + 1 \right) \quad (\text{eq.4})$$

$$\kappa = \frac{1}{2} \left( \frac{\mu^2}{\sigma^2} - 1 \right)$$

$\mu$  = sample mean

$\sigma^2$  = variance

The recurrences of extreme events for different return periods were calculated as shown in the equation below.

$$x_T = u + \frac{\alpha}{\kappa} \left[ 1 - (\lambda T)^{-\kappa} \right]$$

$\kappa$  = shape parameter

$\alpha$  = scale parameter

$\lambda$  = average number of events per year above threshold

$T$  = return period in years

(eq.5)

### STEP 3: Normal Rainfall Correction

Normal rainfall is the range between zero rainfall and the extreme rainfall. Correction in this band is based on the gamma distribution function fitted to past observations and GCMs. The following equation has been adopted:


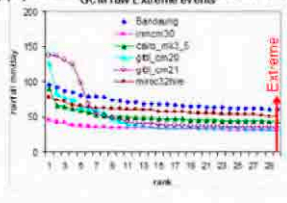
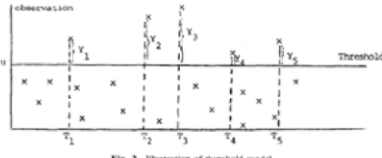

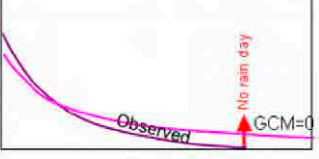

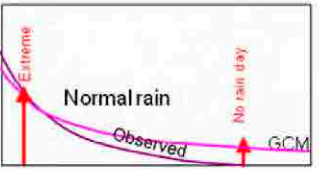
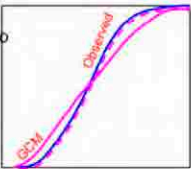
$$f(x) = \frac{\lambda^\beta x^{\beta-1} e^{-\lambda x}}{\Gamma(\beta)} \quad x \geq 0$$

$$\lambda = \frac{\bar{x}}{s_x^2}, \quad \beta = \frac{\bar{x}^2}{s_x^2}$$

$\bar{x}$  = mean of sample  
 $s_x^2$  = variance of sample  
 $\Gamma(\ )$  = Gamma function

The inverse of the gamma distribution for past observed rainfall is used to correct for past GCM rainfall. This is then used as a transfer function for the future normal rainfall correction.

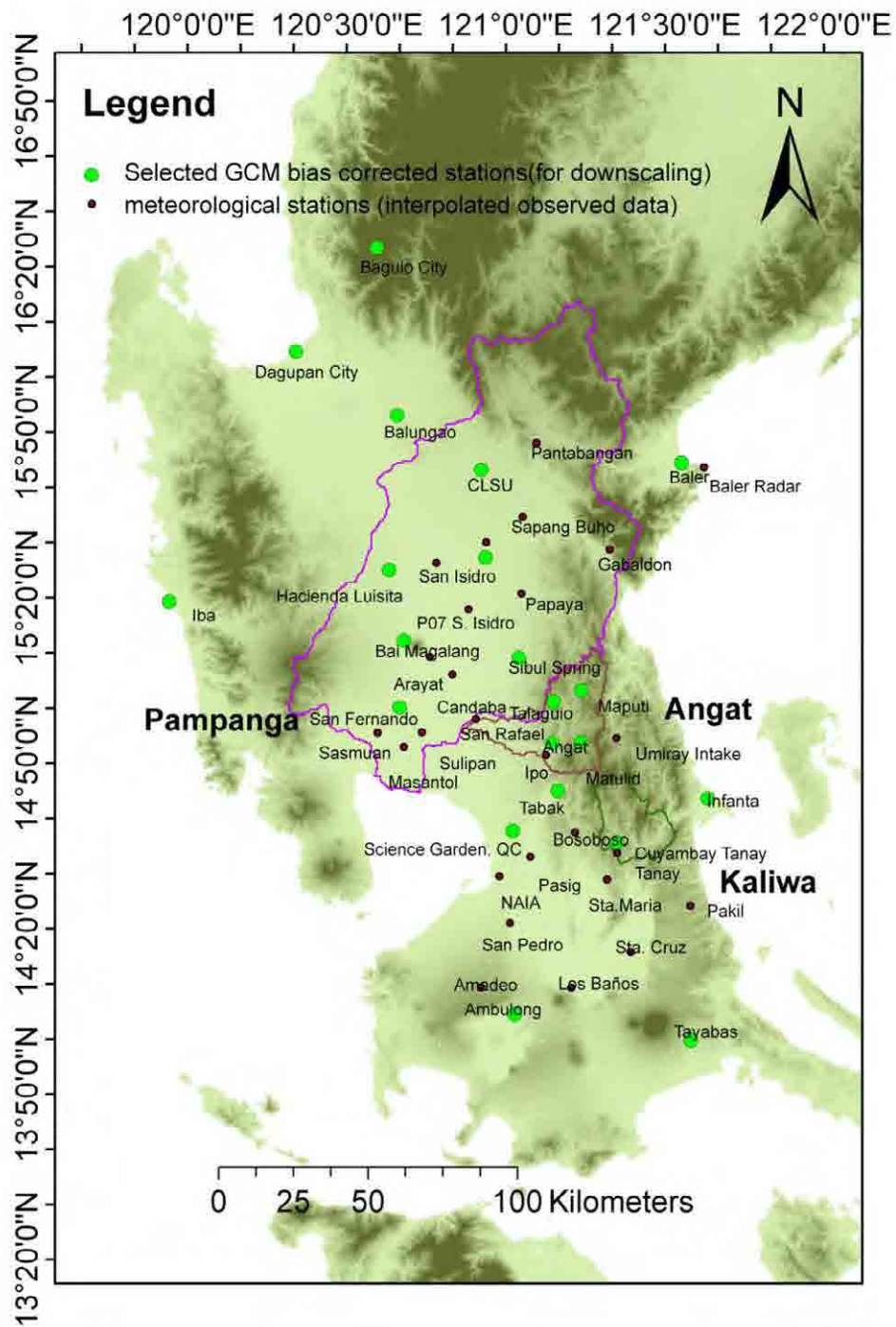
A summary of the 3-step bias correction is given in **Figure 2.3-2** below.

Rain Type	Threshold	Correction
<b>Extreme</b> 	<ul style="list-style-type: none"> <li>- Larger than minimum of annual maxima of station</li> <li>- count the number of extreme events in station (eg. Top of 30 rainfall by ranking all rainfall)</li> <li>- apply same number of extremes in GCM</li> </ul> 	<b>Generalized Pareto Distribution</b> <ul style="list-style-type: none"> <li>- Non every year statistics</li> <li>- Extreme (long or short tailed) fitting</li> <li>- Peak over threshold method</li> </ul>  <p>Fig. 2. Illustration of threshold model.</p>
<b>No rain day</b> 		<b>Ranking order statistics</b> <ul style="list-style-type: none"> <li>- frequency of no rain day in GCM is same as station</li> <li>- less than no rain day threshold change zero rainfall.</li> </ul>
<b>Normal</b> 		<b>Gamma Distribution</b> <ul style="list-style-type: none"> <li>- monthly CDF of GCM mapping to monthly CDF of station</li> <li>- inverse of Gamma CDF in each month is corrected rain</li> </ul> 

**Figure 2.3-2** Summary of the 3-step bias correction.

### 2.3.2 Bias Correction Results

There are 46 observed rain gauges used in this study. 21 of these were used as representative gauges for bias correction. **Figure 2.3-3** shows the distribution of the gauge stations that were bias corrected for this study. **Figure 2.3-4 to 2.3-11** shows a.) the frequency analysis, b.) seasonality of past and future bias corrected rainfall of the selected models and c.) the 10 year, 50 year and 100 year probability of extreme rainfall events of the selected 6 models for the 4 stations (Angat, Matulid, Maputi and Talaguio) within Angat Watershed. These were similarly done to the other stations. **Figures 2.3-12 to 2.3-32** shows the seasonality of the past (1981-2000) and future (2046-2065) bias corrected rainfall stations for the 21 stations that were bias corrected for this study.



**Figure 2.3-3.** Meteorological and synoptic gauges over Central and Southern Luzon with the 21 selected stations for bias correction.

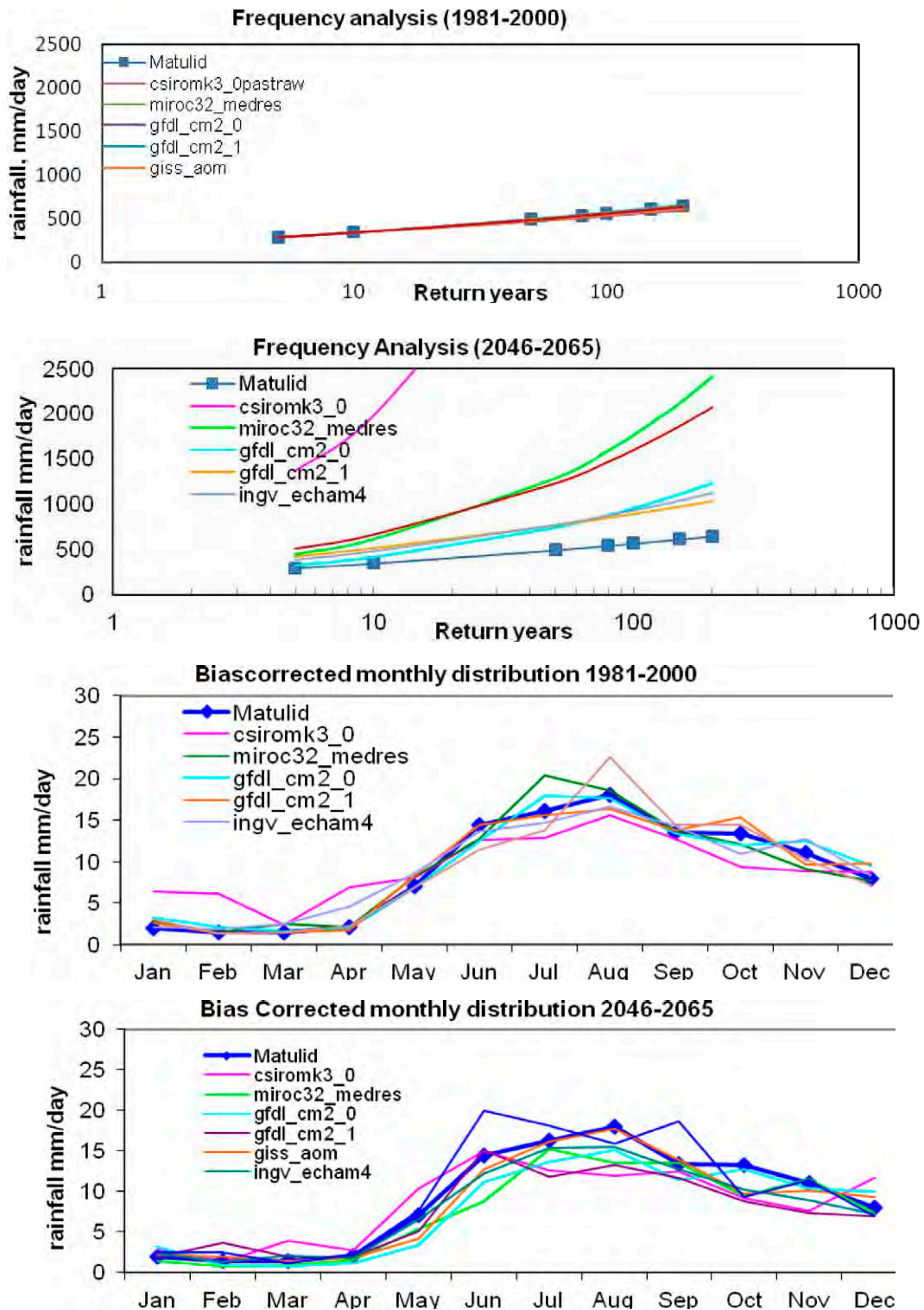


Figure 2.3-4. Bias Corrected Matulid station: frequency distribution and seasonality.

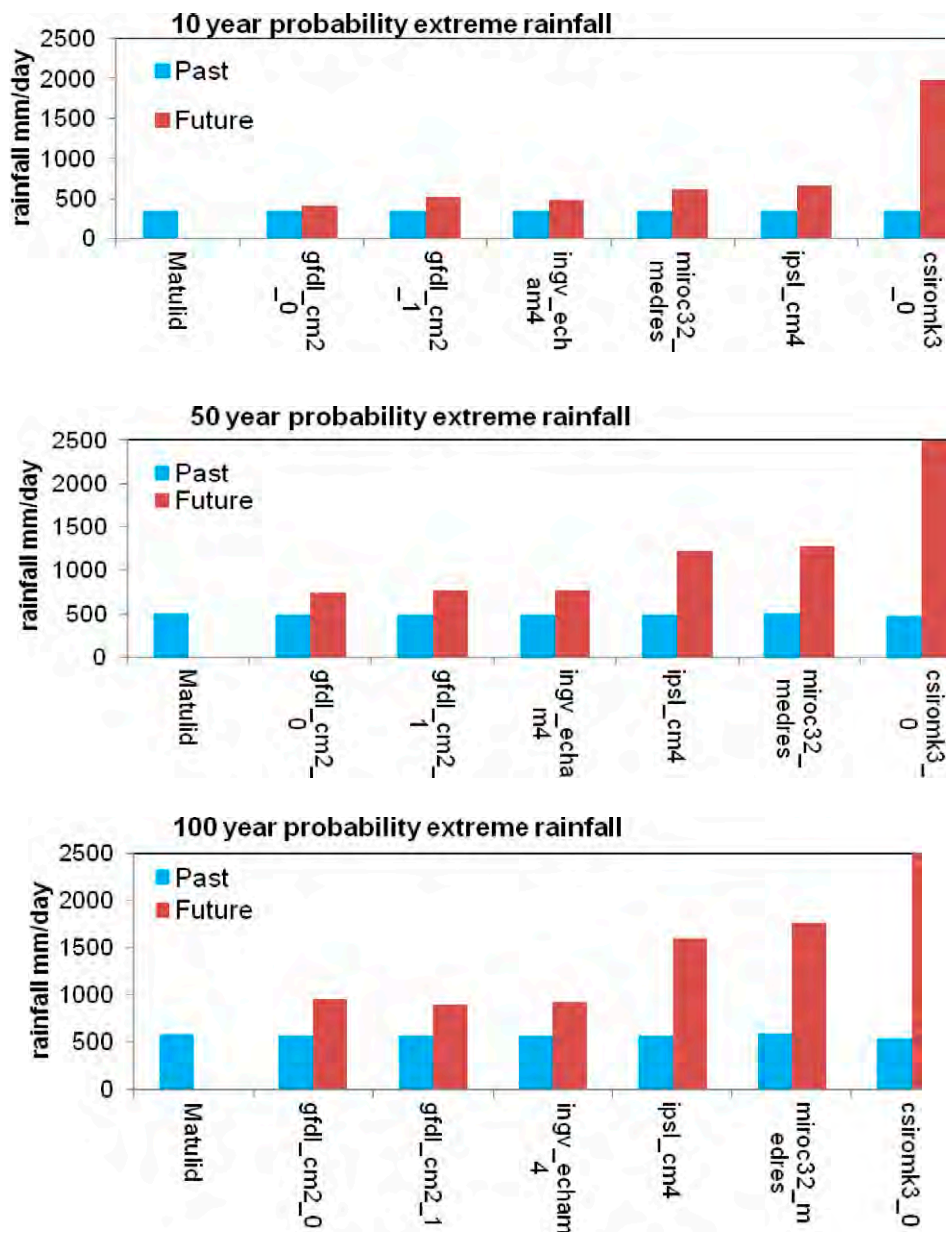


Figure 2.3-5. Bias Corrected Matulid station: 10, 50 and 100-year probability of extreme rainfall.



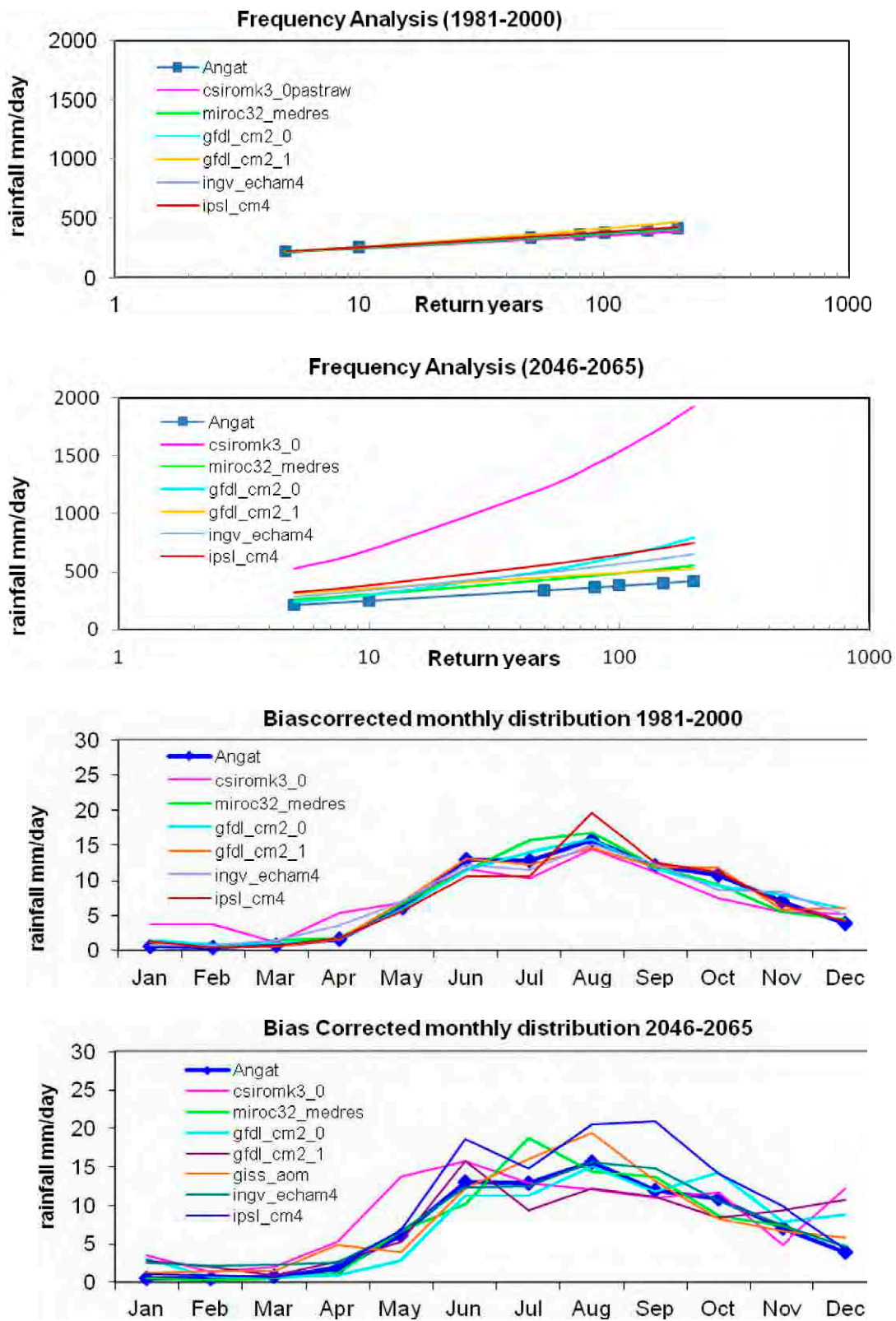


Figure 2.3-6. Bias Corrected Angat station: frequency distribution and seasonality.

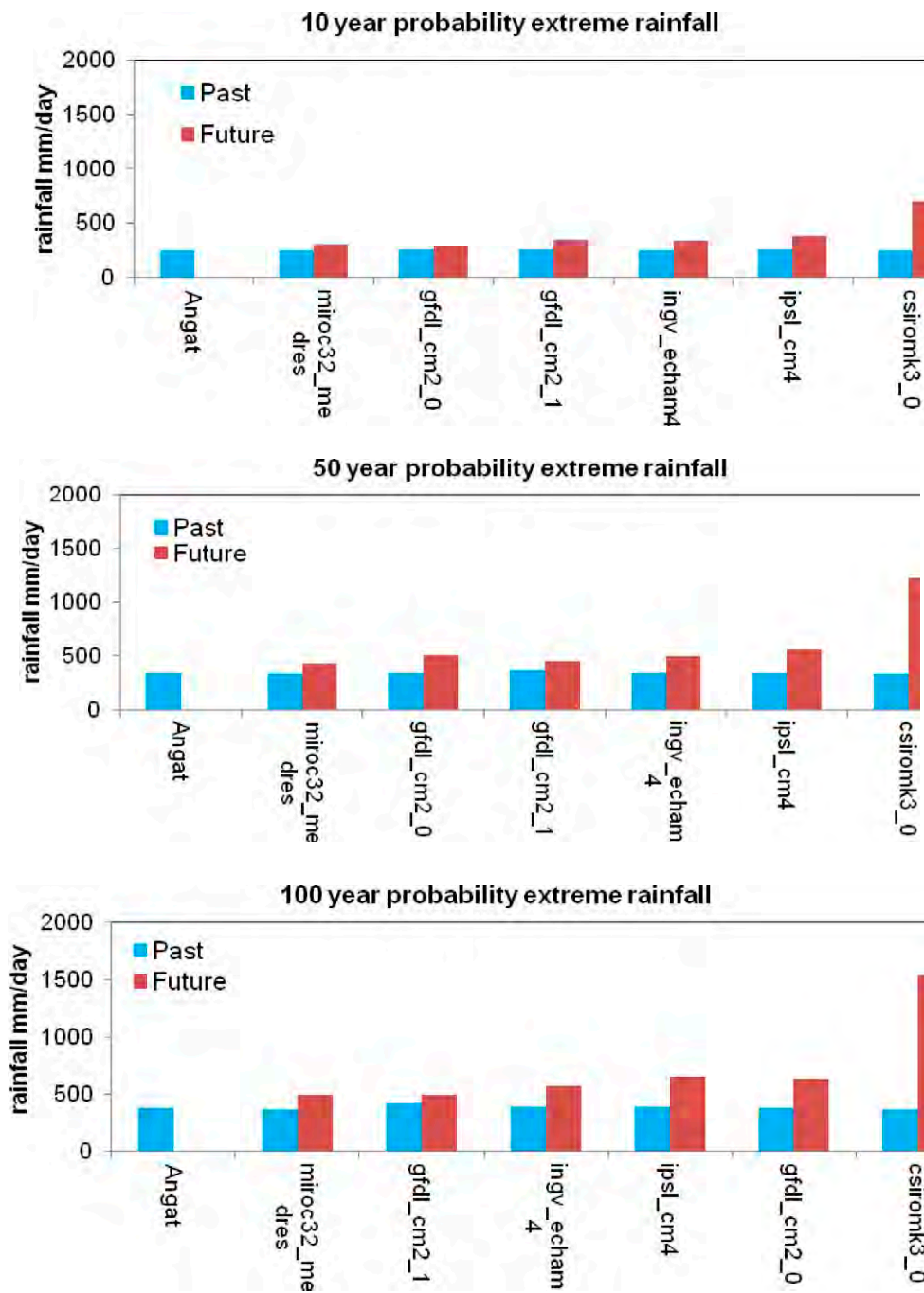


Figure 2.3-7. Bias Corrected Angat station: 10, 50 and 100-year probability of extreme rainfall.

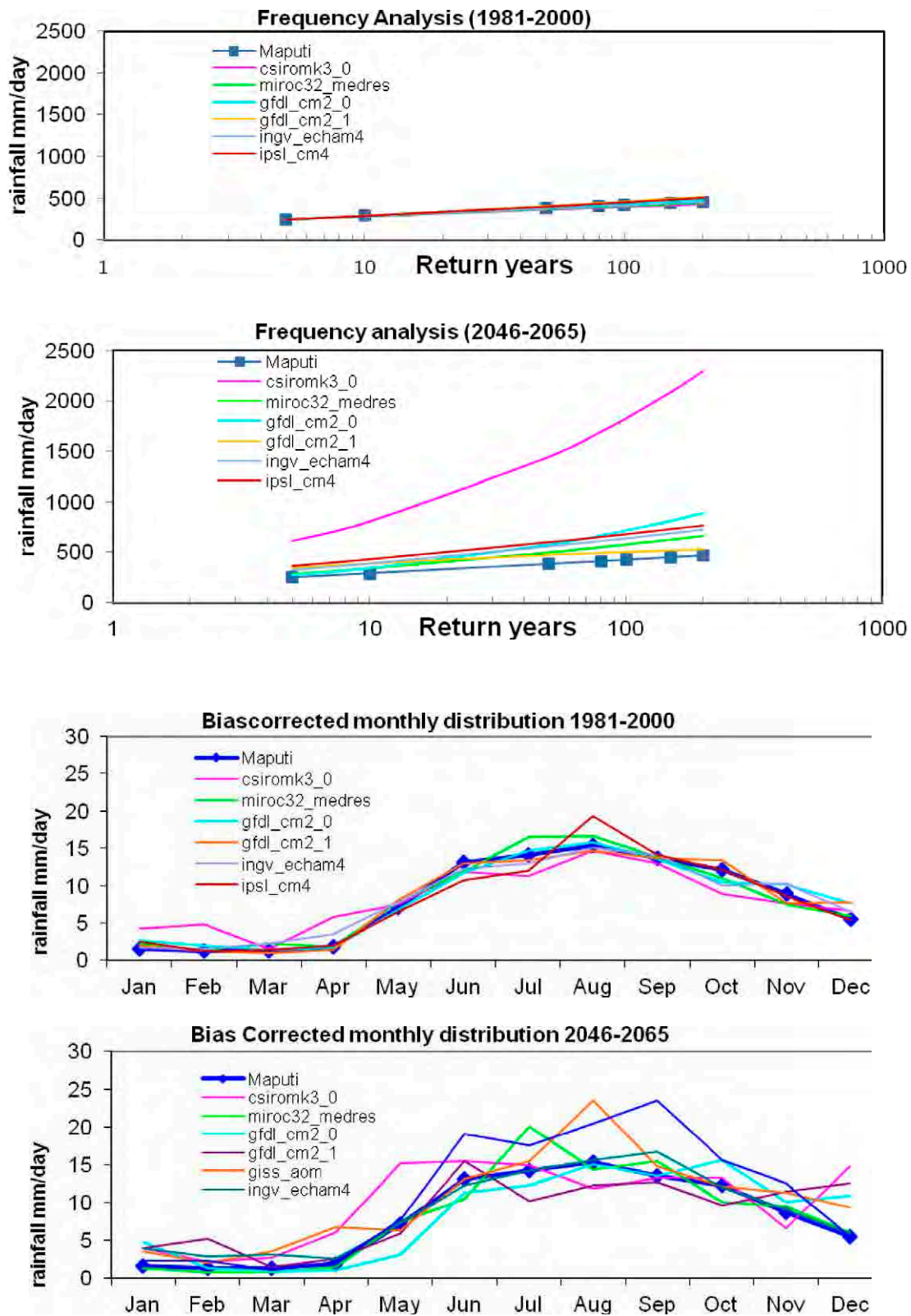


Figure 2.3-8. Bias Corrected Maputi station: frequency distribution and seasonality.



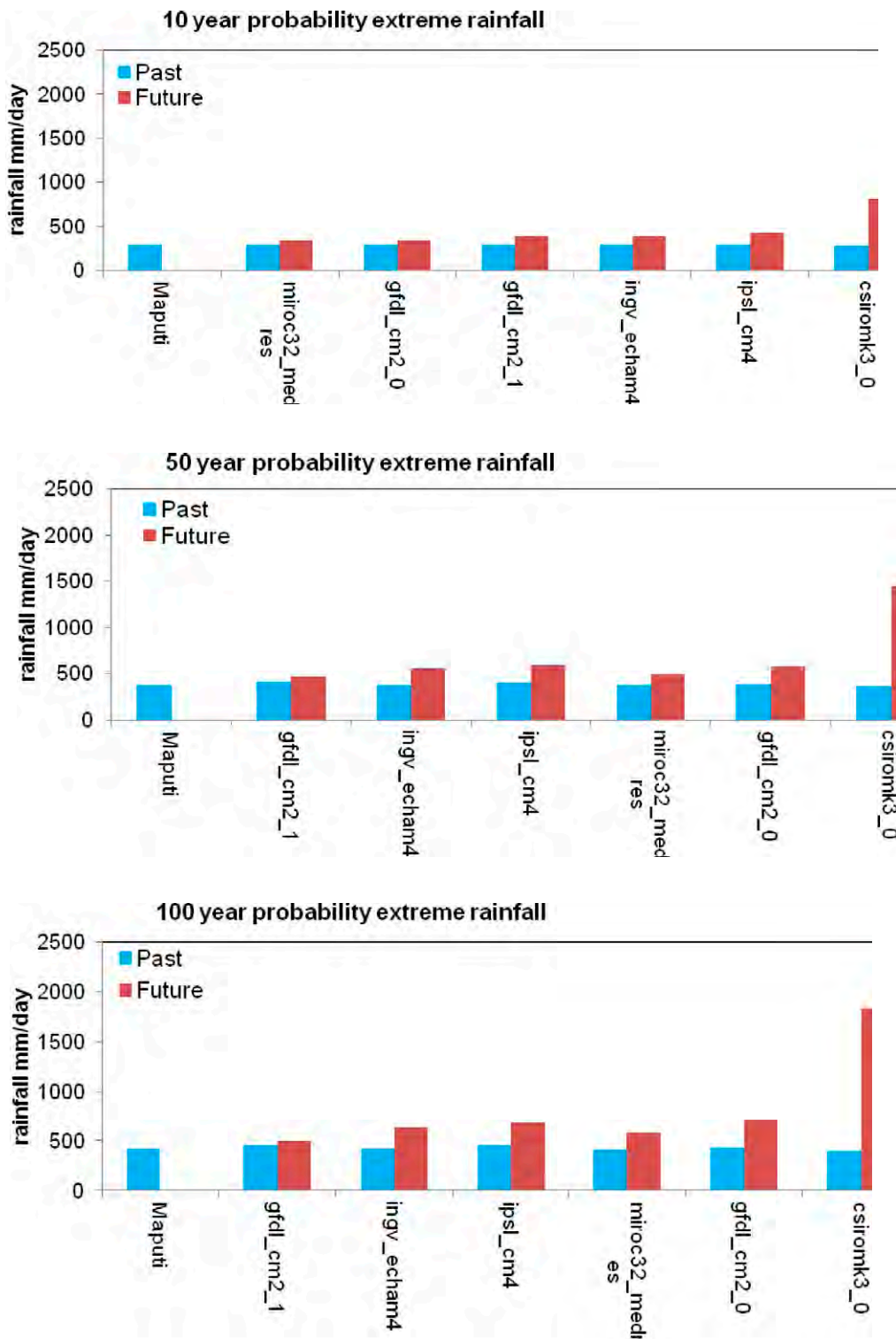


Figure 2.3-9. Bias Corrected Maputi station: 10, 50 and 100-year probability of extreme rainfall.

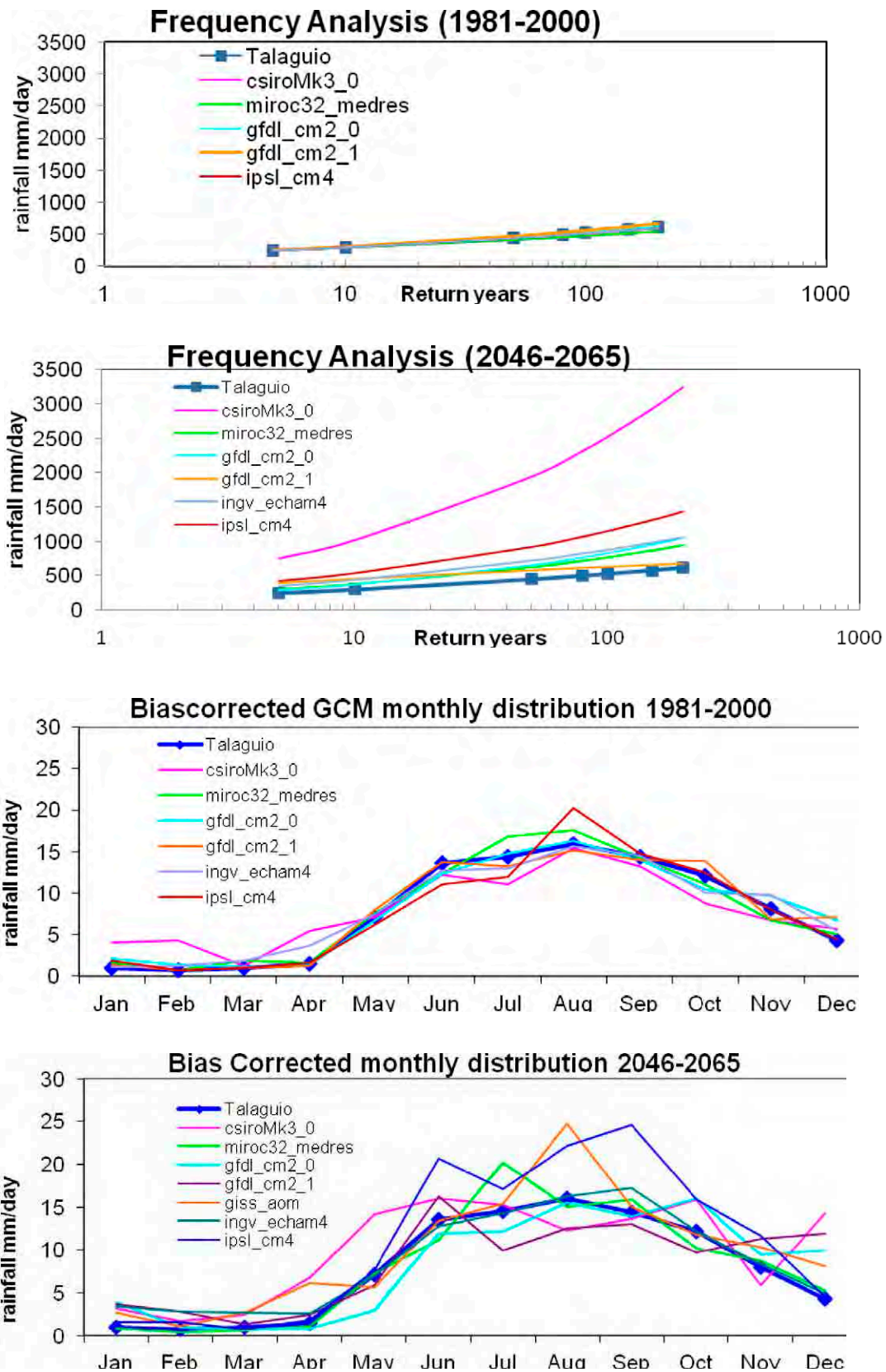


Figure 2.3-10. Bias Corrected Talaguio station: frequency distribution and seasonality.

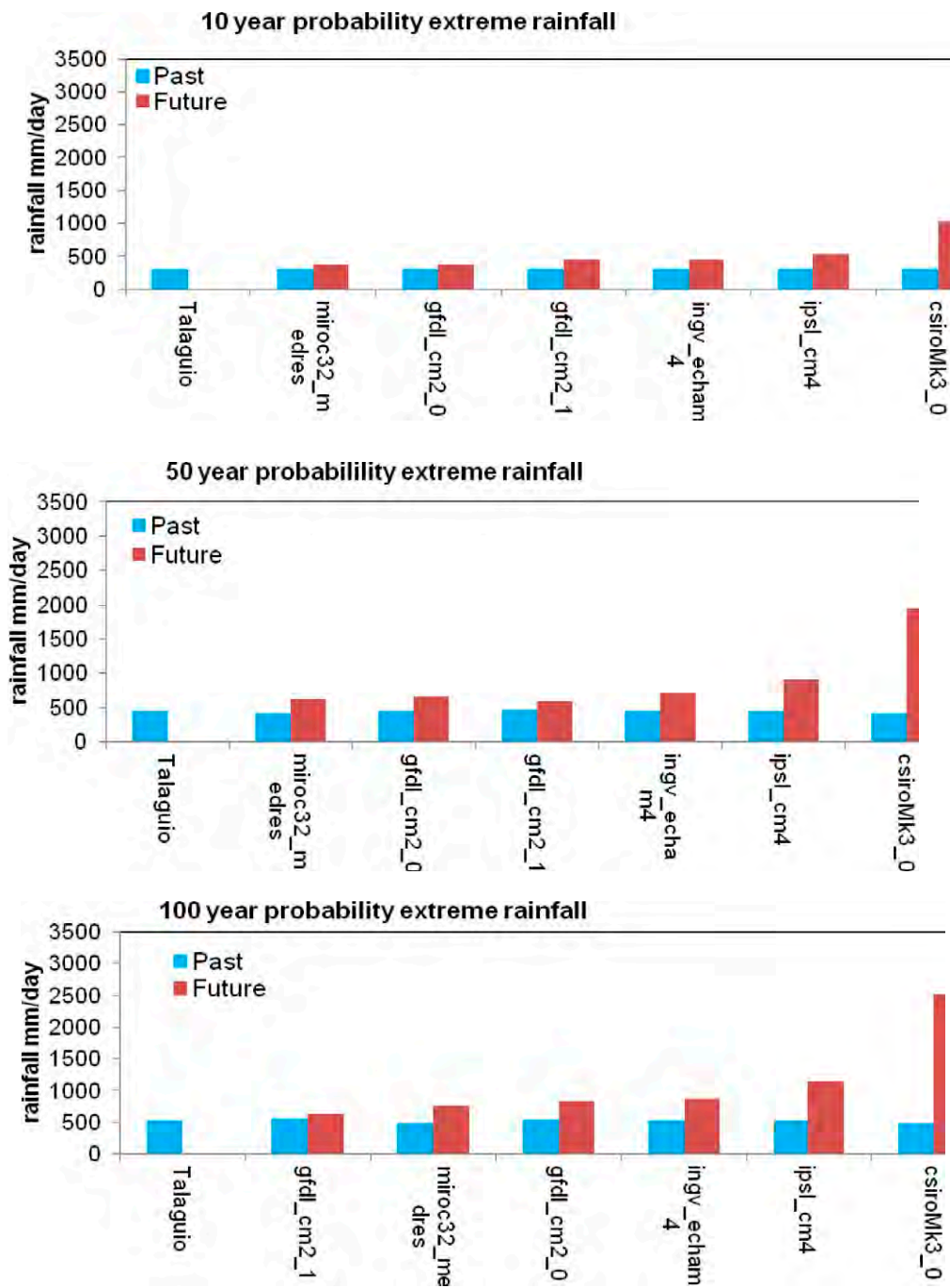


Figure 2.3-11. Bias Corrected Talaguio station: 10, 50 and 100-year probability of extreme rainfall.

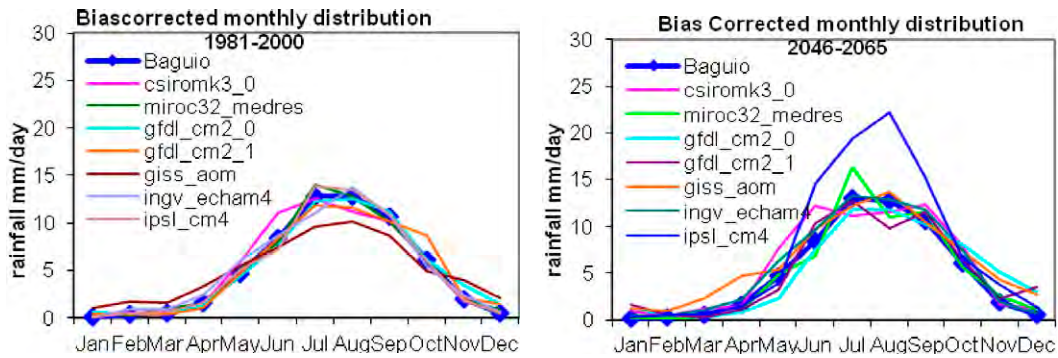


Figure 2.3-12. Bias Corrected past (1981-2000) and future (2046-2065) for Baguio station.

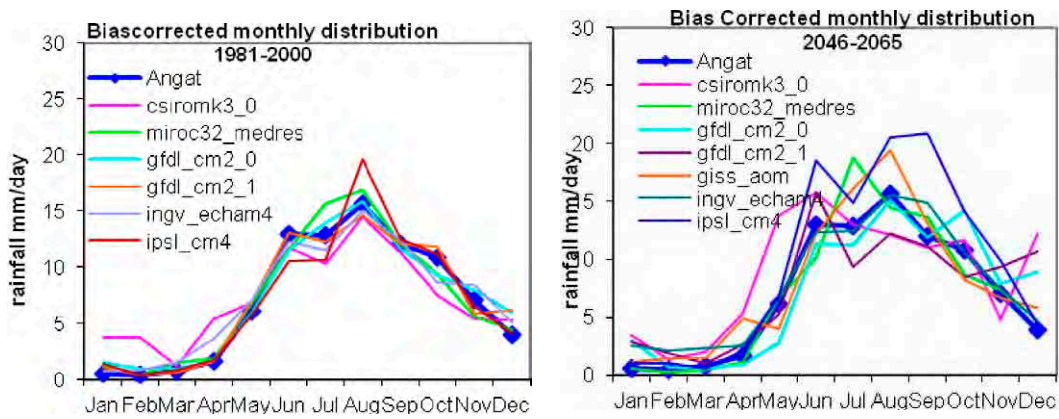


Figure 2.3-13. Bias Corrected past (1981-2000) and future (2046-2065) for Angat station.

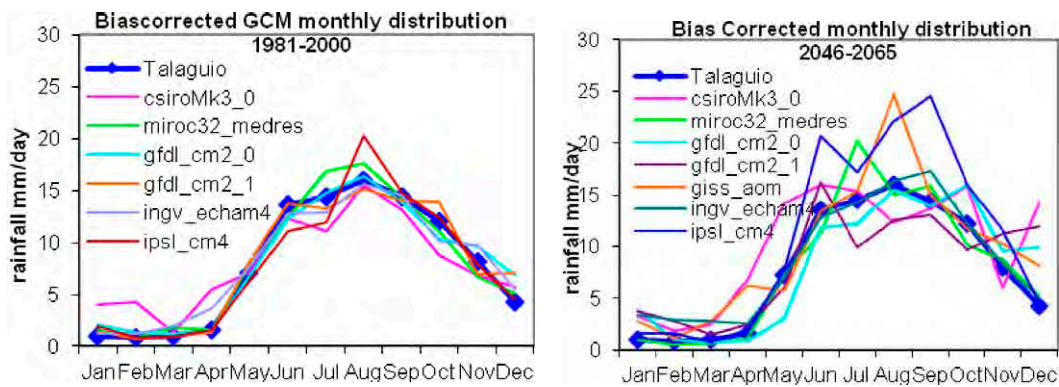


Figure 2.3-14. Bias Corrected past (1981-2000) and future (2046-2065) for Talaguio station.



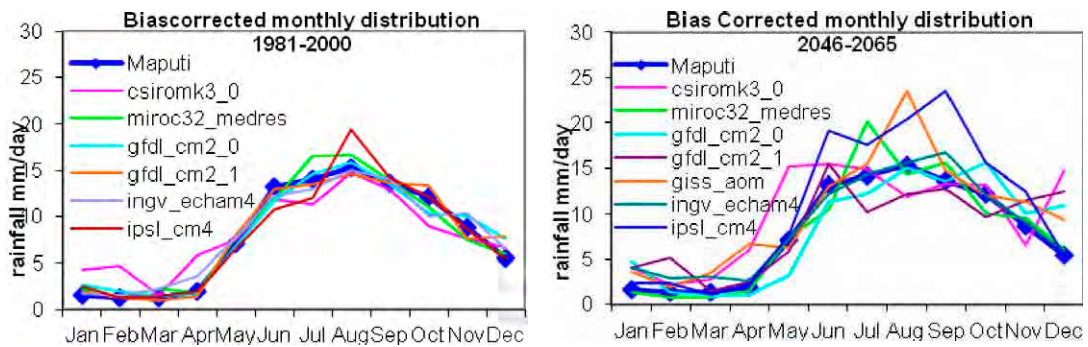


Figure 2.3-15. Bias Corrected past (1981-2000) and future (2046-2065) for Maputi station.

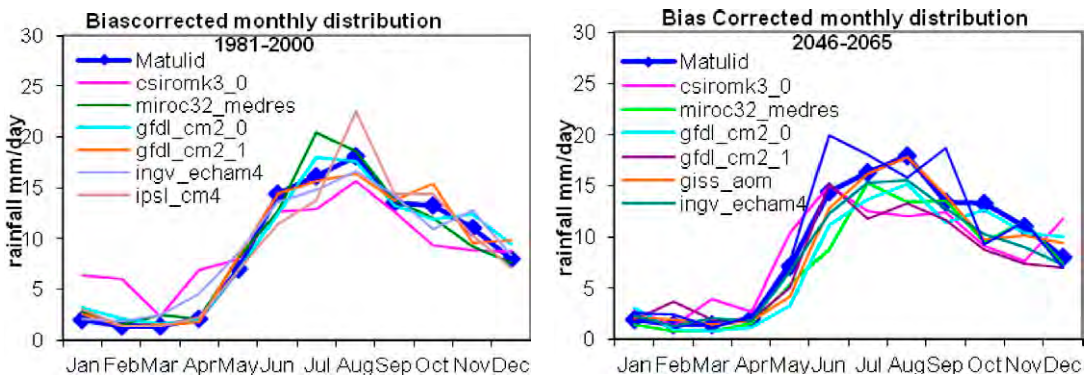


Figure 2.3-16. Bias Corrected past (1981-2000) and future (2046-2065) for Matulid station.

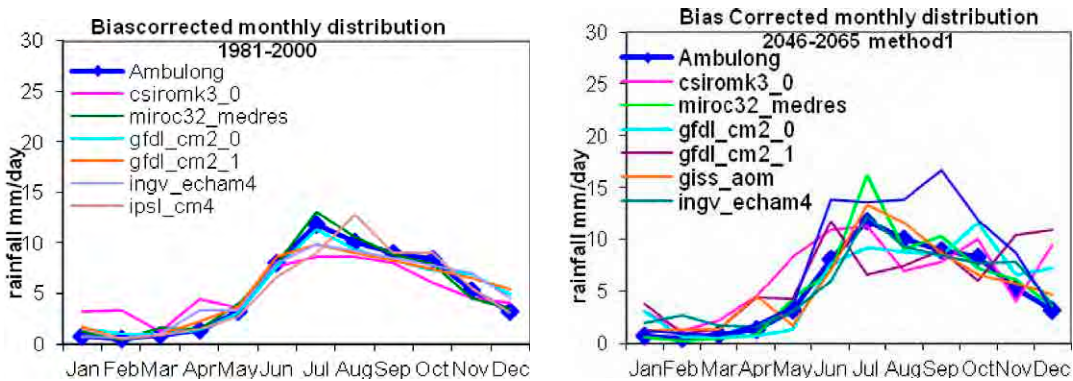


Figure 2.3-17. Bias Corrected past (1981-2000) and future (2046-2065) for Ambulong station.

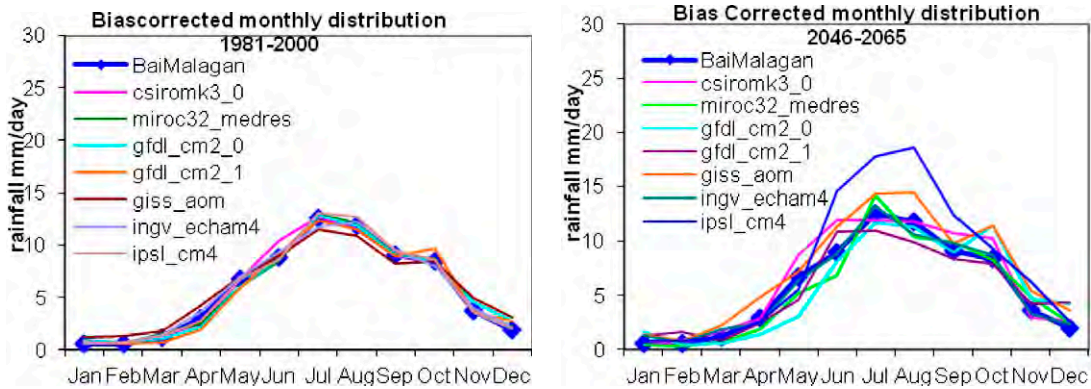


Figure 2.3-18. Bias Corrected past (1981-2000) and future (2046-2065) for Bai Magalang station.

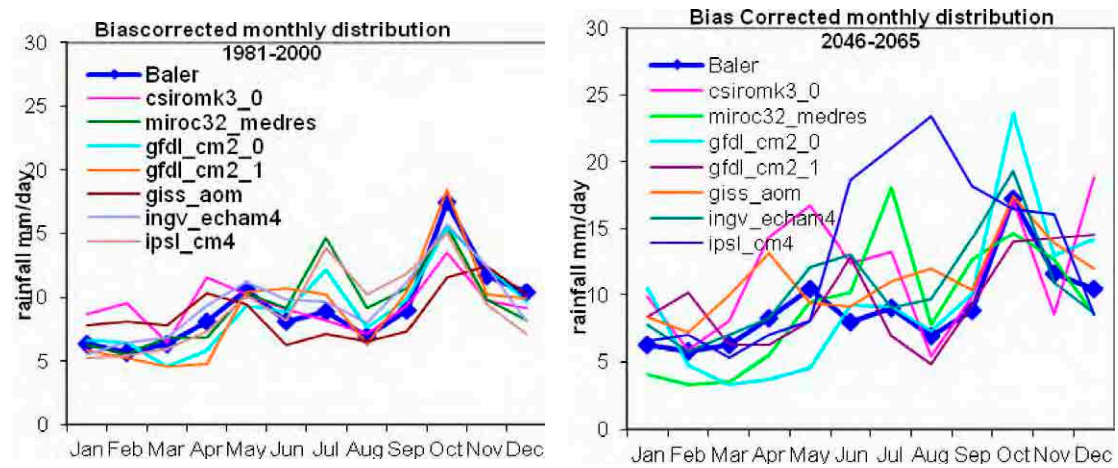


Figure 2.3-19. Bias Corrected past (1981-2000) and future (2046-2065) for Baler station.

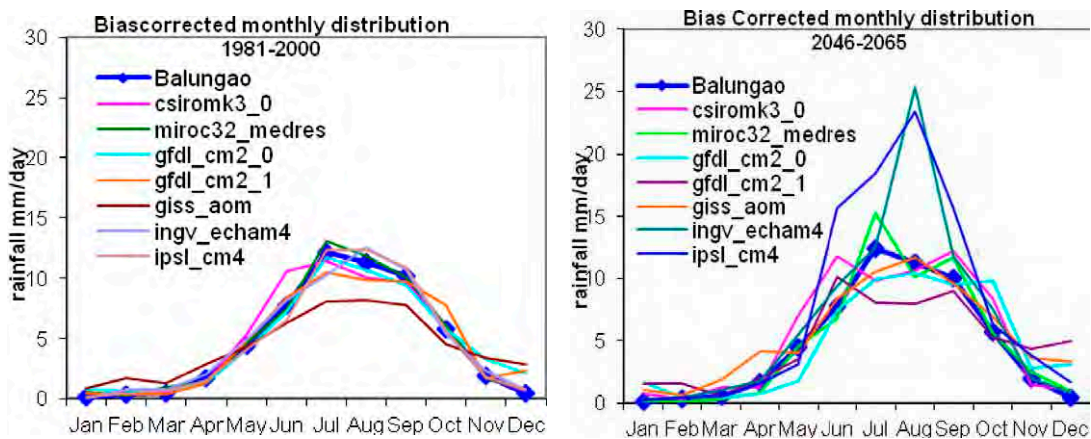


Figure 2.3-20. Bias Corrected past (1981-2000) and future (2046-2065) for Balungao station.

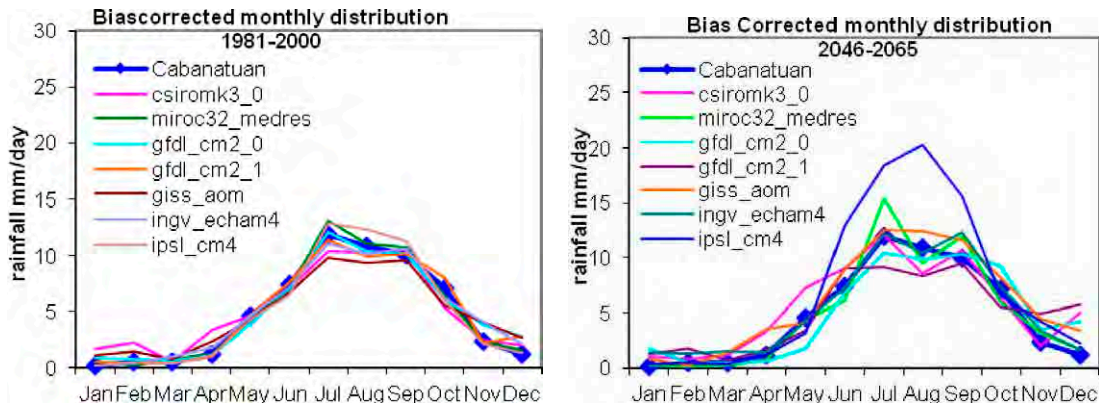


Figure 2.3-21. Bias Corrected past (1981-2000) and future (2046-2065) for Cabanatuan station.

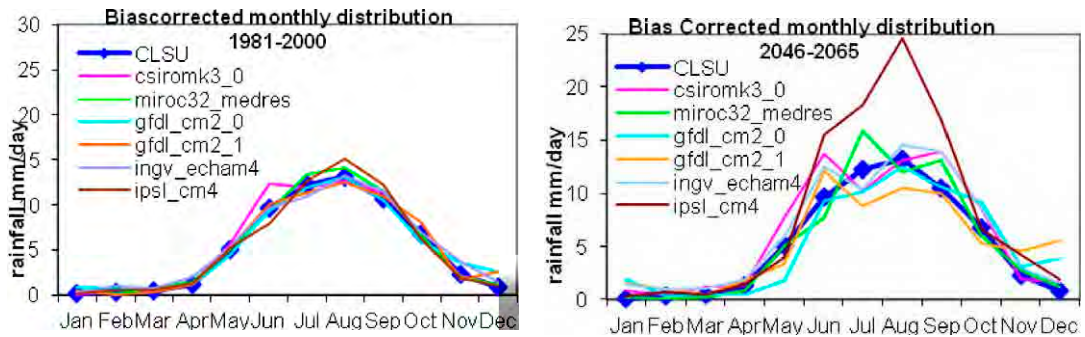


Figure 2.3-22. Bias Corrected past (1981-2000) and future (2046-2065) for CLSU station.

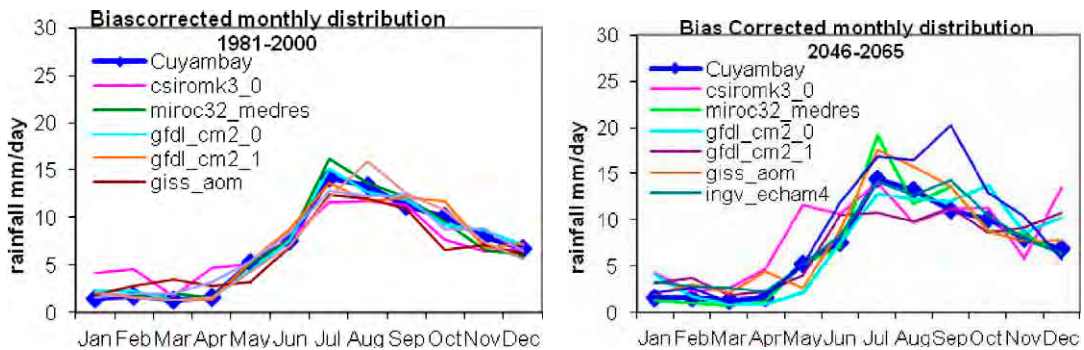


Figure 2.3-23. Bias Corrected past (1981-2000) and future (2046-2065) for Cuyambay station.



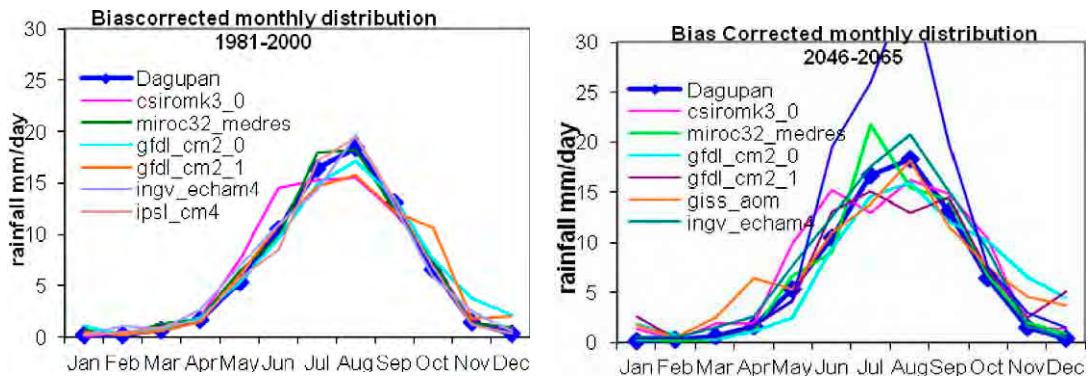


Figure 2.3-24. Bias Corrected past (1981-2000) and future (2046-2065) for Dagupan station.

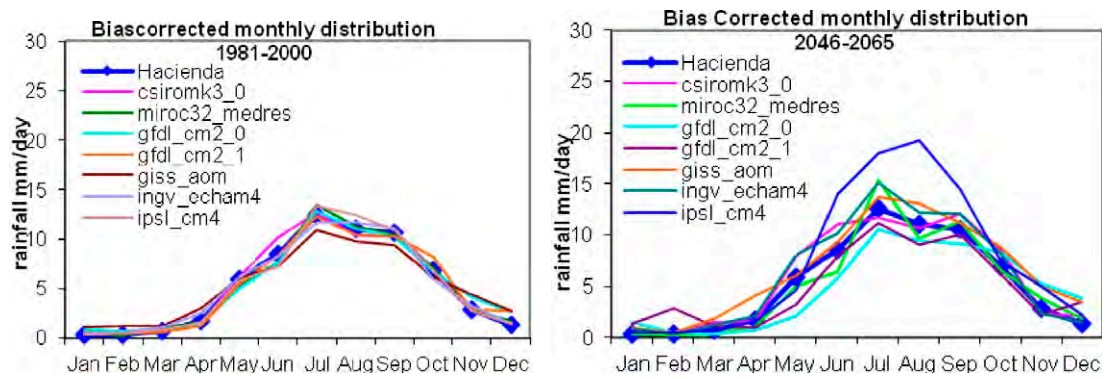


Figure 2.3-25. Bias Corrected past (1981-2000) and future (2046-2065) for Hacienda Luisita station.

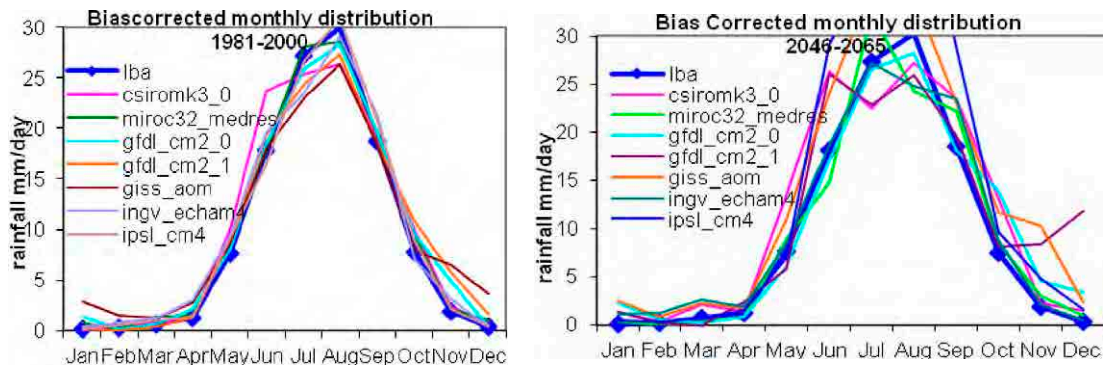


Figure 2.3-26. Bias Corrected past (1981-2000) and future (2046-2065) for Iba station.



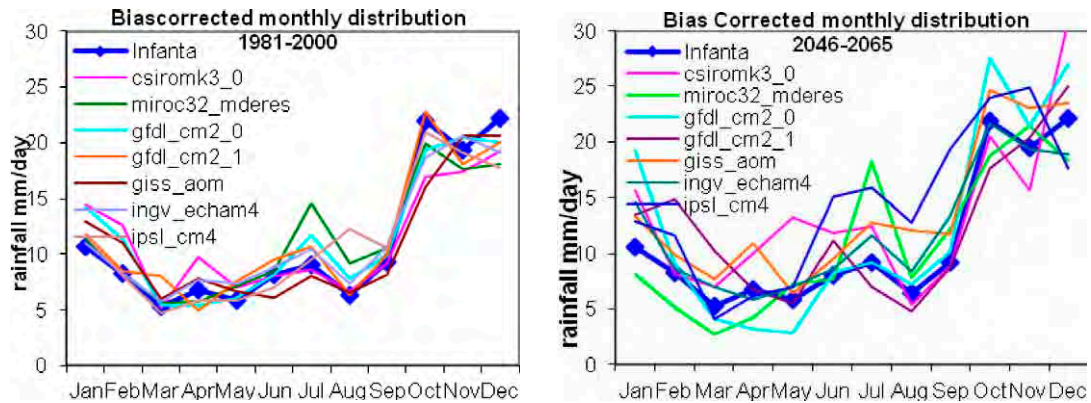


Figure 2.3-27. Bias Corrected past (1981-2000) and future (2046-2065) for Infanta station.

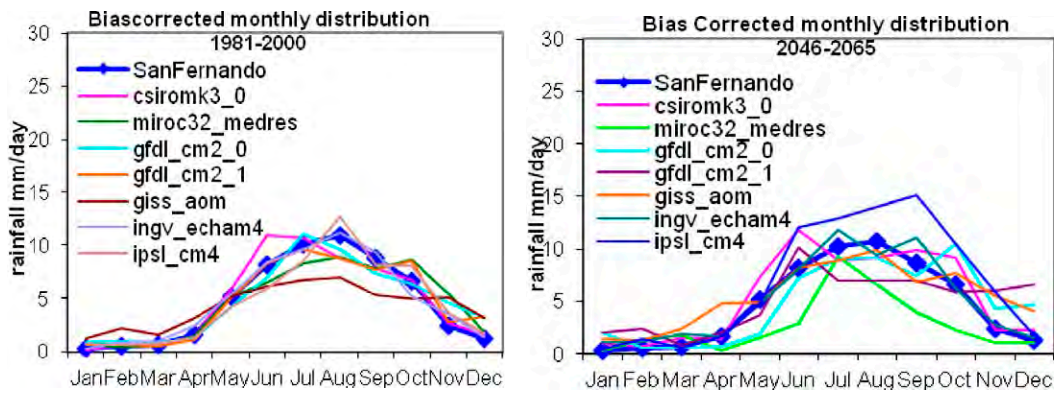


Figure 2.3-28. Bias Corrected past (1981-2000) and future (2046-2065) for San Fernando station.

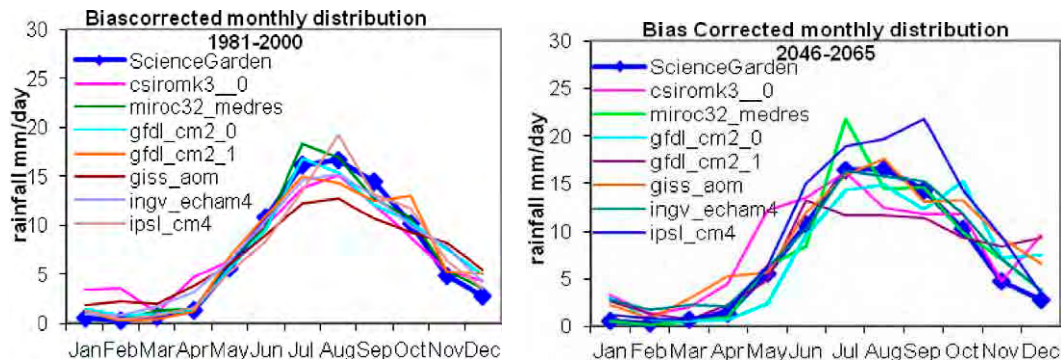


Figure 2.3-29. Bias Corrected past (1981-2000) and future (2046-2065) for Science Garden station.

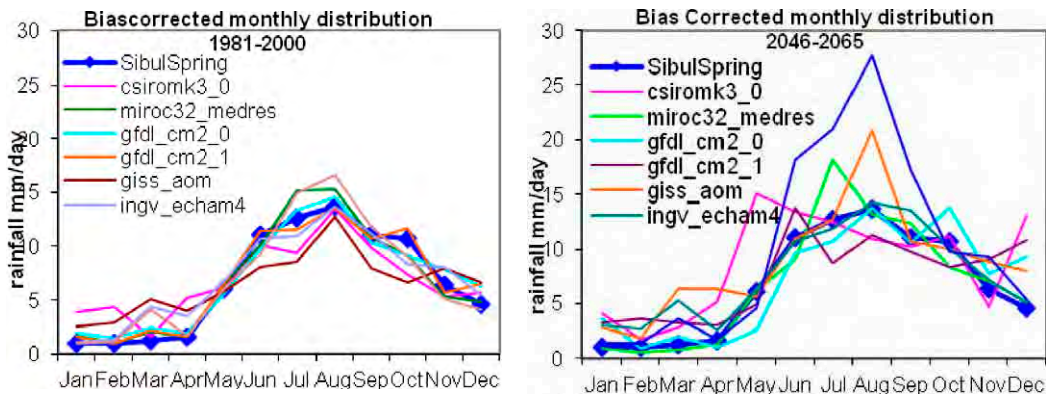


Figure 2.3-30. Bias Corrected past (1981-2000) and future (2046-2065) for Sibul Spring station.

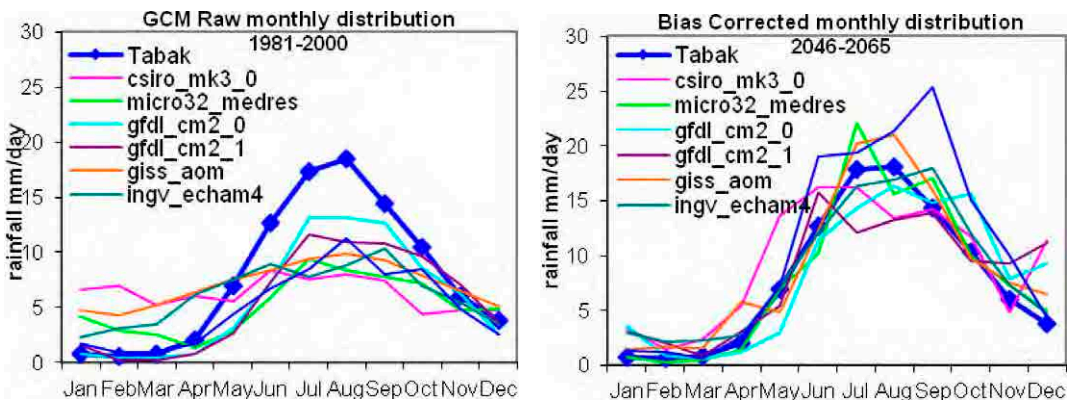


Figure 2.3-31. Bias Corrected past (1981-2000) and future (2046-2065) for Tabak station.

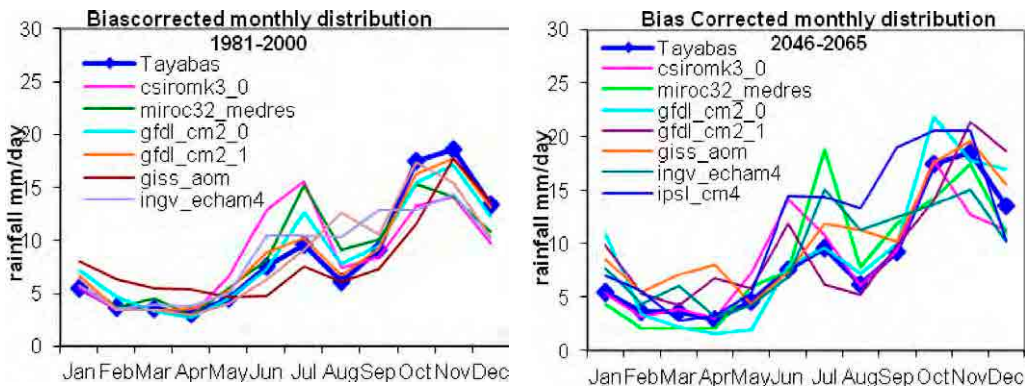


Figure 2.3-32. Bias Corrected past (1981-2000) and future (2046-2065) for Tayabas station.

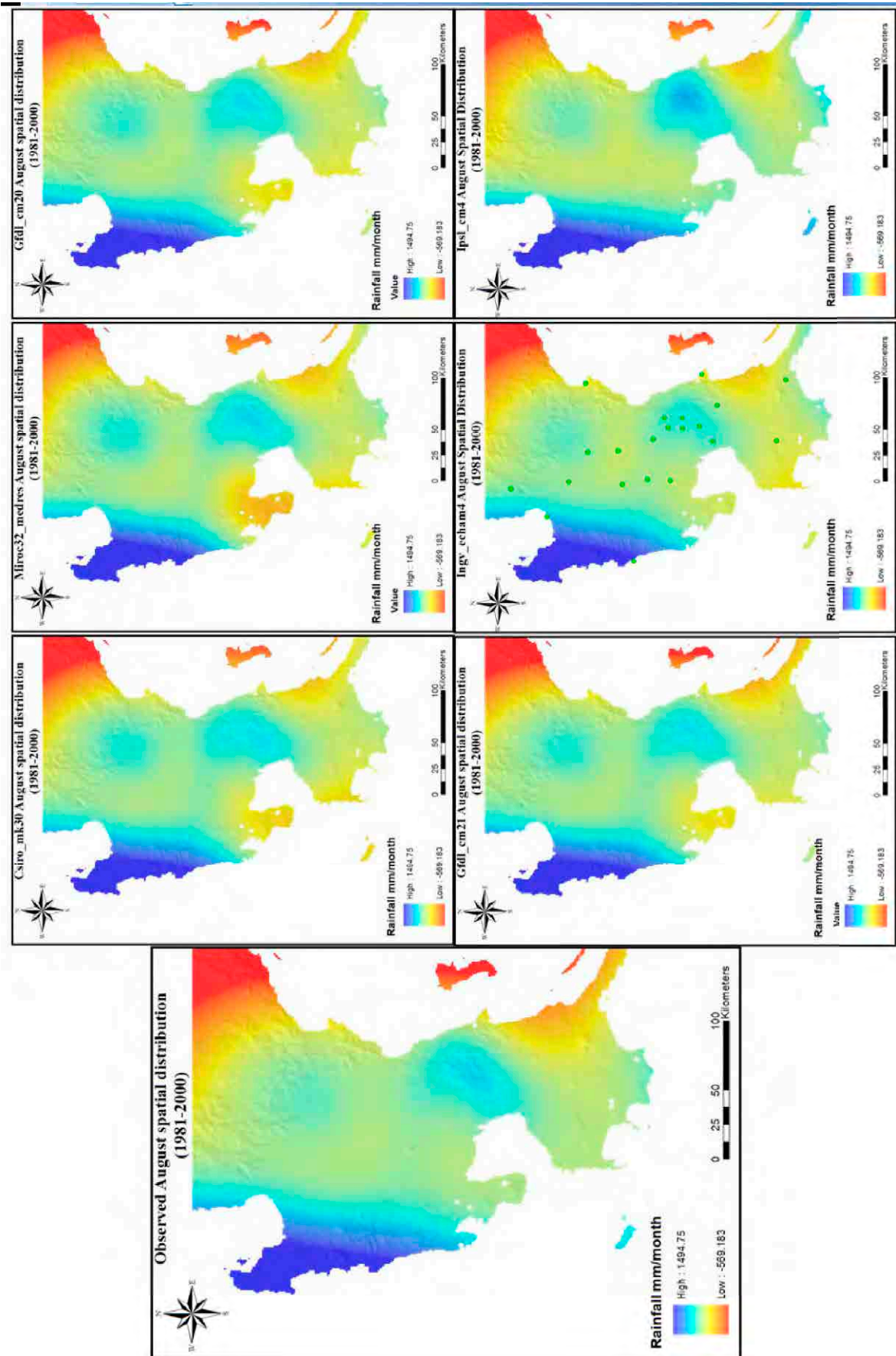
## **2.4 Spatial Downscaling of Rainfall**

Spatial Downscaling was done by correcting the biases on each of the 21 rainfall gauge data distributed throughout the Study area.

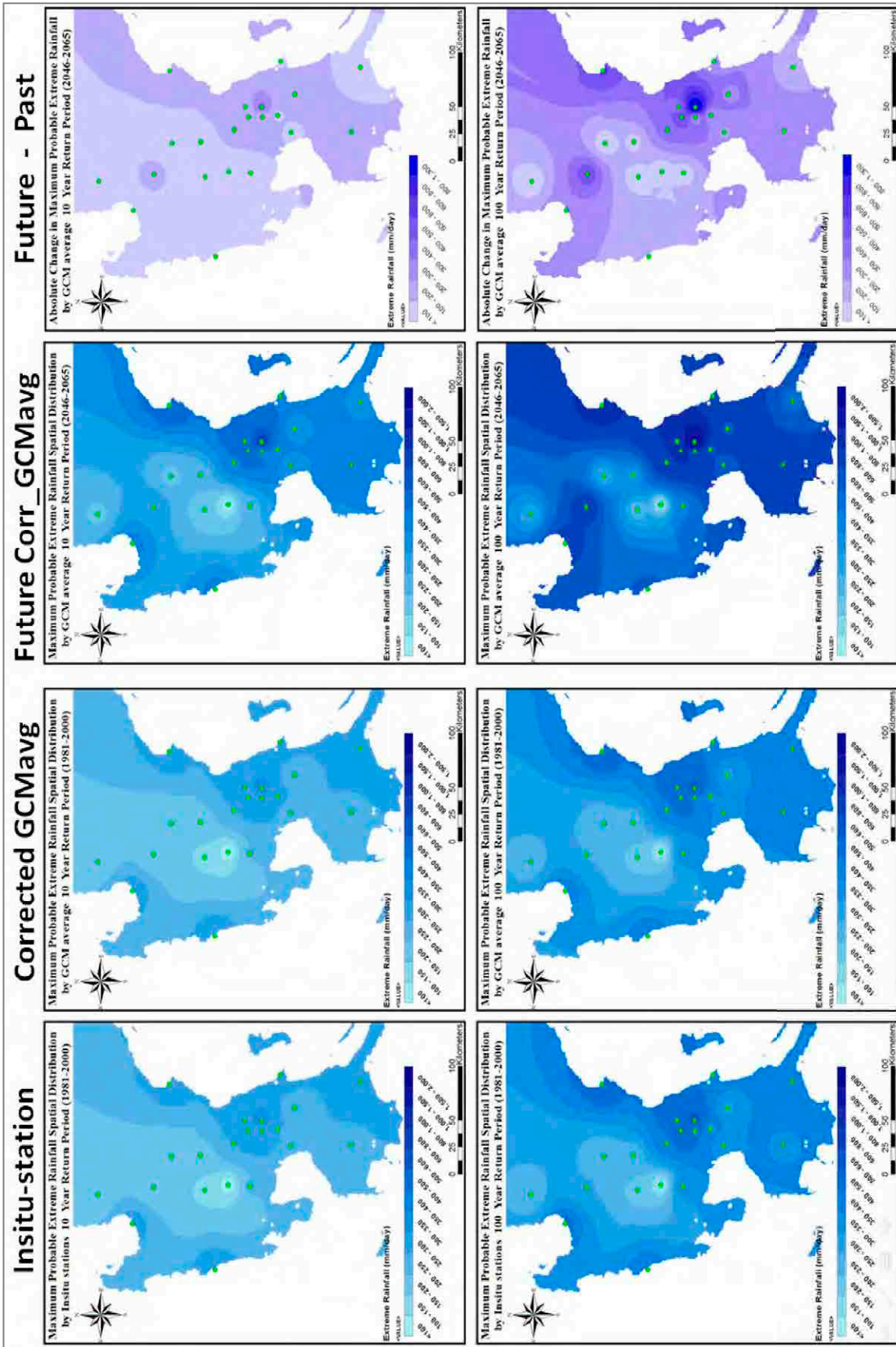
A comparison (**Figure 2.4-1**) of the spatial rainfall distribution for the August climatology for past observed gauge data and the 21 bias corrected points for the selected 6 models show that the spatial distribution of all 6 models are almost identical with that of observed data for 1981-2000. Although there is still large uncertainty on the predictability of future climate, the results from this statistical bias correction of past GCM rainfall gives us more confidence that the method can correct GCM datasets that will produce conditions very similar to past events. Hence, using the same bias correction method on future GCM predictions will reduce the uncertainty of the future and give us a prediction that will show us a better glimpse of the future.

The 10-year and 100-year return periods for extreme rainfall events are given in **Figure 2.4-2** for the spatial distribution of a.) Average In-situ station data; corrected GCM average data for b.) Past and c.) Future, and the d.) Absolute differences between the future and past. The largest differences occur in the western side of Metro Manila corresponding to stations within Angat and Kaliwa basin as well as the upstream portion of Pampanga river basin.





**Figure 2. 4-1.** Sample spatial distribution for the average August rainfall in comparison with the average August rainfall from the corrected 6 GCMs.



**Figure 2.4-2.** In-situ, Corrected GCM average, Future corrected GCM average and absolute change (future – past) for 10 year (upper figures) and 100 year (lower figures) return period.

## 2.5 Climate Change Impact Assessment in the Target Year of 2040

The target projection year of this study is 2040. Rainfall data for the period from 2031 to 2050 was used to represent 2040. However, future simulated daily data set are available for only from 2046 to 2065 for most of GCMs. There are 2 GCMs with available daily data from 2021 to 2050. The period of daily data availability of GCMs are listed in **Table 2.5-1** for CMIP3 (Coupled Model Inter-comparison Project) SRESa1b and shown in **Figure 2.5-1** for 2000-2065.

**Table 2.5-1.** List of daily datasets available on CMIP3 SRESA1B GCMs.

<b>Model</b>	<b>Time slices available</b>
bccr_bcm2_0	2056-2065 / 2081-2100
cccma_cgcm3_1	2046-2065 / 2081-2100 / 2181-2200 / 2281-2300
cccma_cgcm3_1_t63	2046-2065 / 2081-2100 / 2181-2200
cnrm_cm3	2046-2065 / 2081-2100 / 2181-2200 / 2281-2300
csiro_mk3_0	2046-2065 / 2081-2100 / 2181-2200
csiro_mk3_5	2001-2200 / 2281-2300
gfdl_cm2_0	2046-2065 / 2081-2100 / 2181-2200 / 2281-2300
gfdl_cm2_1	2046-2065 / 2081-2100 / 2181-2200 / 2281-2300
giss_aom	2046-2065 / 2081-2100
giss_model_e_r	2046-2065 / 2081-2100 / 2181-2200 / 2281-2300
iap_fgoals1_0_g	2046-2100 / 2181-2200
ingv_echam4	2046-2065 / 2081-2100
inmcm3_0	2046-2125
ipsl_cm4	2046-2065 / 2081-2100 / 2181-2200
miroc3_2_hires	2046-2065 / 2081-2100
miroc3_2_medres	2046-2065 / 2081-2100 / 2181-2200 / 2281-2300
miub_echo_g	2046-2065 / 2081-2100 / 2181-2200 / 2281-2300
mpi_echam5	2046-2065 / 2081-2100 / 2181-2200 / 2281-2300
mri_cgcm2_3_2a	2046-2065 / 2081-2100 / 2181-2200 / 2281-2300
ncar_ccsm3_0	2000-2099
ncar_pcm1	2046-2065 / 2080-2099

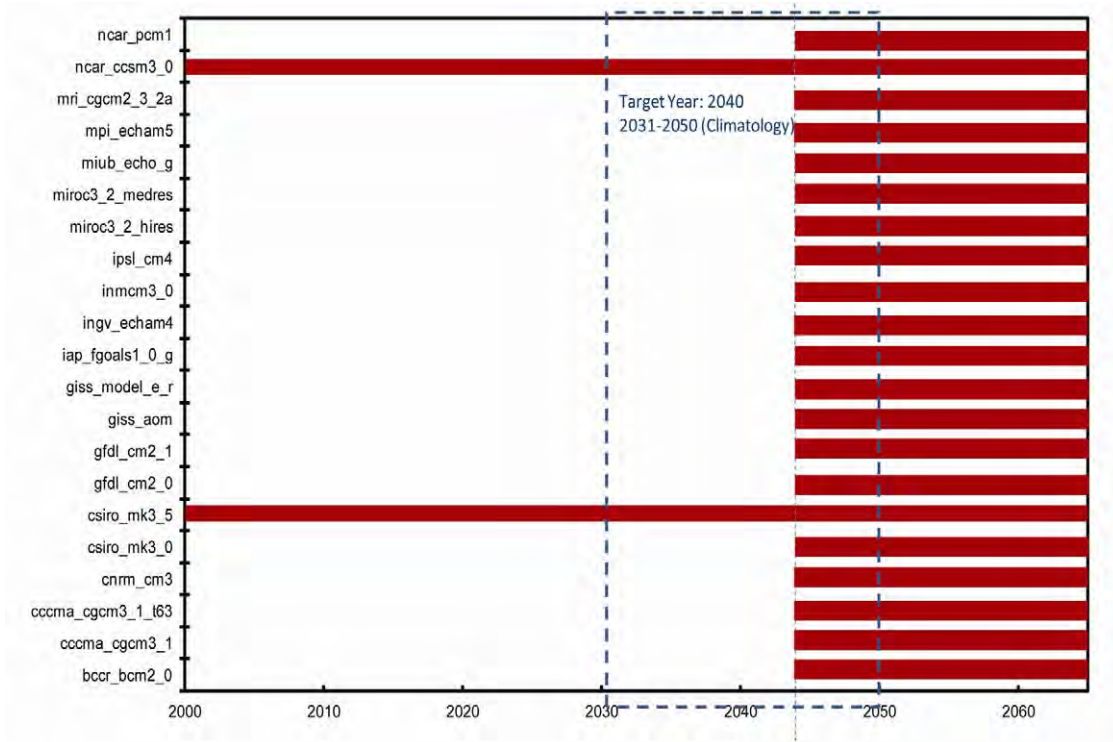


Figure 2.5-1. Availability of Daily Data Set on CMIP3 and the Target Year of This Study.

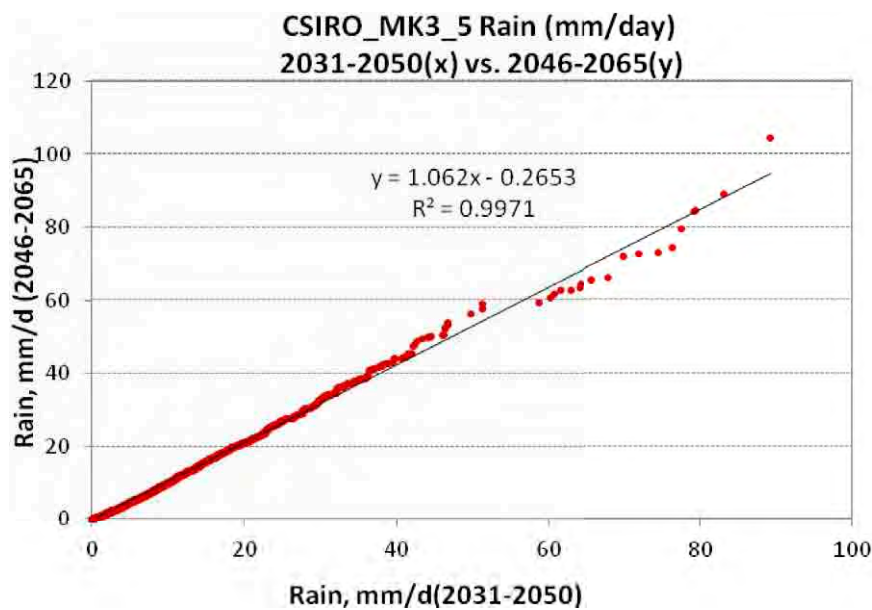
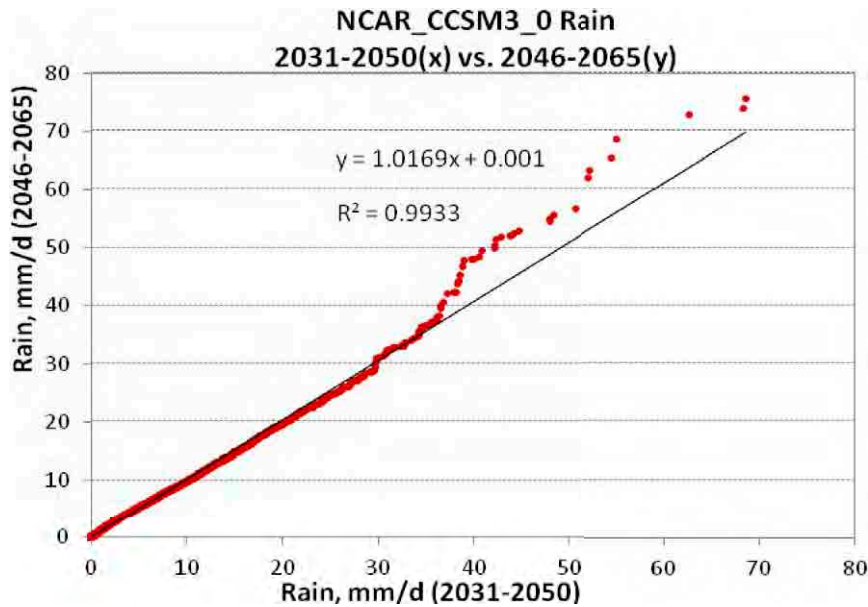


Figure 2.5-2. Comparison of 2031-2050 versus 2046-2065 daily rainfall of csiro\_mk3\_5 in Angat Station.

First, the climatology of the period 2031-2050 and 2046-2065 was compared using the data set of the GCM csiro\_mk3\_5 and near\_ccsm3\_0, whose data set for the period of 2031-2050 is available.



The daily datasets are ranked from highest to lowest values for 2031-2050 and 2046-2065. These are plotted in x-y scatterplots (x-axis for 2031-2050 and y-axis for 2046-2065). Simple linear regression was utilized to determine if there is a significant difference between the time slice 2031-2050 and 2046-2065. This difference is used to adjust the recommended projections from 2046-2065 (either reduced or increased) so it can be used for 2040.



**Figure 2.5-3.** Comparison of 2031-2050 versus 2046-2065 daily rainfall of near\_ccsm3\_0 in Angat Station.

From the csiro\_mk3\_5 daily rainfall data (**Figure 2.5-2**), the time slice from 2046-2065 is higher by 6.2% as compared to the 2031-2050 time slice with a correlation coefficient ( $R^2$ ) of 0.9971. However, for near\_ccsm3\_0 daily rainfall data (**Figure 2.5-3**), the time slice 2046-2065 is higher by 1.02% with a correlation coefficient ( $R^2$ ) of 0.9933. The high correlation coefficients in the two models indicate that there is very high correlation between 2046-2065 and 2031-2050 datasets.

To estimate the projections for the year 2040, results from the simulations should be reduced by around 1.02% to 6.2% to account for this difference. This result will be used in the Water Balance Study following this Study.



## **CHAPTER 3 Hydrological Model Simulations**

### **3.1 Hydrological Model Development and River Runoff Simulations**

Global climate changes have significant effects on regional river runoff and water availability, the most important factors for water resource managers and policy makers. It has been reported that by 2050 drought-affected areas will likely increase in some water-stressed regions, while flood risks are likely to increase in some wet areas. Under these circumstances, it is critical to integrate knowledge regarding the atmospheric science and hydrology for improved capability for prediction of available water resources and possible hazards (floods and droughts). Distributed Hydrological Models (DHMs) can provide a distributed representation of the spatial variation and physical descriptions of runoff generation and routing in river channels from basin to continental scales. It is critically important to simulate regional or basin-scale surface soil moisture distribution and to improve river discharge. The spatial distribution of land surface wetness has been recognized as one of the most important factors representing floods, droughts, and land surface heterogeneity, which can significantly affect energy and water fluxes. Moreover, the DHM to be used in the Study should have an optimization function for operation of existing and planned water resources management facilities.

The WEB-DHM was developed by fully coupling a biosphere scheme (SiB2) with a geomorphology-based hydrological model (GBHM). The model enabled consistent descriptions of water, energy and CO<sub>2</sub> fluxes at the basin scale (Wang et al., 2009a, 2009b). The characteristics of the WEB-DHM are summarized as follows:

- The model physically describes ET using a biophysical land surface scheme for simultaneously simulating heat, moisture, and CO<sub>2</sub> fluxes in the soil-vegetation-atmosphere transfer (SVAT) processes.
- The hydrological sub-model describes overland, lateral subsurface, and groundwater flows using grid-hill slope discretization followed by flow routing in the river network.
- The model has high efficiency for simulations of large-scale river basins while incorporating sub grid topography and effects of water resources management facilities.

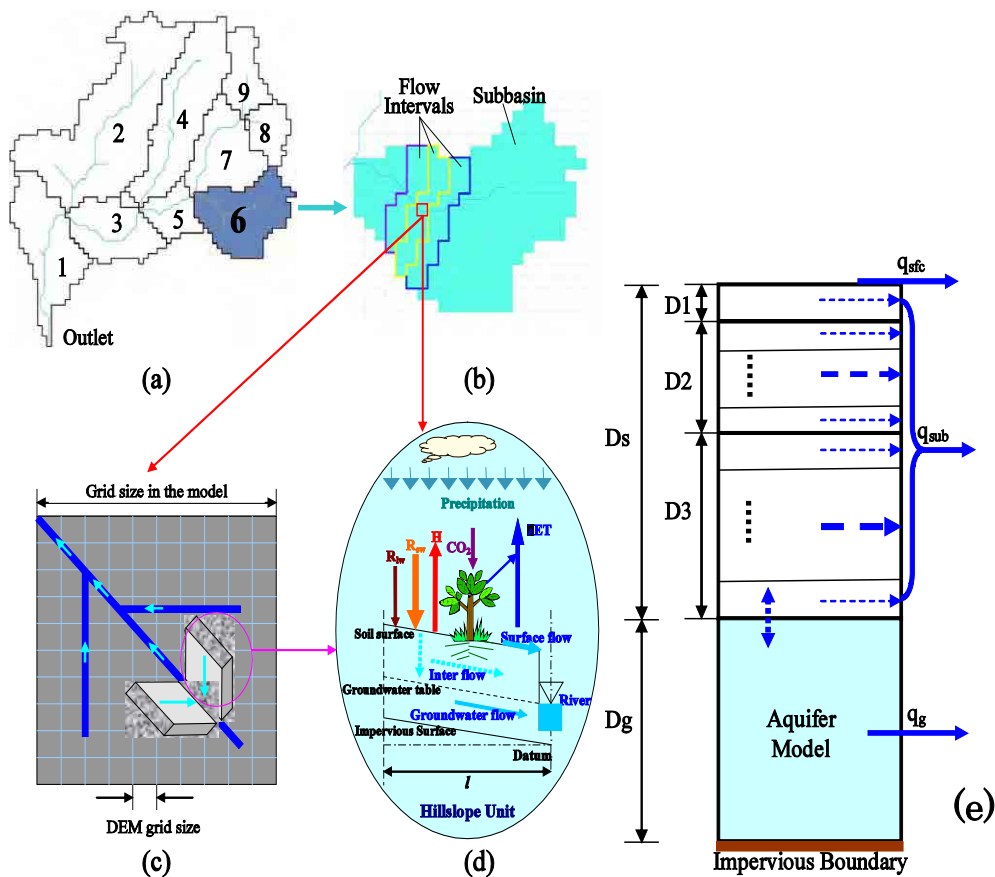
Due to the possible limitation of in-situ data availability, it is necessary to consider satellite-based rainfall products, which can be widely applied to catchment-scale impact studies.

Satellite-based low-frequency microwave brightness temperature is strongly affected by near-surface soil moisture; therefore, it can be assimilated into a land surface model to improve modeling of soil moisture and the surface energy budget. The Study uses the Land Data Assimilation System developed by the University of Tokyo (LDAS-UT) (Yang, K., 2007), to estimate the soil moisture and surface temperature. The LDAS-UT consists of a land surface model (LSM) used to calculate surface fluxes and soil moisture, a radiative transfer model (RTM) to estimate the microwave brightness temperature, and an optimization scheme to search for optimal values of soil

moisture by minimizing the difference between modeled and observed brightness temperatures.

### 3.2 Model Structure

Although improvements over the lumped hydrological models have been made by representing the spatial heterogeneity, DHMs have large uncertainties when used to simulate water exchanges at the soil-atmosphere interface and the time evolution of surface soil moisture owing to the conceptual treatment of the land surface. In most current Land Surface Models (LSMs) (e.g., SiB2), lateral soil moisture redistributions due to topographically driven runoff are usually not well formulated since they were originally developed for application in general circulation models (GCMs).



**Figure 3.2-1.** The WEB-DHM. a.) division from a basin to sub-basins, b.) subdivision from a sub-basin to flow intervals comprising several model grids, c.) discretization from a model grid to a number of geometrically symmetrical hillslopes, d.) process descriptions of water moisture transfer from the atmosphere to river and e.) soil layers coupled with aquifer model in WEBDHM. (Wang et al., 2009a, 2009b)

The coupling of LSMs and DHMs has the potential to improve the land surface representation, benefiting the streamflow prediction capabilities of the hydrological models and providing improved

estimates of water and energy fluxes into the atmosphere.

A distributed biosphere hydrological model, the water and energy budget-based distributed hydrological model (WEB-DHM), has been developed by fully coupling a biosphere scheme (SiB2) with a geomorphology-based hydrological model (GBHM). SiB2 describes the transfer of turbulent fluxes (energy, water, and carbon fluxes) between the atmosphere and land surface for each model grid. The GBHM redistributes water moisture laterally through simulation of both surface and subsurface runoff using grid-hill slope discretization and then flow routing in the river network.

The overall model structure is shown in **Figure 3.2-1** and can be described as follows.

- i. A digital elevation map (DEM) is used to define the target area, after which the target basin is divided into sub basins (see **Figure 3.2-1a**).
- ii. Within a given sub basin, a number of flow intervals are specified to represent time lag and accumulating processes in the river network according to the distance to the outlet of the sub basin. Each flow interval includes several model grids (see **Figure 3.2-1b**).
- iii. For each model grid with one combination of land use type and soil type, the SiB2 is used to calculate turbulent fluxes between the atmosphere and land surface independently (see **Figures 3.2-1b** and **3.2-1d**).
- iv. The GBHM is used to calculate the runoff from a model grid with a sub grid parameterization. Each model grid is subdivided into a number of geometrically symmetrical hill slopes (see **Figure 3.2-1c**), which are the basic hydrological units (BHUs) of the WEB-DHM. For each BHU, the GBHM is used to simulate lateral water redistributions and calculate runoff (see **Figures 3.2-1c** and **3.2-1d**). The runoff for a model grid is the total response of all BHUs in it.
- v. For simplicity, the streams located in one flow interval are lumped into a single virtual channel in the shape of a trapezoid. All flow intervals are linked by the river network generated from the DEM. All runoff from the model grids in the given flow interval is accumulated into the virtual channel and led to the outlet of the river basin.

### **3.3 Input Data**

#### **3.3.1 Static Parameters**

The digital elevation map (DEM) was based on the 90-m Shuttle Radar Topography Mission (SRTM) Digital Elevation Database V4.1 produced by NASA but processed by the Consultative Group of International Agricultural Research Consortium for Spatial Information (CGIAR-CSI) (source: <http://srtm.csi.cgiar.org/>). This DEM has been re-projected from geographic to Universal Transverse Mercator (UTM) coordinate system (zone 51) and re-sampled to 500m x 500m grid size. Local land use map was reclassified into the SiB2 land use classification (**Table 3.3-1**) and re-sampled to 500m x 500m grid (**Figure 3.3-1**). The assumption is that each grid has a

homogeneous land use.

The local soil map was also used and reclassified to FAO classification (**Table 3.3-2**) then resampled to 500m x 500m grid as well (**Figure 3.3-2**). Each grid has a homogeneous soil type. The area distributions of different types of land cover and soil are represented using one-dimensional functions with respect to flow distance from the outlet. In a flow interval at any flow distance, the area fraction of each land cover (and soil) type is known. For representation of the heterogeneity of land cover and soil inside a hillslope, one hillslope is divided into a number of small elements along the slope direction. Each element corresponds to one type of land use-soil combination, which is the simulation unit of the unsaturated zone. The top soil is considered as the unsaturated zone, and the maximum depth of the unsaturated zone is around 4 meters. Below the top soil, the minimum simulation unit of the unconfined aquifer is the whole hillslope above the impermeable bed rock, which is the common groundwater storage of all elements in this hillslope.

Non-uniform vertical distribution of soil water property of root zone is represented assuming an exponentially decreasing function (Robinson and Sivapalan, 1996; Singh et al., 2002):

$$K_s(z) = K_0 \exp(-fz) \quad (\text{eq. 7})$$

Where  $K_s(z)$  is the saturated hydraulic conductivity,  $z$  is the distance taken positive in downward direction normal to surface,  $K_0$  is the saturated hydraulic conductivity of the surface soil,  $f$  is a constant parameter. Many soils, especially forest soils are anisotropic with a higher conductivity parallel to the hillslope. For such soils, an anisotropy ratio can be defined as (Jackson, 1992; Singh et al., 2002):

$$r_a = \frac{K_{sp}}{K_{sn}} \geq 1 \quad (\text{eq. 8})$$

Where  $r_a$  is the anisotropy ratio,  $K_{sp}$  and  $K_{sn}$  is the saturated hydraulic conductivity in the directions normal (n) and parallel (p) to the slope respectively.

These soil parameters were taken from the FAO global soil dataset. Soil parameterization at each basin was done by applying factors to the saturated hydraulic conductivity at the soil surface, the hydraulic conductivity decay factor, hydraulic conductivity in groundwater, manning's roughness for each sub-basin, and the soil anisotropic ratio for each sub-basin.

**Table 3.3-1** Reclassification of Philippine local land use to SiB2 classification.

<b>Local Land Use Classification</b>	<b>SiB2 Reclassification</b>
--	1-Broadleaf Evergreen Trees
Closed Forest, Broadleaved Open Forest, Broadleaved Mangrove forest	2-Broadleaf Deciduous Trees
Open forest mixed Closed forest mixed	3-Broadleaf and Needleleaf trees
Closed forest coniferous Bamboo Formation	4-Needleleaf evergreen trees
	5-Needleleaf deciduous trees
Natural, grassland	6-Short vegetation/C4 grassland
Built up area Natural, Barren land Woodland, fallow	7-Shrubs with bare soil
Wood land, shrubs	8-Dwarf trees and Shrubs
Cultivated, annual crop Wooded land, wooded grassland Cultivated perennial crop	9-Agriculture or C3 Grasslands
Fishpond Inland Water	10-Water, wetlands

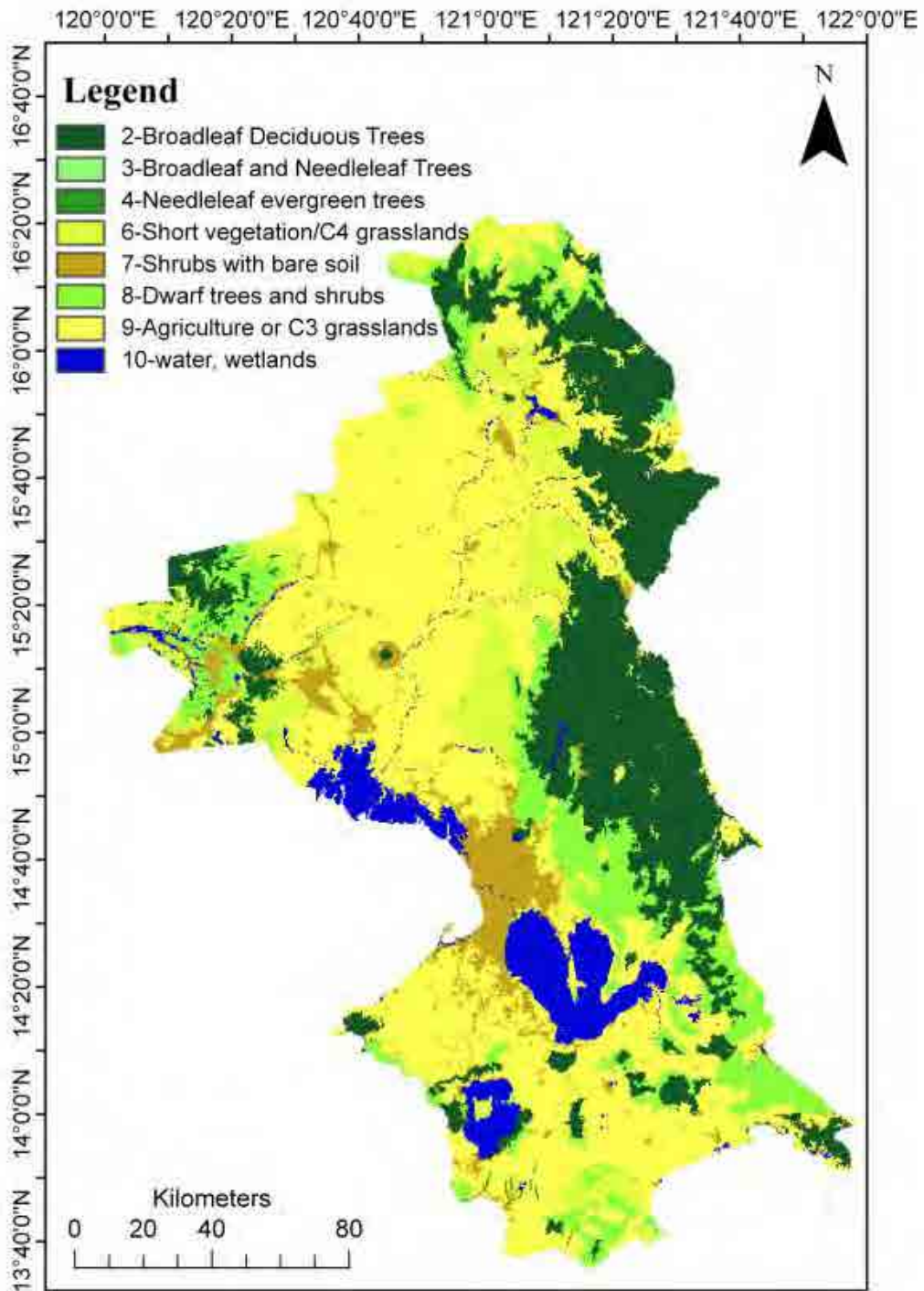


Figure 3.3-1. Local land use map reclassified to SiB2 land use classification.

**Table 3.3-2** USDA 1975 Local soil classification reclassified to FAO soil classification.

<b>USDA 1975; Local soil classification</b>	<b>Soil Class (FAO)</b>	<b>FAO number</b>	<b>% Sand</b>	<b>% Silt</b>	<b>% Clay</b>	<b>Soil Type</b>
Lake,Laguna de Bay,Taal Lake	Water	0	--	--	--	--
Tropudults w/Tropudalfs, Tropepts & Oxisols	NITOSOLS	4413	44.781	22.9154	32.3035	Clay loam
MOUNTAIN SOILS W/ENTISOLS, INCEPTISOLS, ULTISOLS AND ALFISOLS W/THERMIC HYPERThERMIC AND ISOHYPERThERMIC TEMPERATURE REGIMES	ACRISOLS	4465	48.5151	21.7678	29.717	Clay loam
ENTROPEPTS W/DYSTROPEPTS	CAMBISOLS	4478	40.933	25.5137	33.5533	Clay loam
TROPAQUEPTS W/HYDRAQUENTS	GLEYSOLS	4503	64.7694	13.631	21.5997	Sandy clay loam
TROPUDALFS W/TROPEPTS	GLEYSOLS	4504	44.0539	22.9231	33.0231	Clay loam
PELLUSTERTS W/UDALFS, UDORTHENTS AND TROPEPTS; TROPAQUEPTS W/ENTROPEPTS	LUVISOLS	4537	46.47	23.01	30.52	Sandy clay loam
Contested_Area	NITOSOLS	4546	37.6113	24.3273	38.0614	Clay loam
TROPOPSAMMENTS W/TROPORTHENTS	ARENOSOLS	4564	70.002	15.2282	14.7698	Sandy loam
CHROMUSTERTS W/UDALFS, UDORTHENTS AND TROPEPTS	VERTISOLS	4582	28.3164	21.8532	49.8304	Clay
EUTRANDEPTS W/EUTROPEPTS	VERTISOLS	4589	39.5765	15.5437	44.8798	Clay

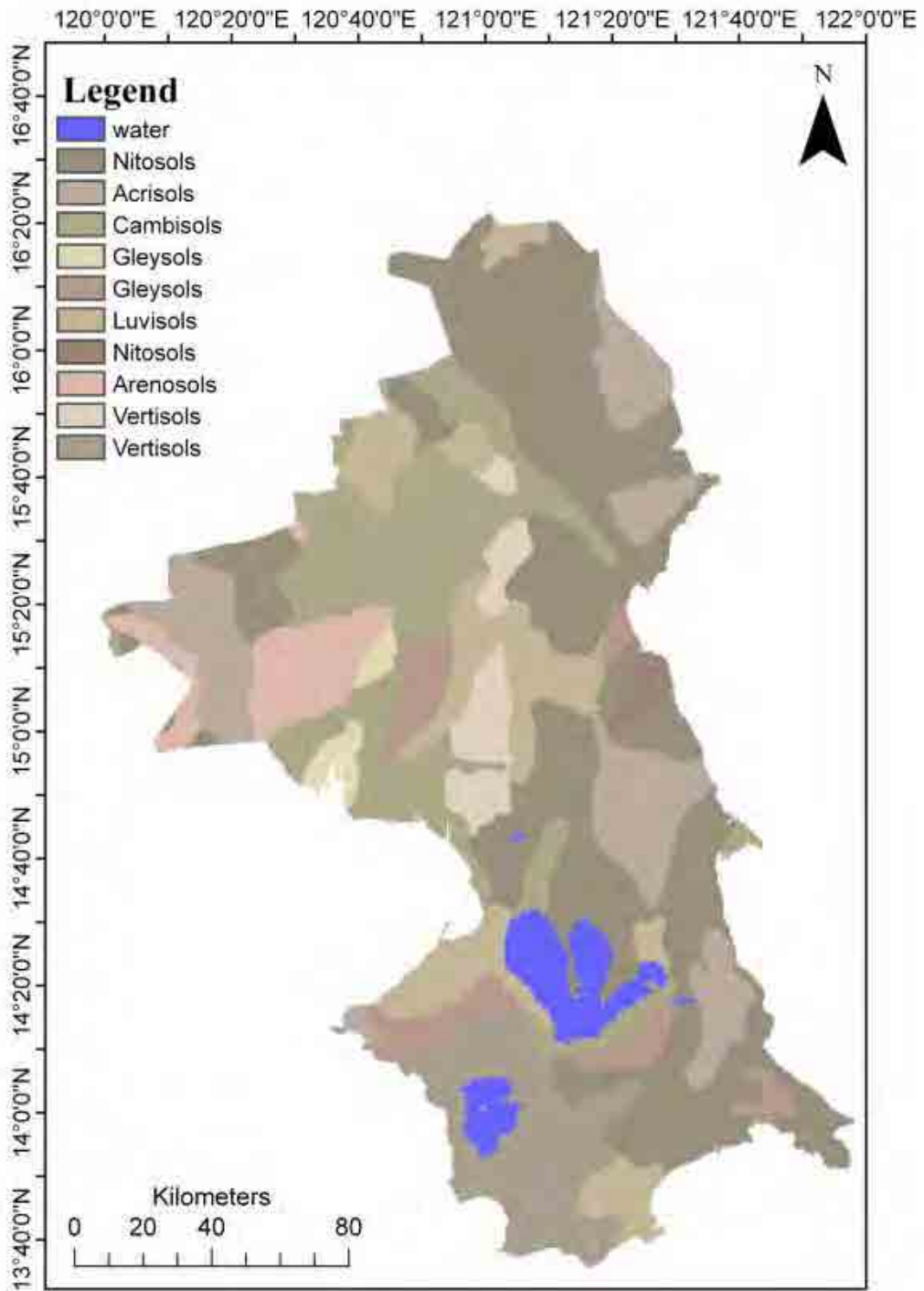


Figure 3.3-2. Local soil map (USDA 1975 classification) reclassified to FAO soil classification.



### **3.3.2 Dynamic Parameters**

The meteorological parameters were taken from both the local meteorological gauges (12 gauges) (surface air temperature (K); relative humidity (%); total cloud cover (%); Downward long wave and short wave radiation flux at surface ( $W/m^2$ )). The downward solar radiation was estimated from sunshine duration, temperature and humidity using a hybrid model developed by Yang et al. (2006). The longwave radiation was estimated from temperature, relative humidity, pressure and solar radiation using the relationship between solar radiation and longwave radiation (Crawford and Duchon, 1999). Rainfall was taken from daily data in 12 meteorological gauge stations and 35 synoptic stations. These were spatially distributed and downscaled by inverse distance weighing interpolation (IDW).

From the Japan Reanalysis data (JRA-25), (surface pressure (Pa); surface 10m zonal wind (m/s) and surface 10m meridional wind (m/s)).

#### **3.3.2.1 Temporal Downscaling of Observed Rainfall Data**

The observed rainfall data collected from the Philippines is mostly in daily time scale. However, for the runoff model, the hourly rainfall data is preferable in general since in tropical regions such as the Philippines, there is a significant periodical rainfall cycle during the day. The diurnal cycle is applied for rainfall with intensities 0-50mm/day, 50-100mm/day, 100-250mm/day and above 250mm/day based on some stations with available hourly data. Since the available hourly rainfall in Luzon is limited to a few gauges only, the average ratio of hourly rainfall to total daily rainfall from the first hour to the twenty-fourth hour was calculated for the different rainfall intensities.

To illustrate, given five samples of daily rainfall with equal or above 250mm/day (250 mm/day, 255 mm/day, 256 mm/day, 257 mm/day, 258mm/day). If the first hour of each of the five values are 5mm/hour, 10mm/hour, 15mm/hour, 20mm/hour and 30 mm/hour, then the average ratio for the first hour is  $[5/250+10/255+15/256+20/257+30/258]/5$  values = 0.062. This method is utilized for the rainfall intensity ranges: 0-50mm/day, 50-100mm/day, 100-250mm/day, and above 250 mm/day for each hour. The average intensity ratio per hour is multiplied to the available daily rainfall data for each gauge belonging to that range. This simplification is one of the current limitations of this study since rainfall throughout the country does not necessarily follow a unique temporal pattern. Hence, for the analysis of the simulations, only daily outputs are presented.

The ratio used for diurnal variation of the different rainfall intensities using hourly rainfall record of Pampanga basin are given in **Figure 3.3-3**. The highest rainfall intensities usually occur in the afternoon until late in the evening which is somewhat what is commonly observed especially during the wet season and in upland areas in the country.

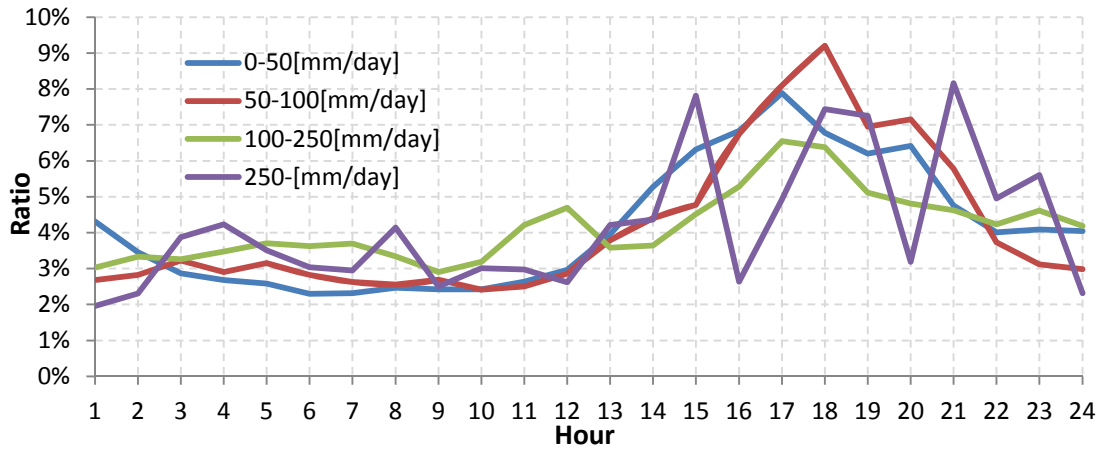


Figure 3.3-3. Diurnal variation used for different intensities.

The WEB-DHM is a grid based distributed model and the model can reflect the distribution of the rainfall in the discharge. The gridded rainfall was developed by Nippon Koei team using spatial interpolation technique from the ground station data. The inverse distance weighted (IDW) interpolation technique was applied for this purpose with a weighting factor of 2.

### 3.3.2.2 Temporal Downscaling of Observed Temperature Data

Hourly temperature data were interpolated from daily maximum and minimum data based on the TM model (Figure 3.3-4) proposed by Cesaraccio et al., (2001).

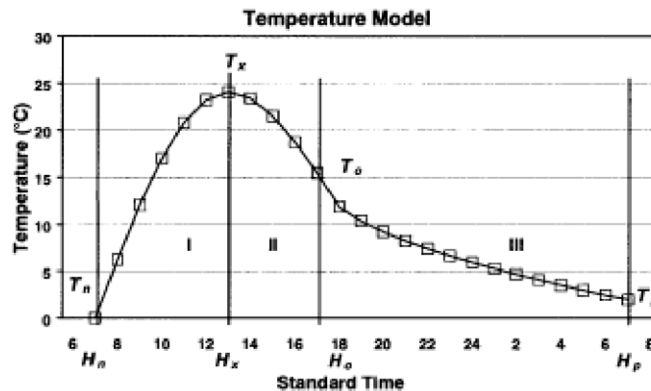


Figure 3.3-4. Example of Hourly Temperature Calculation by the TM Model.

The procedure of the temporal interpolation of the TM model is described as follows:

$$T(t) = \begin{cases} T_n + \alpha \sin \left[ \left( \frac{t - H_n}{H_x - H_n} \right) \frac{\pi}{2} \right]; H_n < t \leq H_x \\ T_o + R \sin \left[ \frac{\pi}{2} + \left( \frac{t + H_x}{4} \right) \frac{\pi}{2} \right]; H_x < t \leq H_p \\ T_o + b\sqrt{t - H_o}; H_o < t \leq H_p \end{cases} \quad (\text{eq.9})$$

$$T_o = T_x - c(T_x - T_p) \quad (\text{eq.10})$$

$$\alpha = T_x - T_n \quad (\text{eq.11})$$

$$R = T_x - T_o \quad (\text{eq.12})$$

- 1) Divide the day in to three segments: from the sunrise hour ( $H_n$ ) to the time to maximum temperature ( $H_x$ ), from  $H_x$  to the sunset hour ( $H_o$ ) and from  $H_o$  to the sunrise hour for the next day ( $H_p$ ).
- 2) The model uses two sine-wave functions in the daylight and a square-root decrease in temperature at night.
- 3)  $H_n$  and  $H_o$  are determined as a function of the site latitude and the day of the year.  $H_p$  is calculated as  $H_p = H_n + 24$ .
- 4) The time of the maximum temperature is set 4 hours before sunset ( $H_x = H_o - 4$ )

Generally, the spatial distribution of surface temperature is not very localized. However, it is dominated by surface elevation. The assumed temperature lapse rate of 0.6 °C per 100m elevation was applied in this study. The procedures of the gridded temperature data generation are as follows:

- 1) Select four nearest stations to the target grid point which has the valid data for the target date.
- 2) Obtain the elevation of the target grid point DEM data, here  $Z_{grid}$  [El.m] is the elevation.
- 3) Correct the temperature of surrounding stations ( $T_{i\_observed}$ ) at the elevation of the target grid ( $Z_{grid}$ ) from the elevation of the station locates ( $Z_i$ ) using the temperature lapse rate;

$$T_{i\_corrected} = T_{i\_observed} + 0.006(Z_i - Z_{grid}) \quad (\text{eq.13})$$

- 4) The temperature of the target grid ( $T_{grid}$ ) is obtained by the spatial interpolation method: IDW, the temperature data ( $T_{i\_corrected}$ ) of 4 nearest stations corrected to the elevation of the target grid;

$$T_{grid} = \frac{\sum_{i=1}^4 \frac{T_{i\_corrected}}{l_i}}{\sum_{i=1}^4 \frac{1}{l_i}} \quad (\text{eq.14})$$

where,  $l_i$ : distance from the station  $i$  to the target grid.

### 3.3.2.3 Photosynthetic Activity Considered with LAI and FPAR

Other dynamic parameters considered in the study are the Leaf Area Index (LAI) and Fractional Photosynthetically Active Radiation (FPAR) are biophysical variables which describe canopy structure and are related to functional process rates of energy and mass exchange. These parameters were used to account for the photosynthetic activity within the basin. FPAR measures the proportion of absorbed photosynthetic active radiation that a canopy absorbs for photosynthesis and growth (400-700 nm spectral range). LAI is the biomass equivalent of FPAR and is also dimensionless ( $m^2/m^2$ ) of leaf area covering a unit of ground area. This is the ratio of total upper leaf surface of vegetation divided by the surface area of the land on which vegetation grows (range from 0 for bare ground to 6 for a dense forest). Monthly datasets from the AVHRR (the Advanced Very High Resolution Radiometer; resolution: 16km x 16km grid) were used for simulations from 1980-2000 and 8-day MODIS datasets for simulations from 2001-2009.

After incorporating together all the necessary inputs and outputs of the WEBDHM, the model is debugged for errors and run for selected calibration years.

### 3.4 Hydrological Model Development and Parameter Tuning

Calibration of the outputs was done by comparing simulated daily discharges with observed streamflow or dam inflows. The Nash coefficient (NS) and the relative error (RE) were used to compare observed and simulated discharges. The equations are given below.

$$NS = 1 - \frac{\sum_{i=1}^N (Q_{oi} - Q_{si})^2}{\sum_{i=1}^N (Q_{oi} - \bar{Q}_{oi})^2} \quad (\text{eq.15})$$

$$RE = \frac{\sum_{i=1}^N (Q_{si} - Q_{oi})}{\sum_{i=1}^N Q_{oi}} \quad (\text{eq.16})$$

For NS and RE equations above,  $Q_{oi}$  is observed daily discharge,  $Q_{si}$  is simulated daily discharge,  $\bar{Q}_{oi}$  is the average of all the daily observed discharge. A summary of the calibration locations and the selected years for each of the basins are given in **Figure 3.4.1** including specific land uses for each of the 3 basins. The characteristics of Angat and Kaliwa and very similar forested areas while Pampanga is dominated by agricultural land use. The corresponding upstream drainage area for each of the calibrated gauge locations are also included in this figure summary. Drainage area for Pantabangan dam is 1179.25 km<sup>2</sup> (dependent on digital elevation map so upstream political boundary draining to the other side of the Cordillera mountain range is excluded); Cabanatuan

upstream drainage area is 1965.25 km<sup>2</sup>; Zaragosa upstream drainage area is 4437.75 km<sup>2</sup>; San Isidro upstream drainage area is 5428.5km<sup>2</sup>; Arayat upstream drainage area is only within the sub-basin for Arayat = 90.75 km<sup>2</sup>; and upstream drainage area above Angat dam is 712.25 km<sup>2</sup>. Specific details on the basin geophysical and hydrologic characteristics, calibrations and validations of each basin are given in the succeeding sections.

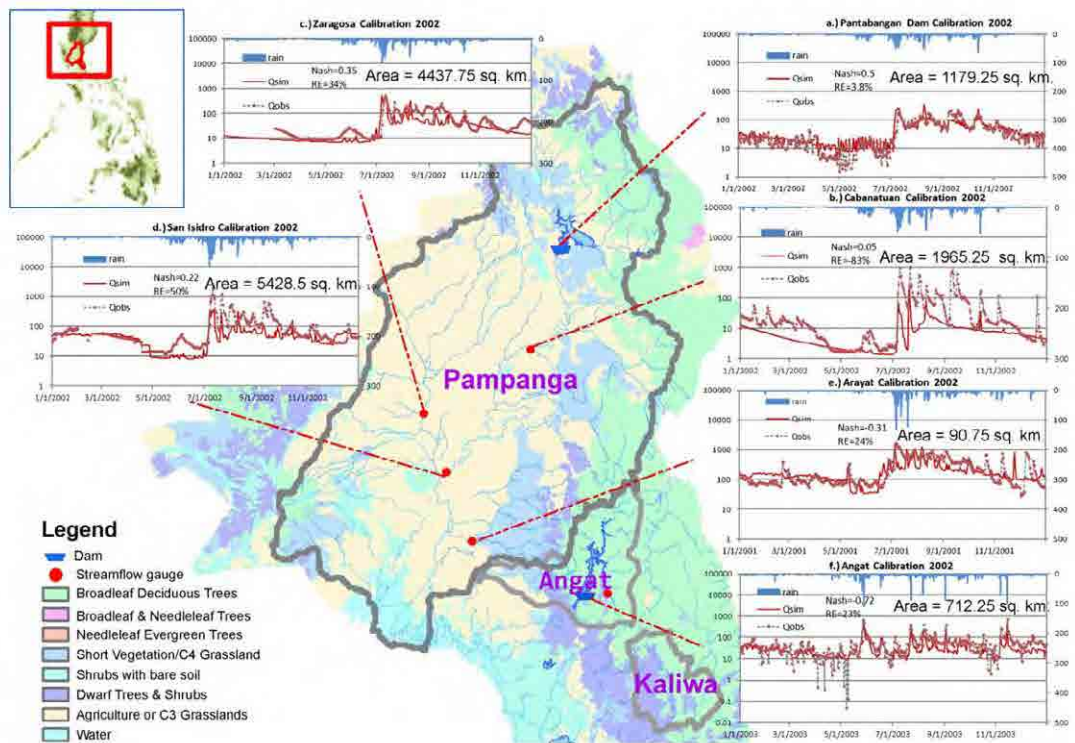
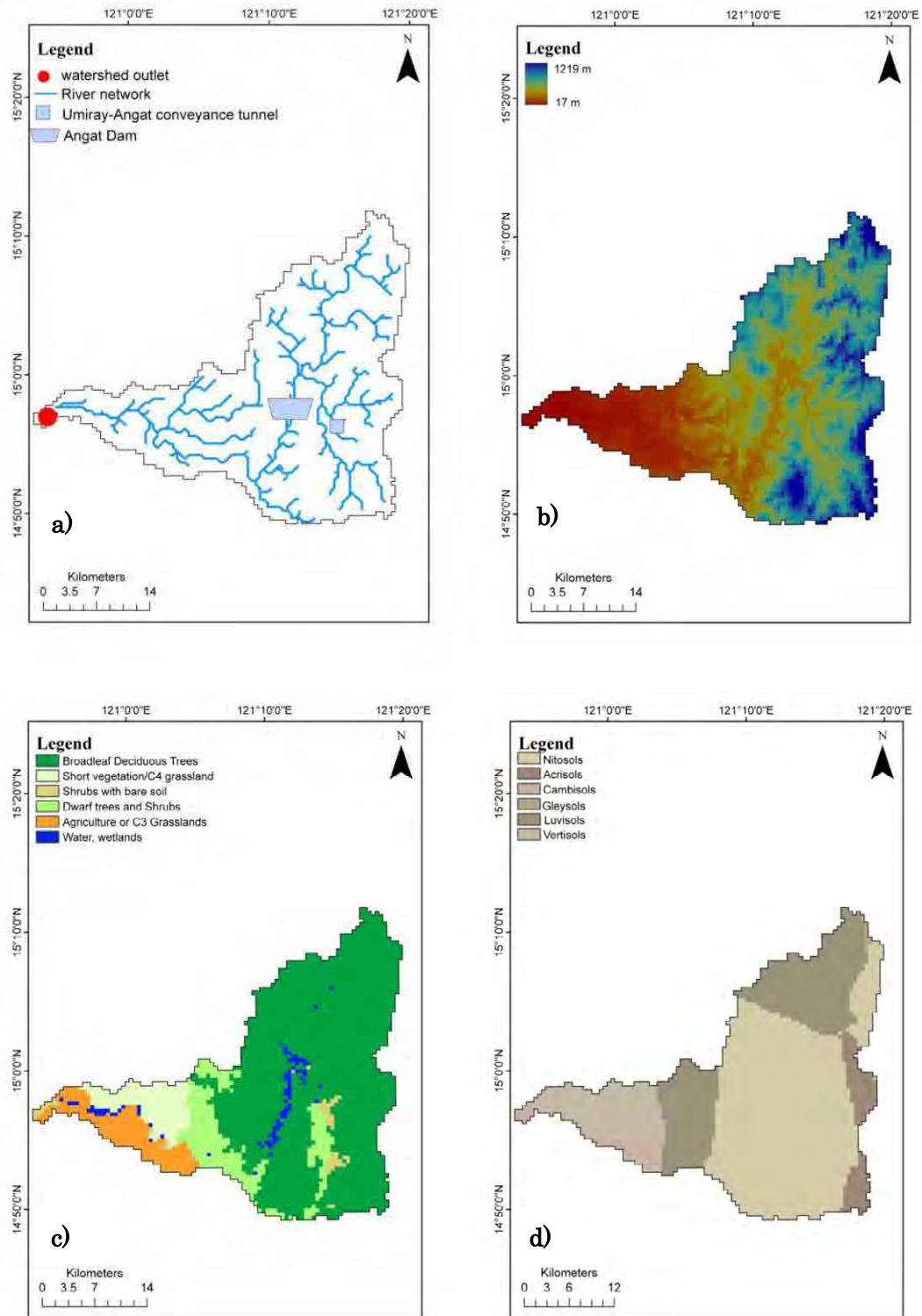


Figure 3.4-1. River network, land use and calibrations in Pampanga, Angat and Kaliwa river basins.

### 3.4.1 Angat River Basin

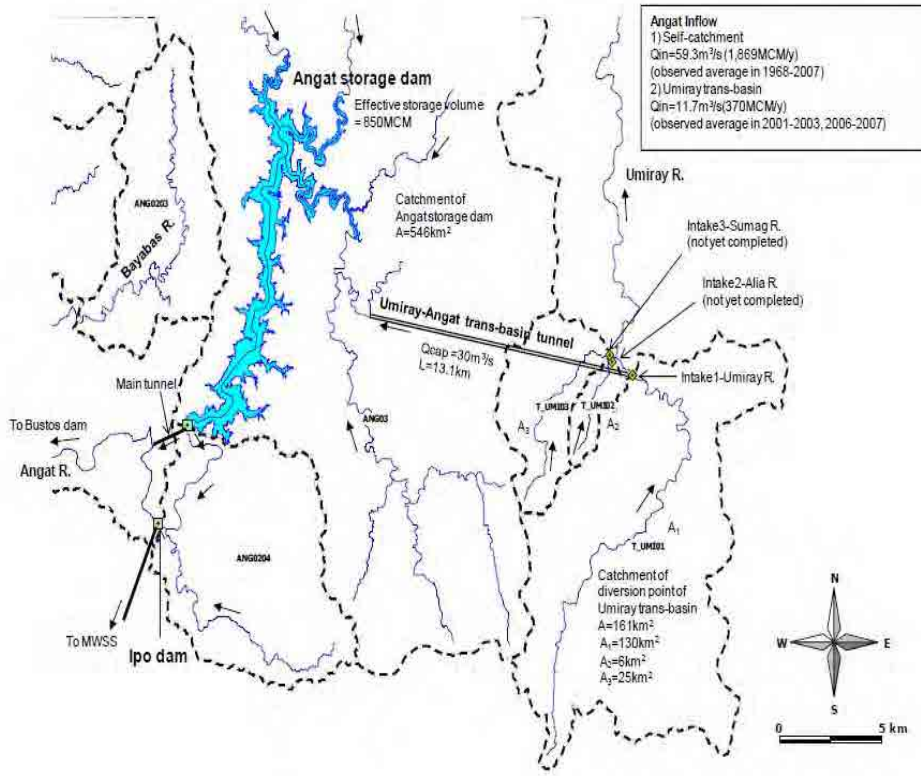
The total area considered for simulation in the Angat watershed delineated by using the DEM (to reduce errors that very flat areas may cause during simulation) is 888km<sup>2</sup>. From the Shuttle Radar Topography Mission (SRTM) DEM, minimum elevation is 17m amsl in the Bulacan area while maximum elevation is 1219 m in the Cordillera Mountain Ranges (Figure 3.4-2b). Angat dam is the main domestic water source of Metro Manila. Additionally water from the dam is used for irrigation of agricultural areas in Bulacan and utilized for hydropower generation. Hence, this river basin is one of the most important water resource in the country. Hydrological simulation considers static and dynamic parameters that would closely represent the present conditions of this basin.



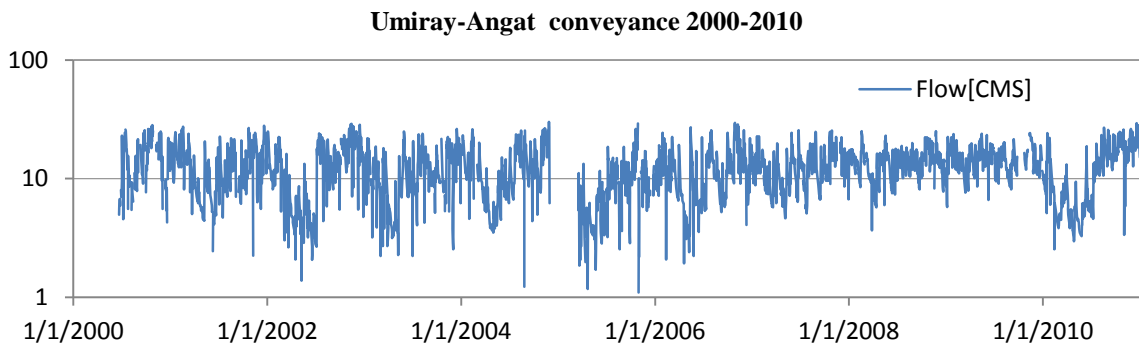
**Figure 3.4.-2.** Static parameters of Angat River basin: **a.)** River Network, **b.)** Digital Elevation, **c.)** Local land use and **d.)** Local soil.



Land use using the Sib2 reclassification (**Figure 3.4-2c**) consist of mostly broadleaf deciduous trees (69.93%), short vegetation C4 grassland (6.95%), shrubs with bare soil (1.8%), dwarf trees and shrubs (11.15%) agriculture or C3 grasslands (7.69%) and water (2.48%). The local soil in the basin as reclassified to FAO classification (**Figure 3.4-2d**) consist of mostly clay, clay loam or sandy clay loam. Nitosols comprise 53.49%, Acrisols (5.6%), Cambisols (2.25%), Gleysols(0.37%), Luvisols (26.25% and Vertisols (11.94%).



**Figure 3.4-3.** The Umiray Angat conveyance tunnel.

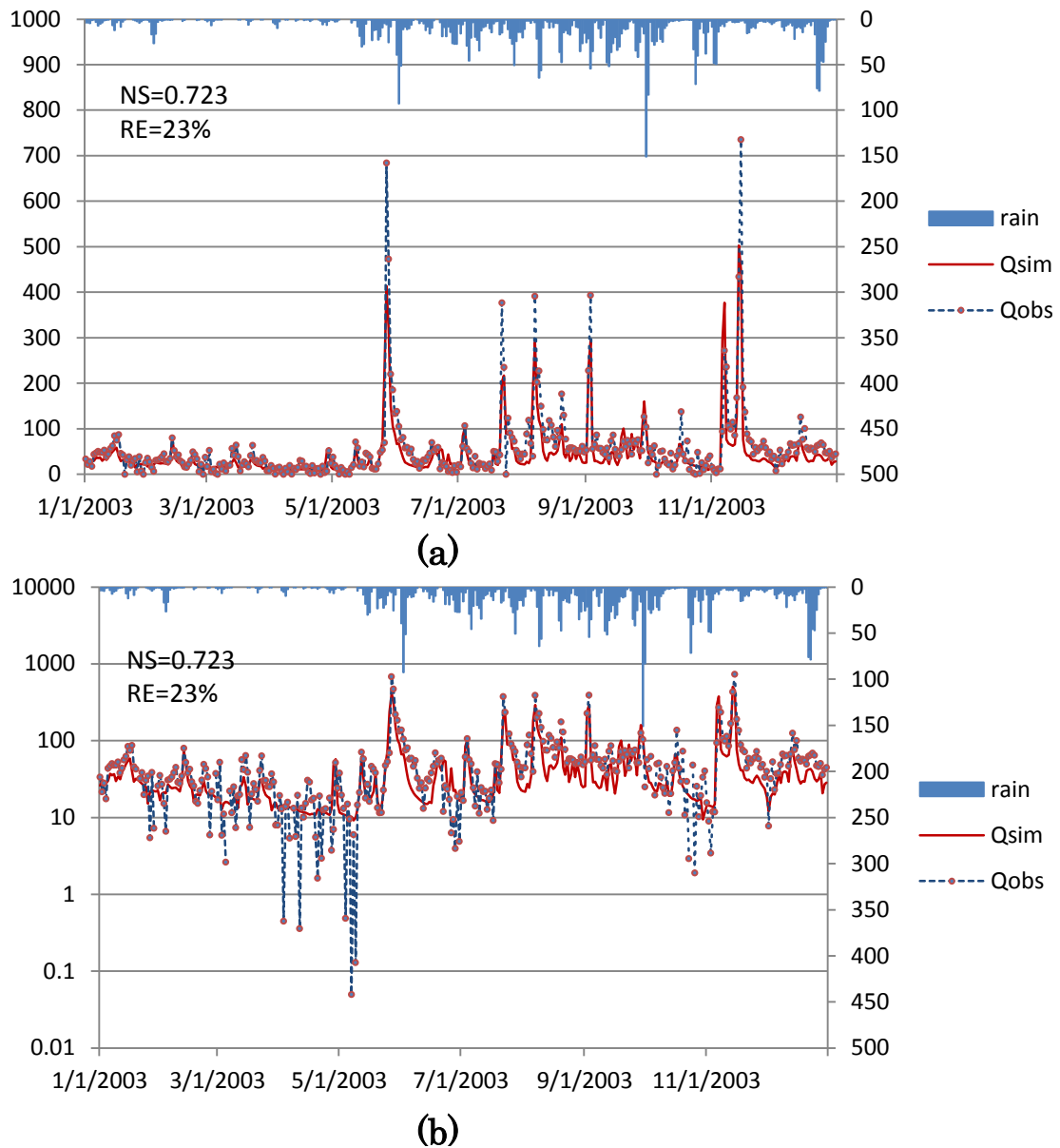


**Figure 3.4-4.** The flow in the Umiray-Angat conveyance tunnel ranged from 0 to 30 m<sup>3</sup>/s.

Aside from natural river flow within the basin (**Figure 3.4-2a**), for calibration and validation of Angat river basin, the Umiray-Angat conveyance channel was included in the

hydrological simulations (**Figure 3.4-3** and **Figure 3.4-4**). This channel supplements from 0-30 m<sup>3</sup>/s of water into the basin since early 2000. Unfortunately, data collection for this channel is only from mid-2000 to the present. Missing information from 1981-2000 were considered as 0 discharge which resulted to possible data gaps in the hydrological simulations. WEB-DHM simulations are only limited by the available input data. Calibration considered simulations for 2003 for the soil parameterization. Validation of the basin was from 2001-2010.

### 3.4.1.1 Angat River Basin Calibration (2003) and Validation



**Figure 3.4-5.** Calibration of Angat dam inflow for 2003, **a)** normal scale, **b)** log-scale.

Calibration of Angat Dam was done by comparing dam inflows for the year 2003 considering peak discharges and low flows. **Figure 3.4-5** shows the dam calibration for Angat dam in 2003 with NS=0.723 and RE=23%. The log-scale (**Figure 3.4-5b**) was illustrated to check if the baseflows are captured during the simulations. The observed records were originally collected as reservoir elevation hence the low flows in the observed data had very large day to day variation. The differences in some of the peak flows are as a result of the simplification in the temporal downscaling of daily to hourly rainfall. The calibrated soil parameters (**Table 3.4-1 to Table 3.4-3**) for each a.) soil type, b.) Manning’s roughness for each sub-basin and c.) soil anisotropy ratio for each landuse classification are provided. These soil parameters are adjusted from baseline information available in the FAO global dataset for that were downscaled to the basin.

**Table 3.4-1.** Calibrated Soil Parameters for Angat River Basin.

Calibrated soil parameters (FAO SOIL TYPES)	4413	4465	4478	4504	4537	4582
Saturated hydraulic conductivity for soil surface (mm/h)	20.07	24.47	13.01	12.775	16.46	6.44
Hydraulic conductivity decay factor	2.01	2.44	1.30	1.28	1.65	0.64
Hydraulic conductivity of groundwater (mm/h)	6.92	12.24	4.49	5.68	5.68	2.22

**Table 3.4-2.** Manning’s roughness for each sub-basin in Angat River Basin

	ws100	ws200	ws300	ws400	ws500	ws600	ws700	ws800	ws900
Manning’s n	0.045	0.045	0.045	0.045	0.045	0.045	0.045	0.045	0.05

**Table 3.4-3.** Soil anisotropy ratio for each land use type in Angat River Basin

Land Use Type (Sib2 reclassification)	1	2	3	4	5	6	7	8	9
Soil anisotropy ratio	30	30	30	30	30	9	3	12	9

**Figure 3.4-6** shows validated dam inflows for long-term simulations (2001-2009) in Angat Dam. The simulations consistently represent the daily historical conditions of the basin without recalibration of existing soil parameters. This indicates that the hydrological parameters considered for calibration are representative of past basin conditions. These assumptions for the past conditions are considered to have minimal change when utilizing the hydrological model for projecting basin-scale climate changes in succeeding chapters.

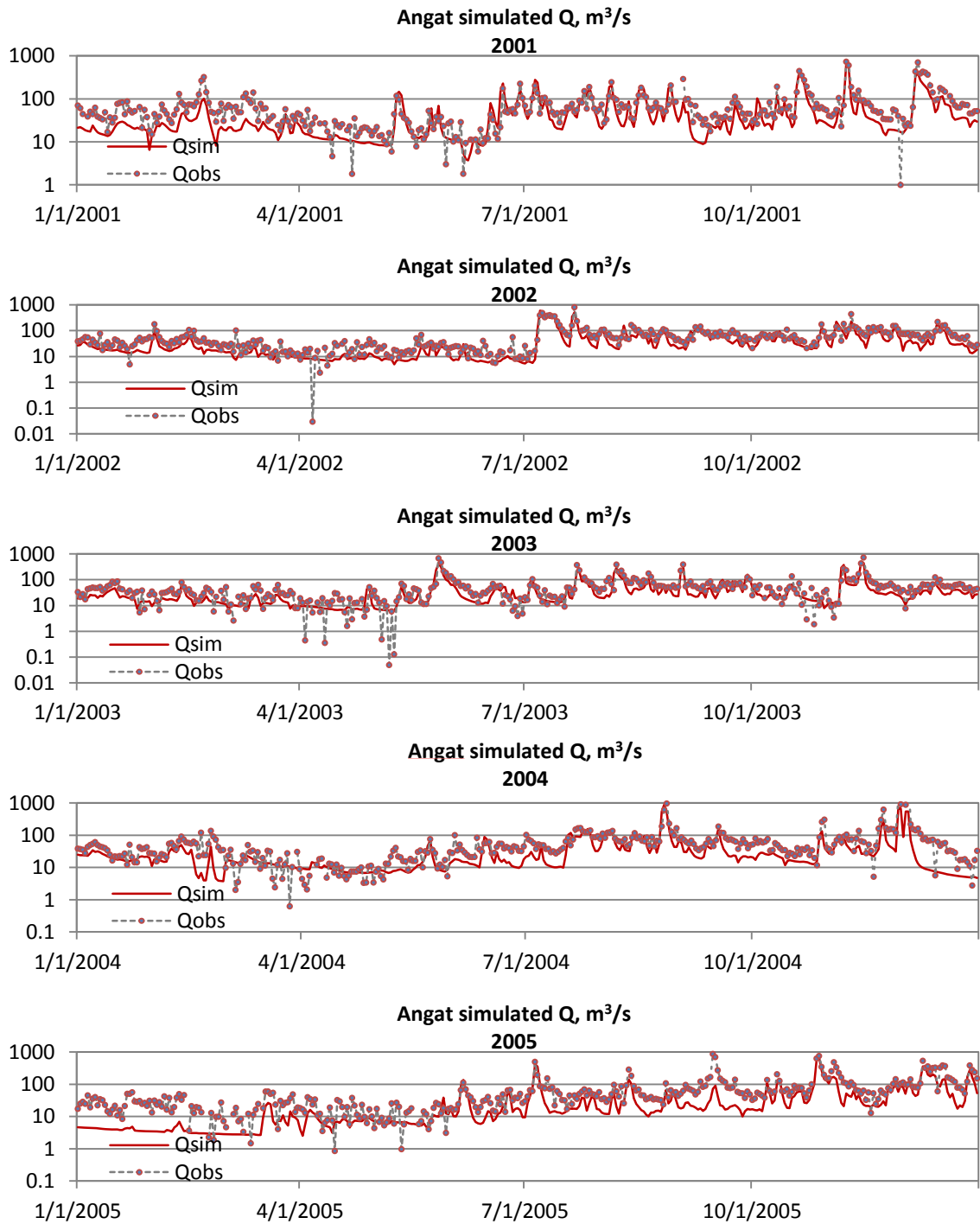


Figure 3.4-6. Validation of Angat dam inflows from 2001-2009 (cont.)

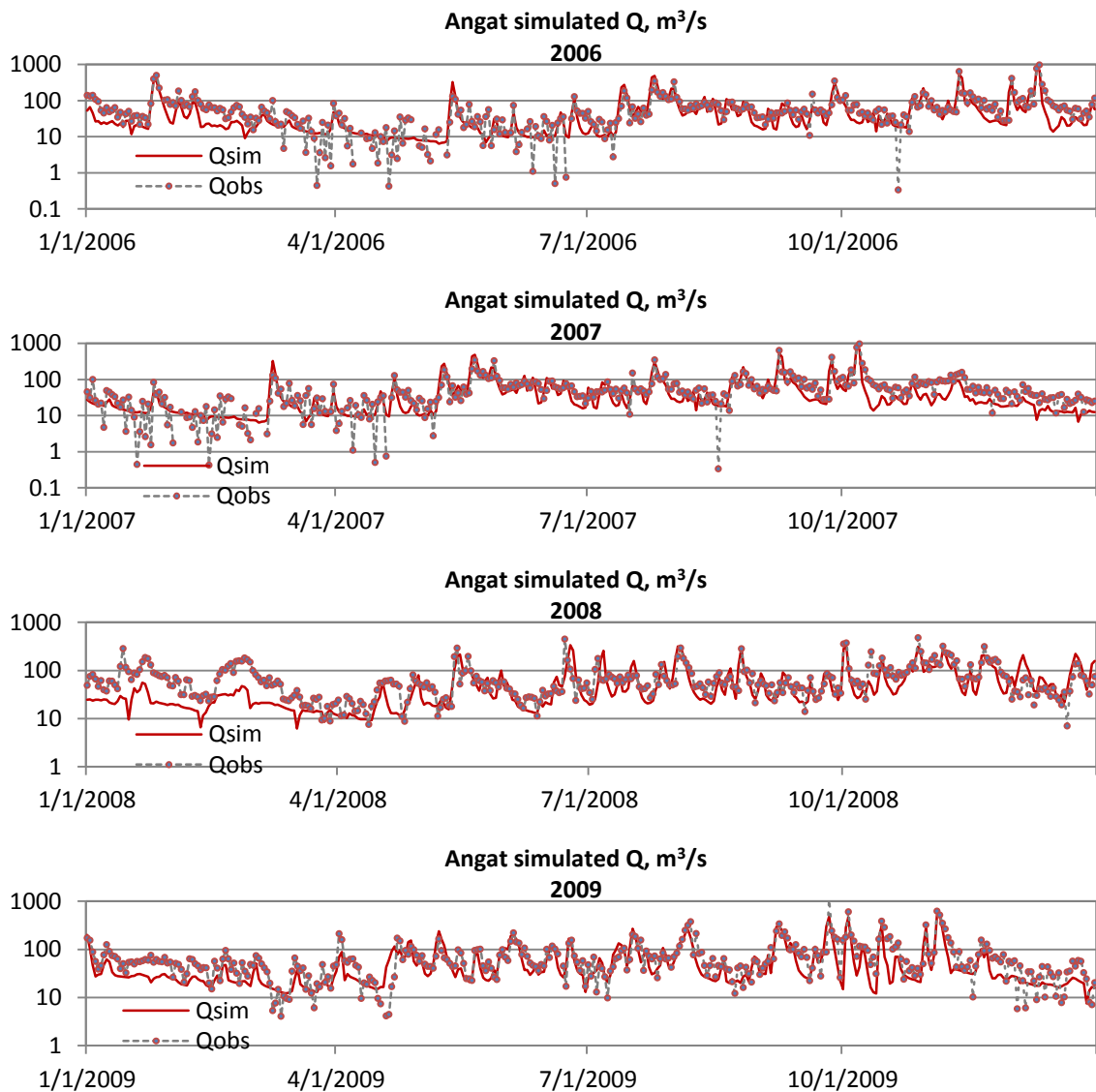
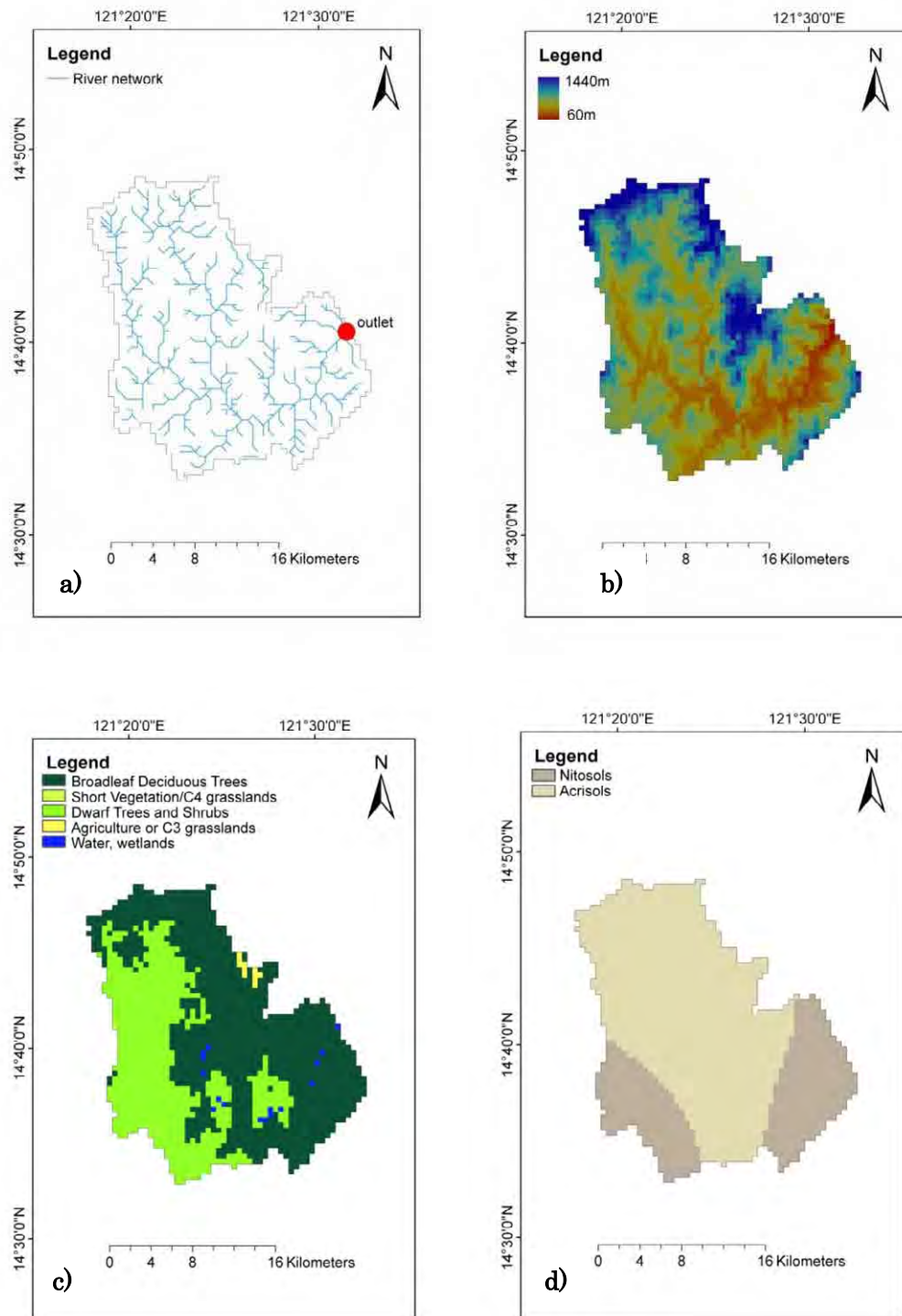


Figure 3.4-6. Validation of Angat dam inflows from 2001-2009 (cont.).

### 3.4.2 Kaliwa River Basin

The Kaliwa river basin is located in the southwestern part of the Agos River Basin. The total area considered for simulation in the Kaliwa watershed is 479.5km<sup>2</sup>. From the Shuttle Radar Topography Mission (SRTM) digital elevation map, minimum elevation is 60m amsl while maximum elevation is 1440 m along the Cordillera Mountain Ranges (Figure 3.4-7b). Land use using the Sib2 reclassification (Figure 3.4-7c) consist of mostly broadleaf deciduous trees (60.58%), short vegetation C4 grassland (0.05%), dwarf trees and shrubs (37.96%) agriculture or C3 grasslands (0.57%) and water (0.84%). The local soil in the basin as reclassified to FAO classification (Figure 3.4-7d) consist of mostly clay loam (Nitosols (31.09%), Acrisols (68.91%).



**Figure 3.4.-7.** Kaliwa River Basin: a) River Network, b) Digital Elevation, c) Local land use and d) Local soil.



### 3.4.2.1 Kaliwa River Basin Validation

There is no observed data which can be used for calibrating parameters of a model of Kaliwa watershed. However, due to its proximity to Angat river basin and the similarity in basin characteristics, the same soil types in Angat and Kaliwa are assumed to have the same soil properties. These are given in **Table 3.4-4** for the 2 soil types, **Table 3.4-5** for Manning’s roughness, and **Table 3.4-6** for soil anisotropy ratio of each soil type. Validation of the model are given from 1981-2009 in **Figure 3.4-8**.

**Table 3.4-4.** Calibrated Soil Parameters of Kaliwa River Basin.

Calibrated soil parameters (FAO SOIL TYPES)	4413	4465
Saturated hydraulic conductivity for soil surface (mm/h)	20.07	24.47
Hydraulic conductivity decay factor	2.01	2.44
Hydraulic conductivity of groundwater (mm/h)	6.92	12.24

**Table 3.4-5.** Manning’s roughness for each sub-basin in Kaliwa River Basin.

	ws100	ws200	ws300	ws400	ws500	ws600	ws700	ws800	ws900
Manning’s n	0.045	0.045	0.045	0.045	0.045	0.045	0.045	0.045	0.05

**Table 3.4-6.** Soil anisotropy ratio for each land use type in Kaliwa River Basin.

Land Use Type (Sib2 reclassification)	1	2	3	4	5	6	7	8	9
Soil anisotropy ratio	30	30	30	30	30	9	3	12	9

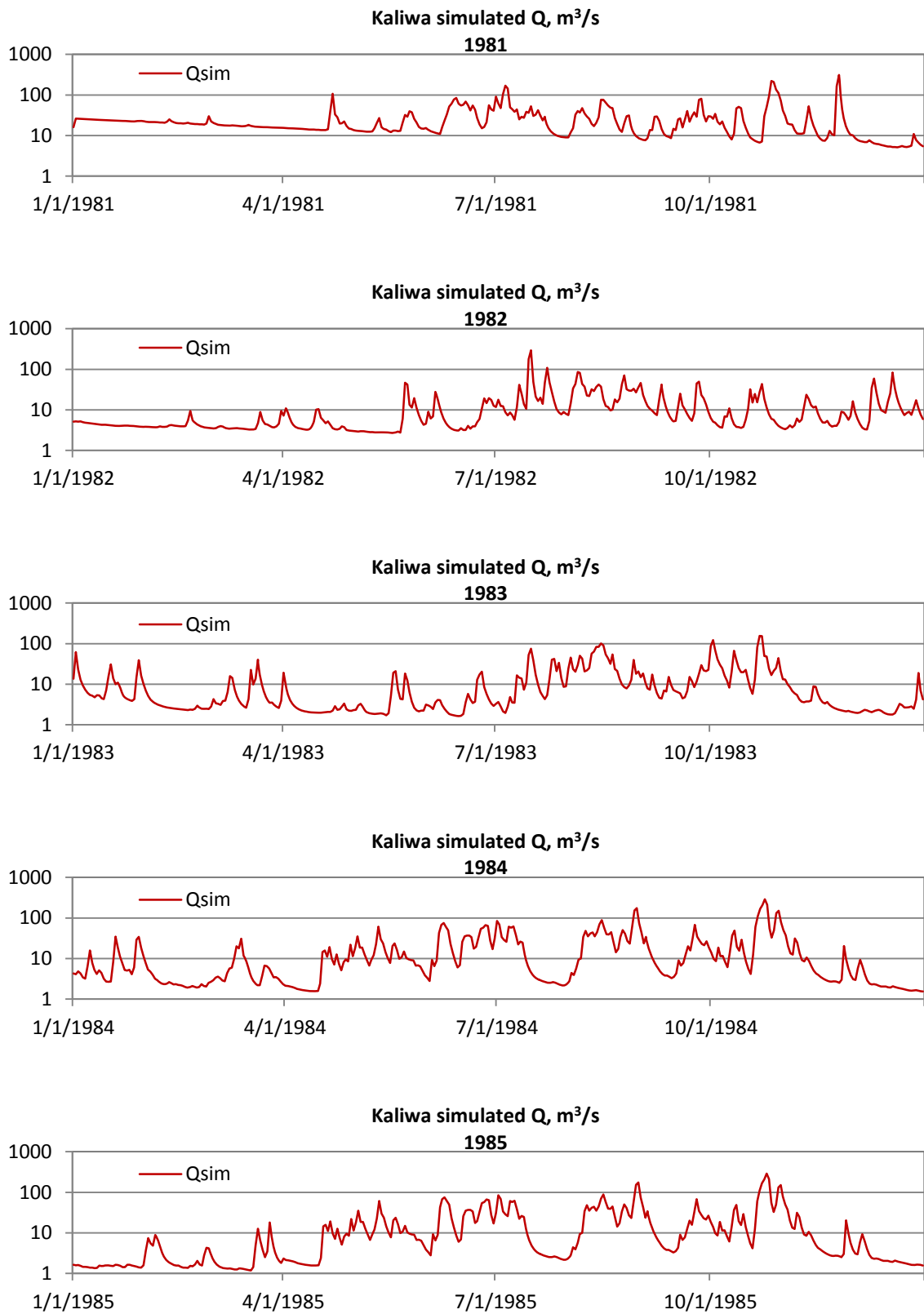


Figure 3.4-8. Validation of Kaliwa River Basin from 1981-2009 (cont.).

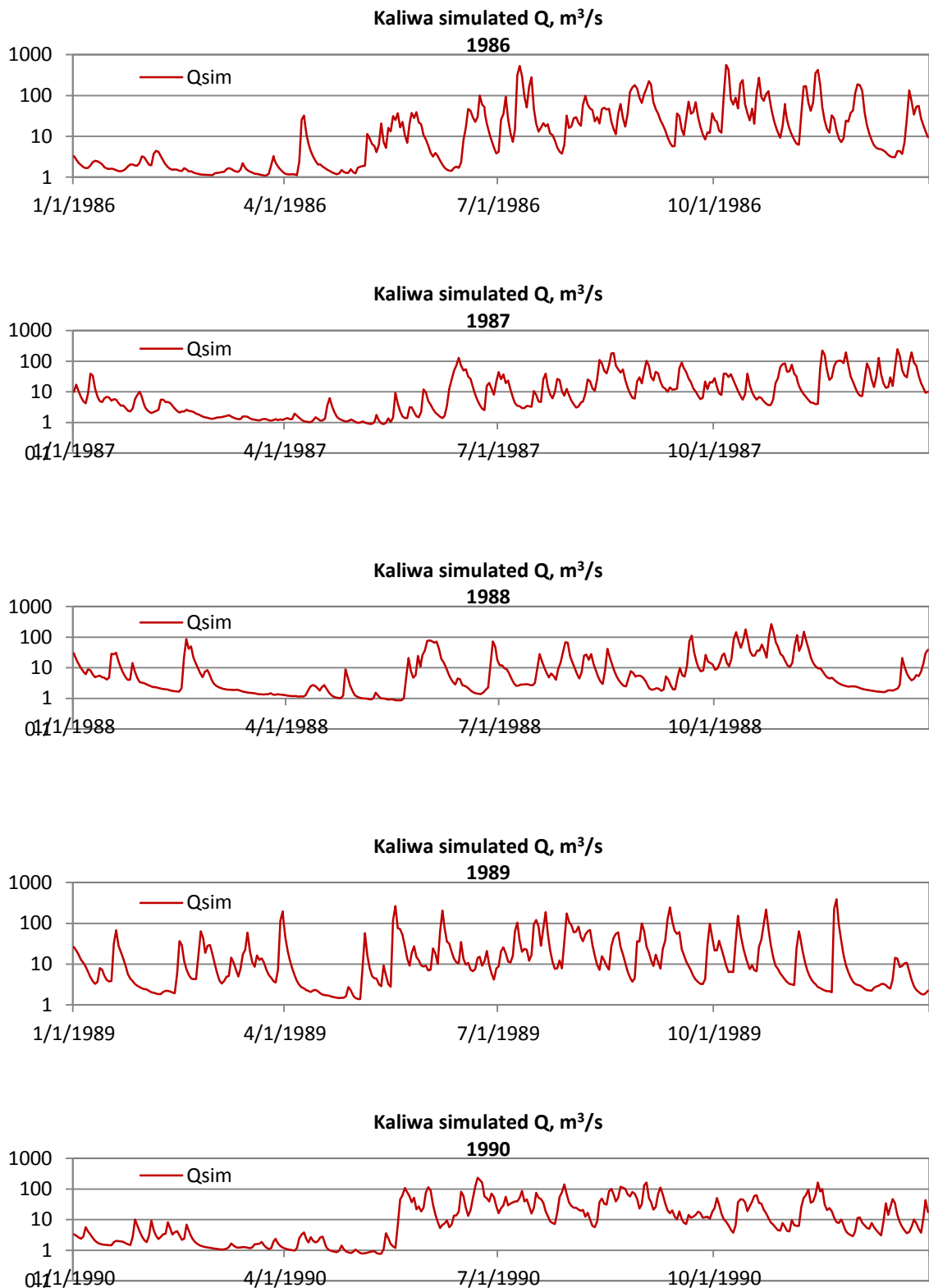


Figure 3.4-8. Validation of Kaliwa River Basin from 1981-2009 (cont.).

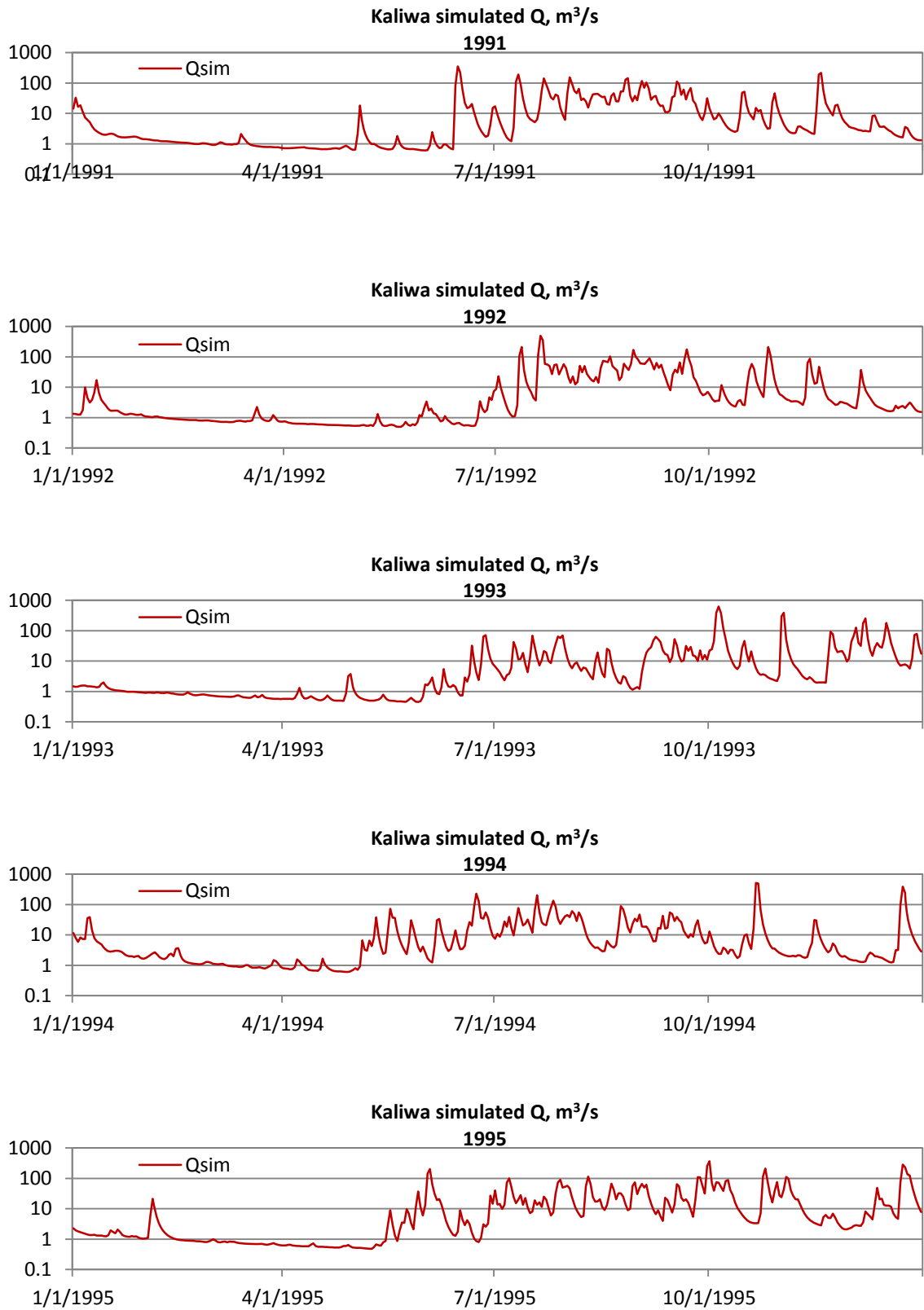
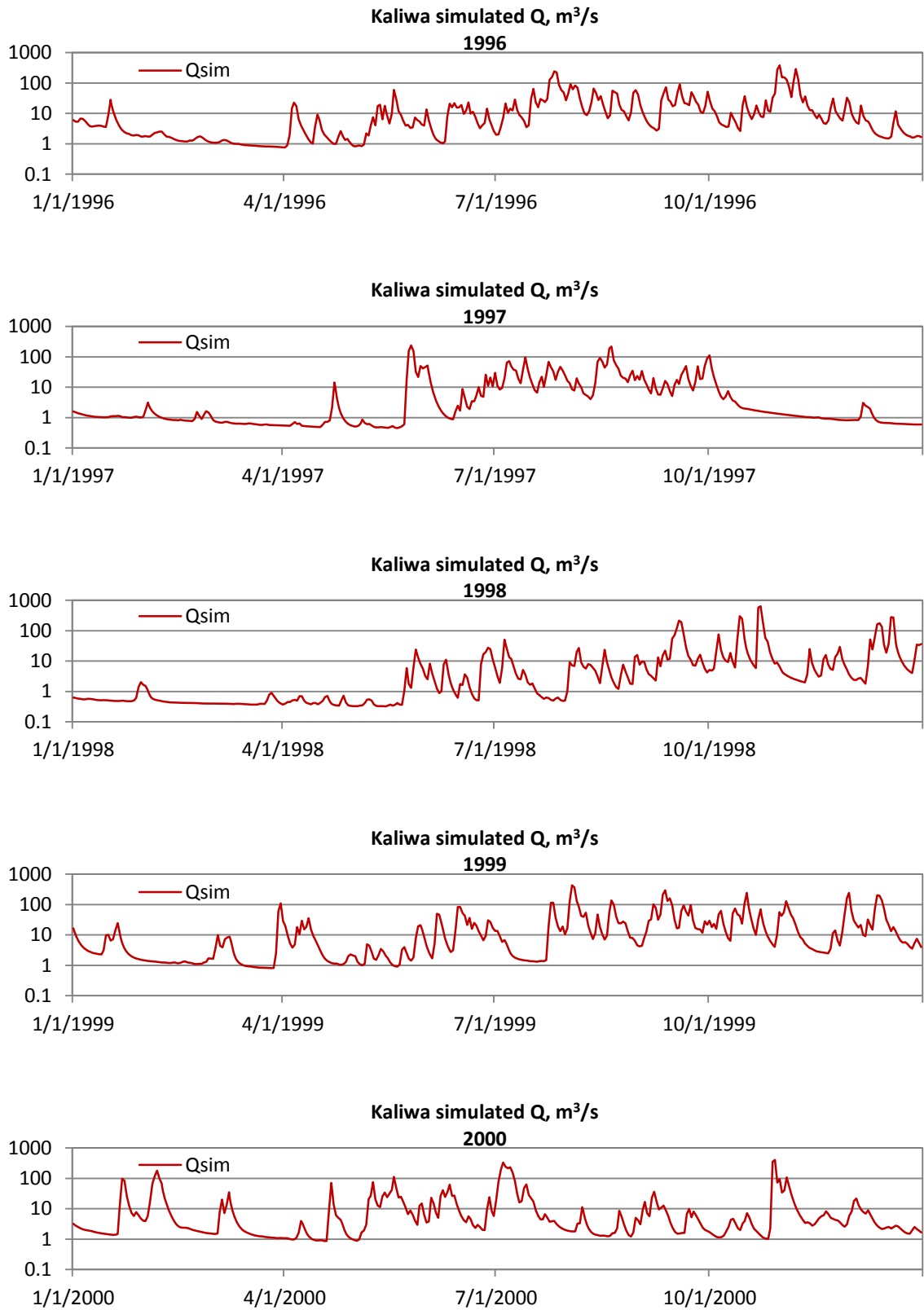


Figure 3.4-8. Validation of Kaliwa River Basin from 1981-2009 (cont.).



**Figure 3.4-8.** Validation of Kaliwa River Basin from 1981-2009 (cont.).

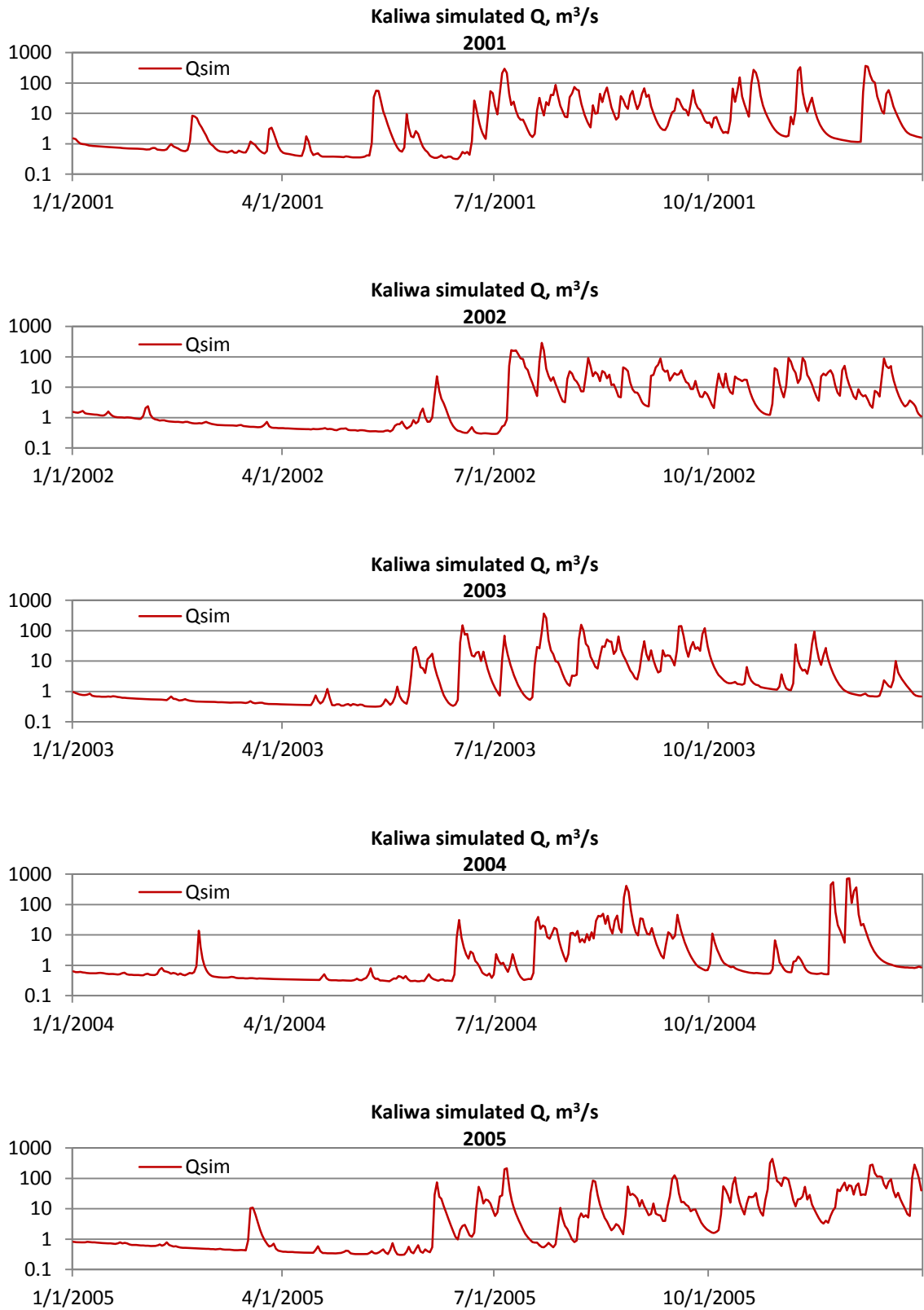


Figure 3.4-8. Validation of Kaliwa River Basin from 1981-2009 (cont.).

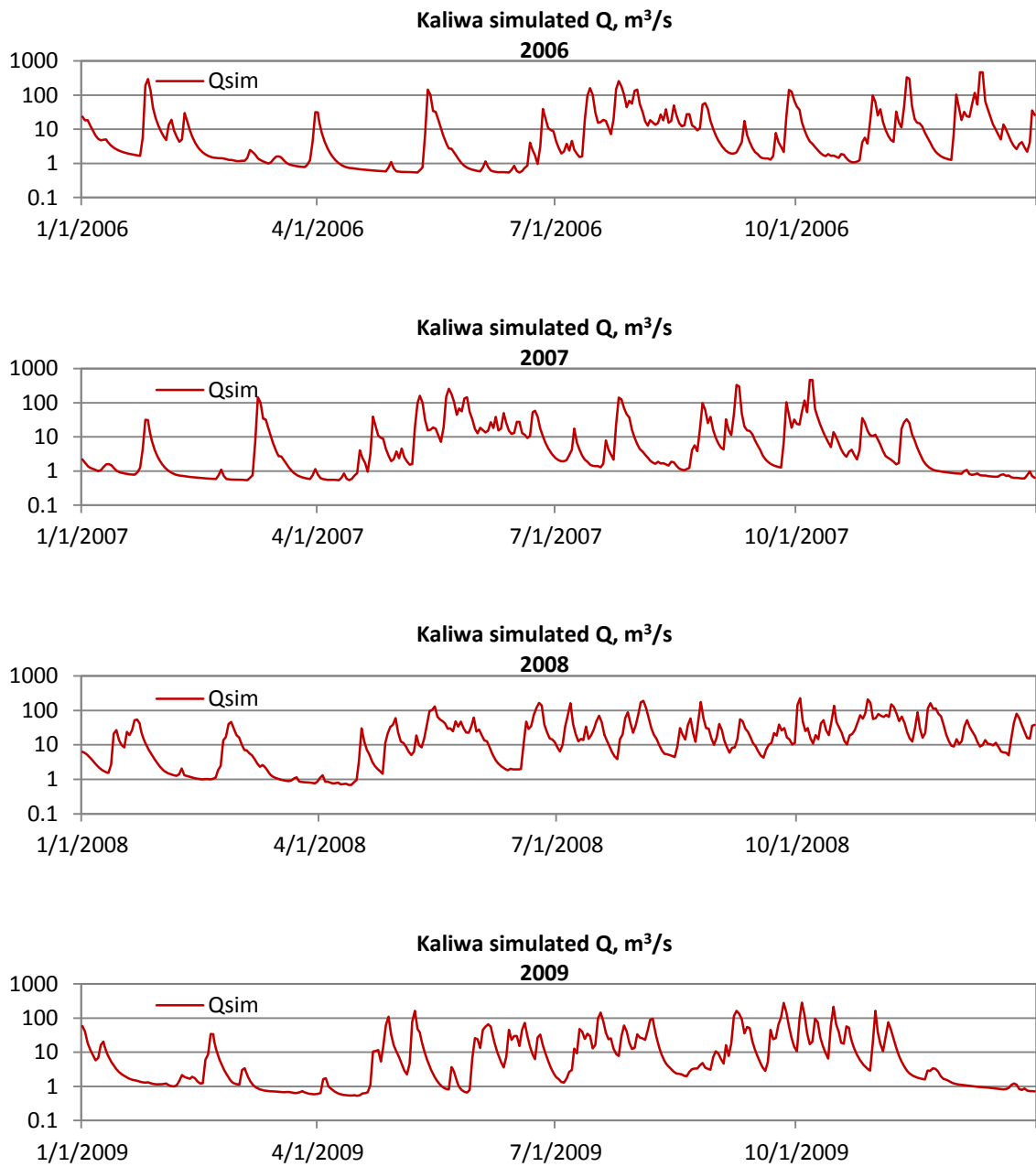


Figure 3.4-8. Validation of Kaliwa River Basin from 1981-2009 (cont.).



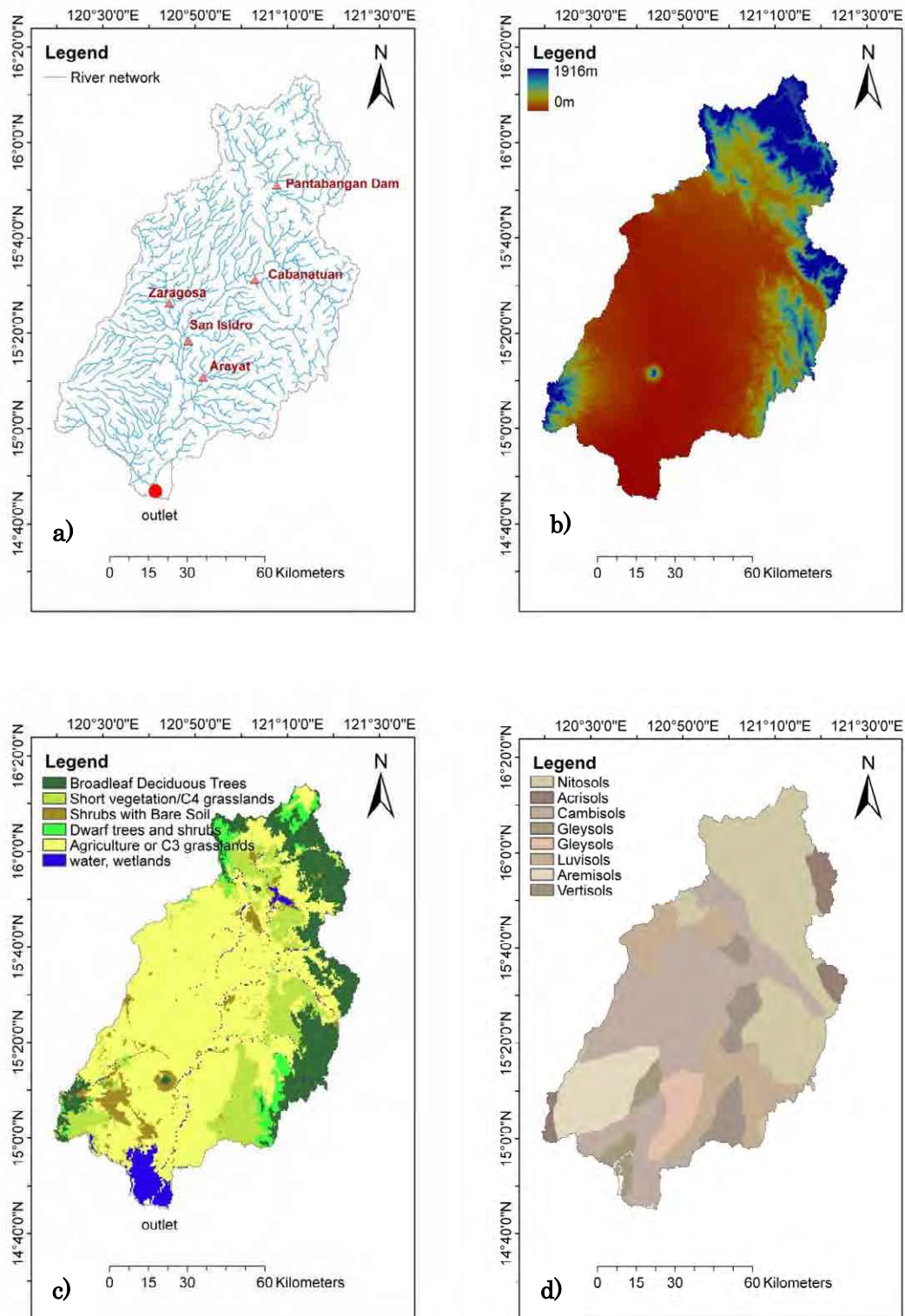
### **3.4.3 Pampanga River Basin**

Pampanga river basin is the largest basin considered in the study with a simulation area of 7,837.75 km<sup>2</sup>. From the SRTM digital elevation map, minimum elevation is at mean sea level (msl) while maximum elevation is 1916 m on the Cordillera Mountain Ranges (**Figure 3.4-9b**).

This basin (dubbed the “Philippine rice bowl”) is one of the most agriculturally important basins in the country producing rice in the central plains of the basin as well as other agricultural products (corn, sugarcane and tilapia (fish)).

Land use using the Sib2 reclassification (**Figure 3.4-9c**) consist of mostly agriculture or C3 grasslands (58.84%) ,broadleaf deciduous trees (15.75%), short vegetation C4 grassland (14.05%),shrubs with bare soil (4.50%), dwarf trees and shrubs (3.54%) and water (3.32%). The local soil in the basin as reclassified to FAO classification (**Figure 3.4-9d**) consist of mostly clay loam, sandy clay loam, sandy loam and clay. Nitosols comprise 29.4%, Acrisols (3.47%), Cambisols (31.83%), Gelysols (6.89%), Luvisols (14.10%, Aremisols (8.61%) and Vertisols (5.72%).

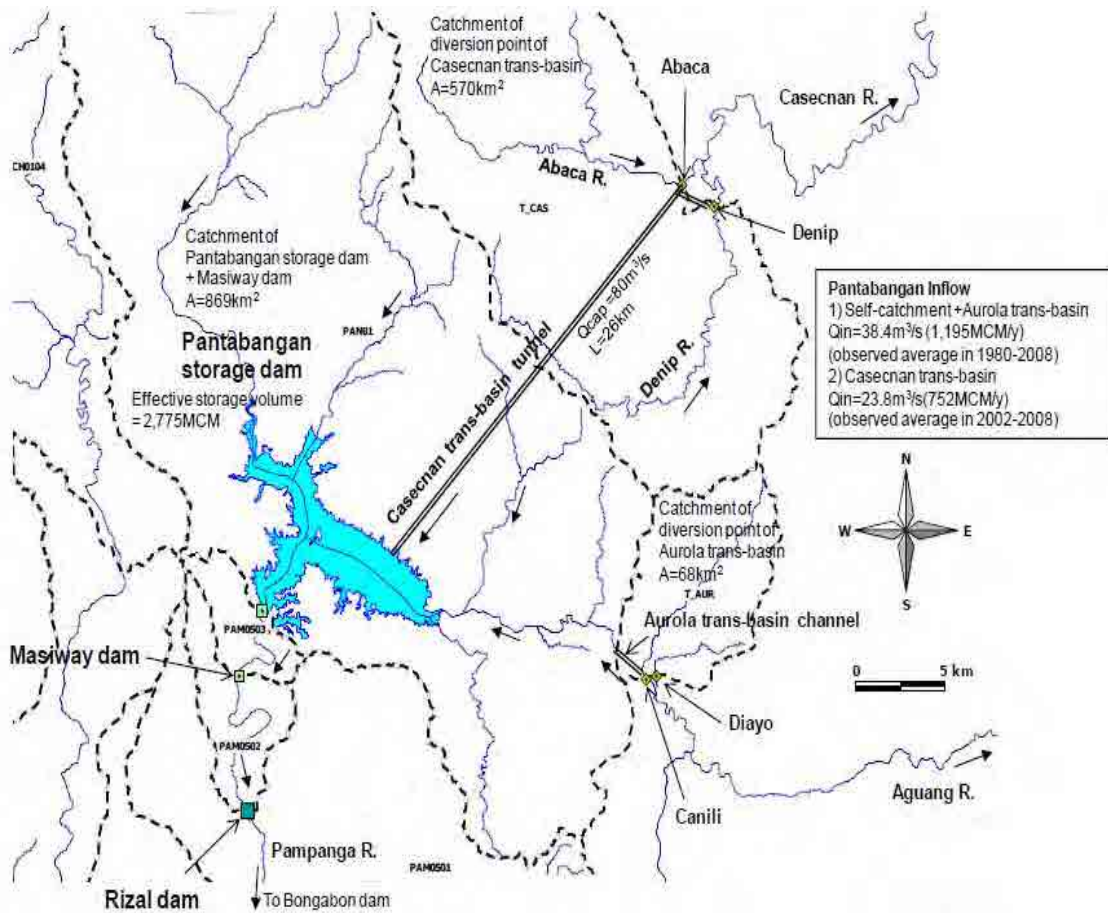
Unlike the smaller basins Angat and Kaliwa, this basin does not have very dense observation network for rainfall distribution within the basin. Hence results from this basin are limited to the interpolated values that were used during the simulations.



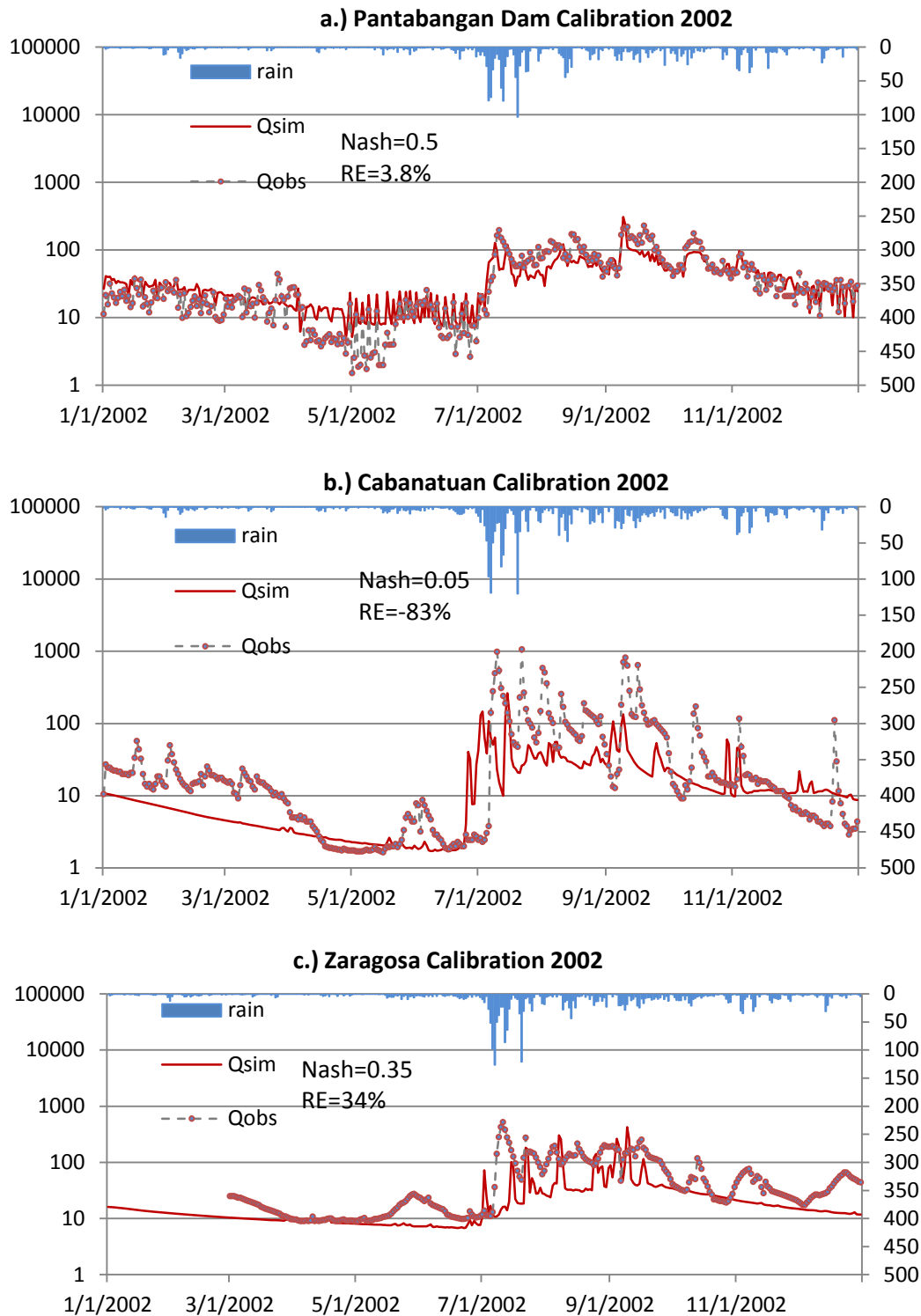
**Figure 3.4-9.** Pampanga River basin: a) River Network, b) Digital Elevation, c) Local land use and d) Local soil.

### 3.4.3.1 Pampanga River Basin Calibration (2002) and Validation

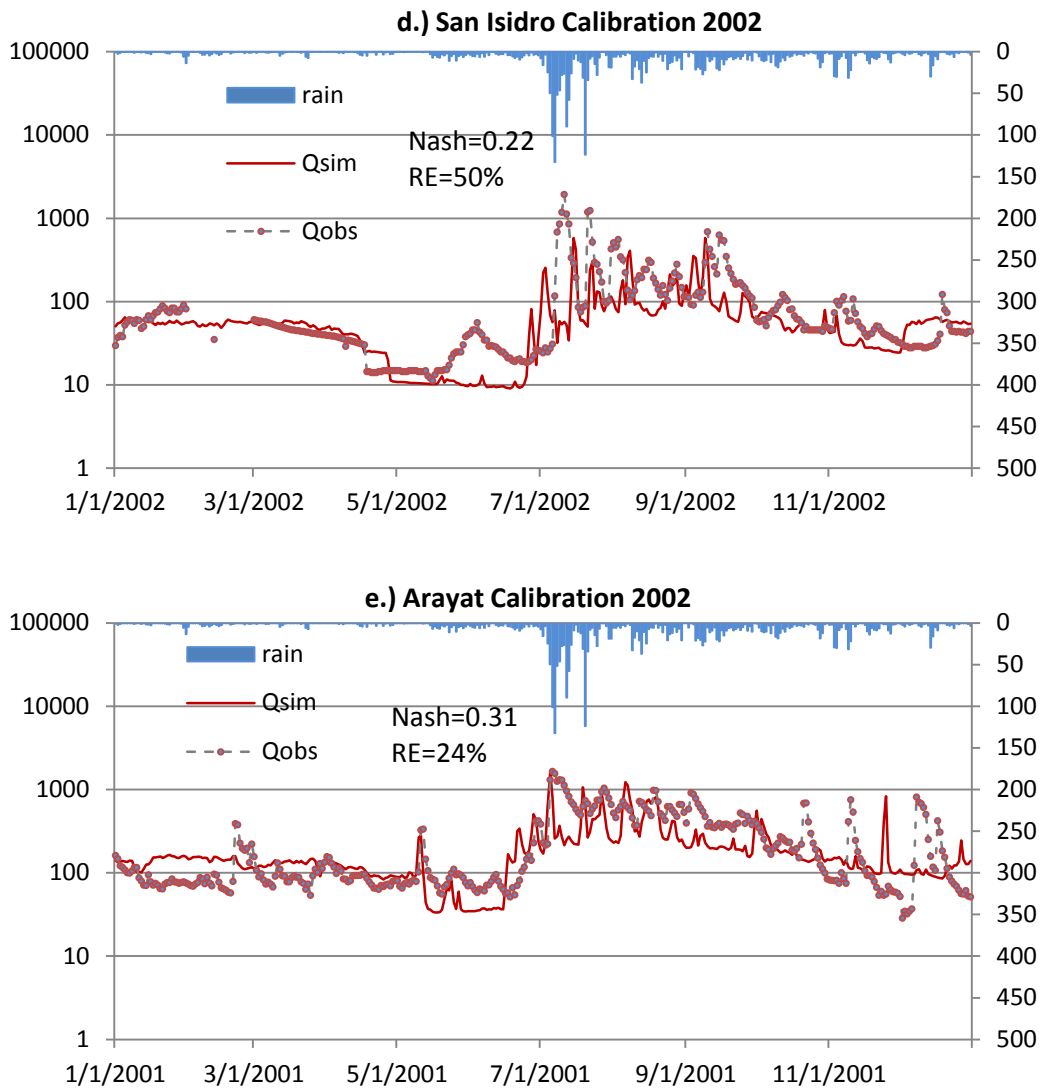
Calibration in the Pampanga river basin was done for the year 2002. This considered inflows from the upstream catchment and inflow from the Aurora –transboundary channel (data was available from 2000-2011). In addition, the Casecnan trans-basin was also included (data available from 2002-2011). The Masiway outflow was also incorporated (data available from 1981-2011) for calibrating the downstream (Arayat stream gauge). No data was incorporated from Rizal Dam and Bongabon Dam (See **Figure 3.4-10**). The limitations in available data for this basin are large sources of errors during calibration (**Figure 3.4-11**). Calibrations for Pantabangan Dam inflow (NS=0.65, RE=11%), Cabanatuan (NS=0.05, RE=83%), Zaragosa (NS=0.35, RE=34%), San Isidro (NS=0.22, RE=50%) were done for 2002 and for Arayat (NS=0.31, RE=24%) it was done for 2001.



**Figure 3.4-10.** The Casecnan trans-basin tunnel and the Aurora trans-basin channel upstream of Pantabangan dam and the Masiway dam outflows were considered for downstream calibration.



**Figure 3.4-11.** 2002 daily data calibration in a.) Pantabangan Dam, b.) Cabanatuan, c.) Zaragosa, d.) San Isidro and e.) Arayat stream gauges.(cont.)



**Figure 3.4-11.** 2002 daily data calibration in a.) Pantabangan Dam, b.) Cabanatuan, c.) Zaragosa, d.) San Isidro and e.) Arayat stream gauges.

The calibrated parameters are listed in **Table 3.4-7 to Table 3.4-9** while the validated discharges for simulations (2001-2009) in the 5 discharge gauges (Pantabangan, Cabanatuan, Zaragoza, San Isidro and Arayat) within the basin are shown in **Figure 3.4-12 to Figure 3.4-16**. Unfortunately, not all the observed daily discharges are available for comparison with the simulated discharges. Additionally, imperfect simulations due to sparse upstream rainfall gauges are considered as some of the limitations of the Study. Additionally, since the hydrological model is based on the hill-slope scheme, hydrological simulations in the plains are more difficult to fit perfectly (as evidenced by simulations from San Isidro, Cabanatuan and Zaragoza). However, Note that the intensities of the baseflows and peaks of the simulated discharges are similar with baseflows and peaks from all the gauges.

**Table 3.4-7.** Calibrated Soil Parameters for Pampanga River Basin.

Calibrated soil parameters (FAO SOIL TYPES)	4413	4465	4478	4503
Saturated hydraulic conductivity for soil surface (mm/h)	109.61	111.18	22.43	22.07
Hydraulic conductivity decay factor	10.96	11.12	2.24	2.21
Hydraulic conductivity of groundwater (mm/h)	115.38	63.35	6.73	6.62

**Table 3.4-7.** Calibrated Soil Parameters for Pampanga River Basin (cont).

Calibrated soil parameters (FAO SOIL TYPES)	4504	4537	4564	4582
Saturated hydraulic conductivity for soil surface (mm/h)	22.03	28.39	213.82	11.10
Hydraulic conductivity decay factor	2.20	2.84	21.38	1.11
Hydraulic conductivity of groundwater (mm/h)	6.61	8.52	64.14	3.33

**Table 3.4-8.** Manning's roughness for each sub-basin for Pampanga River Basin.

	ws100	ws200	ws300	ws400	ws500	ws600	ws700	ws800	ws900
Manning's n	0.05	0.05	0.05	0.01	0.01	0.01	0.05	0.01	0.01

**Table 3.4-9.** Soil anisotropy ratio for each land use type for Pampanga River Basin.

Land Use Type (Sib2 reclassification)	1	2	3	4	5	6	7	8	9
Soil anisotropy ratio	50	50	50	50	50	15	5	20	15

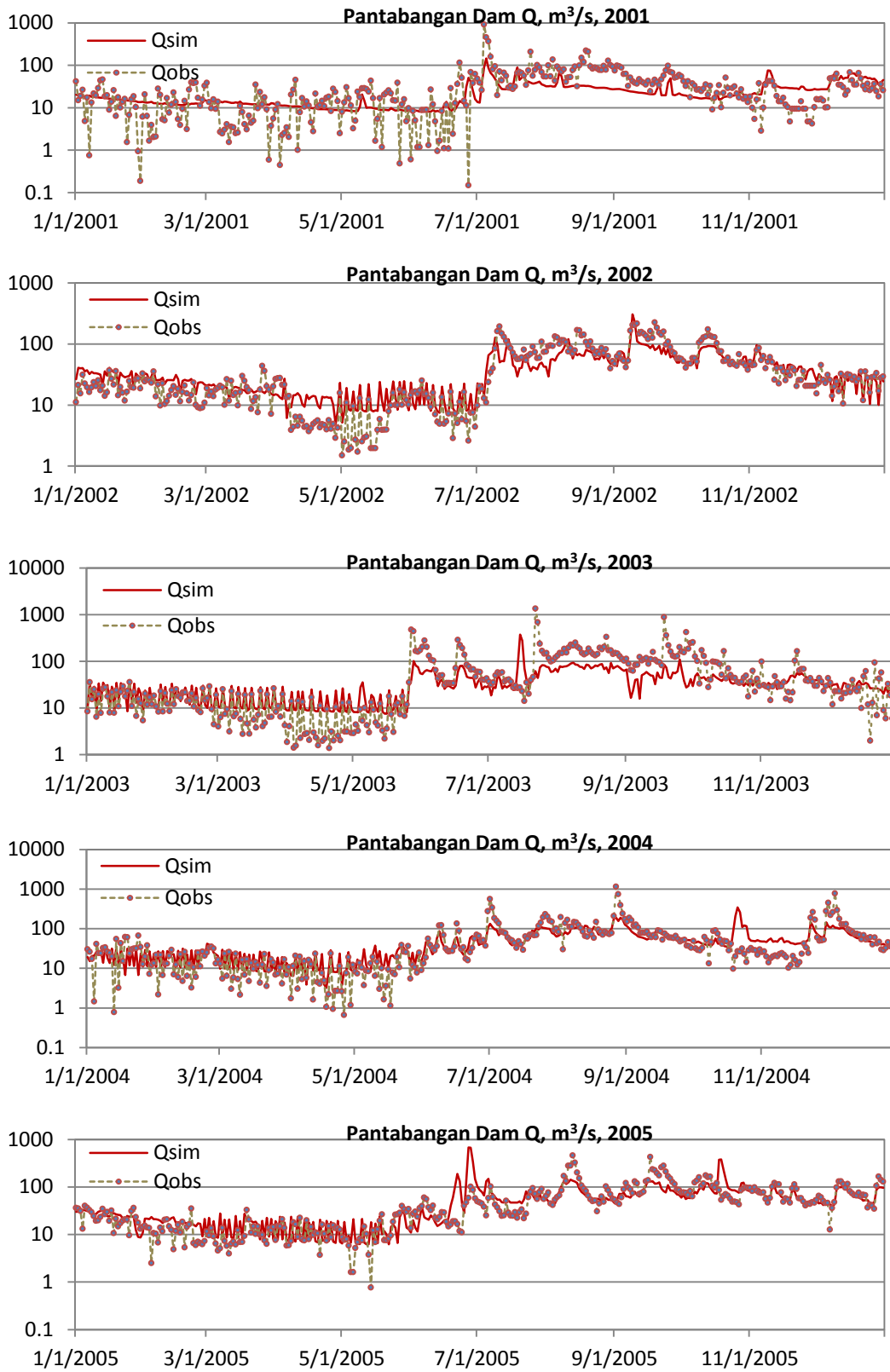
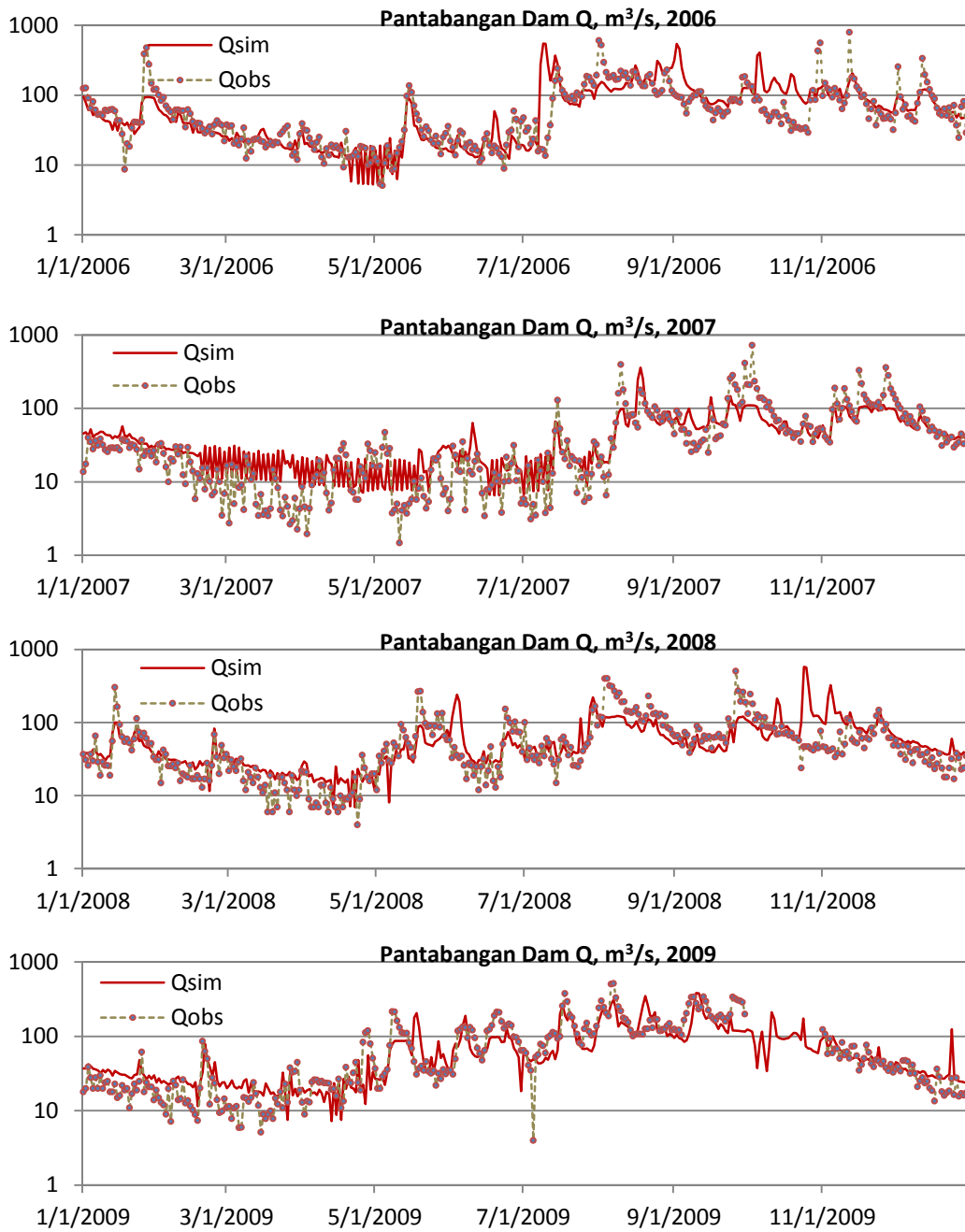
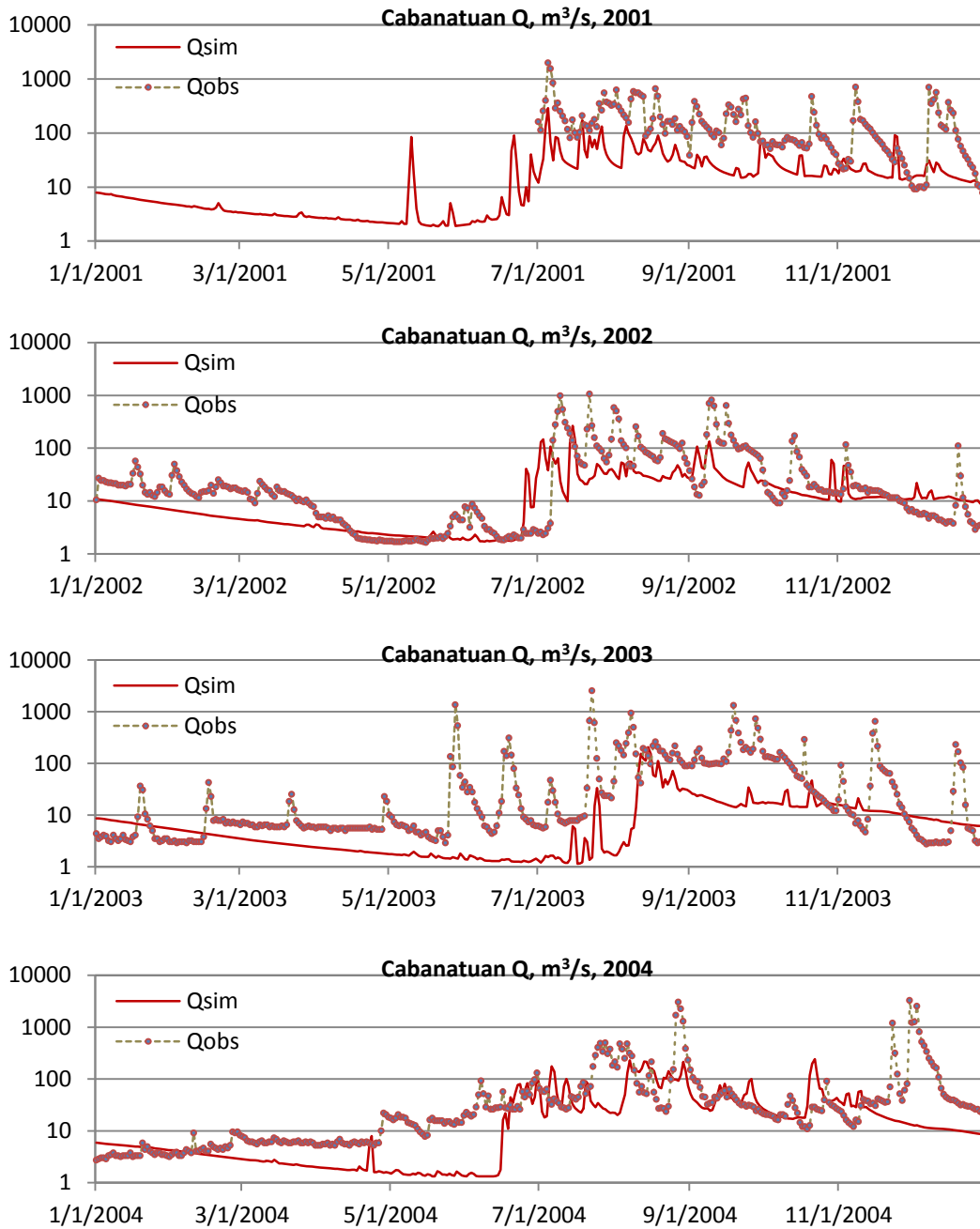


Figure 3.4-12. Validation for Pampanga River Basin (2001-2009): Pantabangan Dam inflow.





**Figure 3.4-12.** Validation for Pampanga River Basin (2001-2009): Pantabangan Dam inflow.



**Figure 3.4-13.** Validation for Pampanga River Basin (2001-2009): Cabanatuan

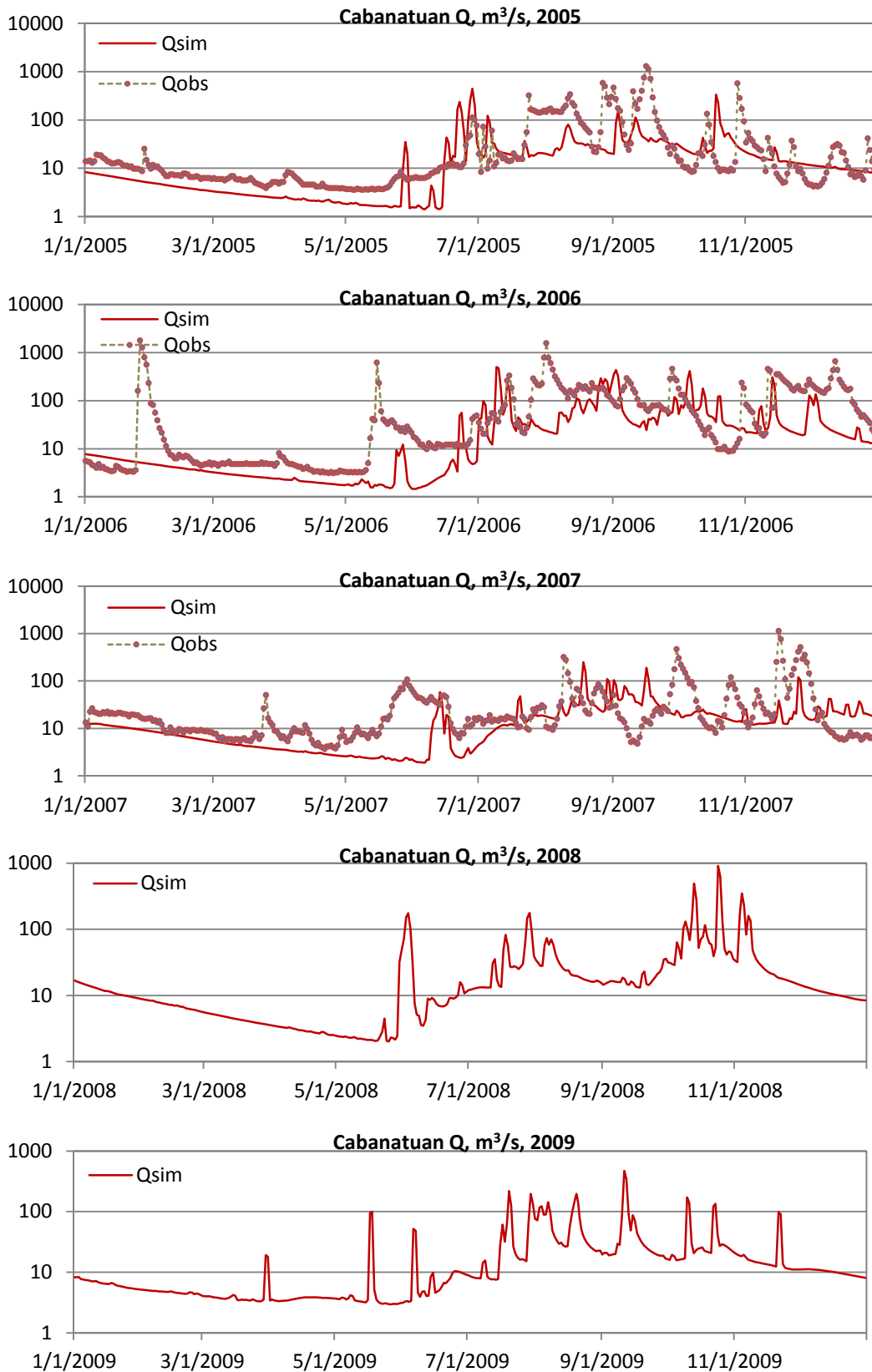


Figure 3.4-13. Validation for Pampanga River Basin (2001-2009): Cabanatuan

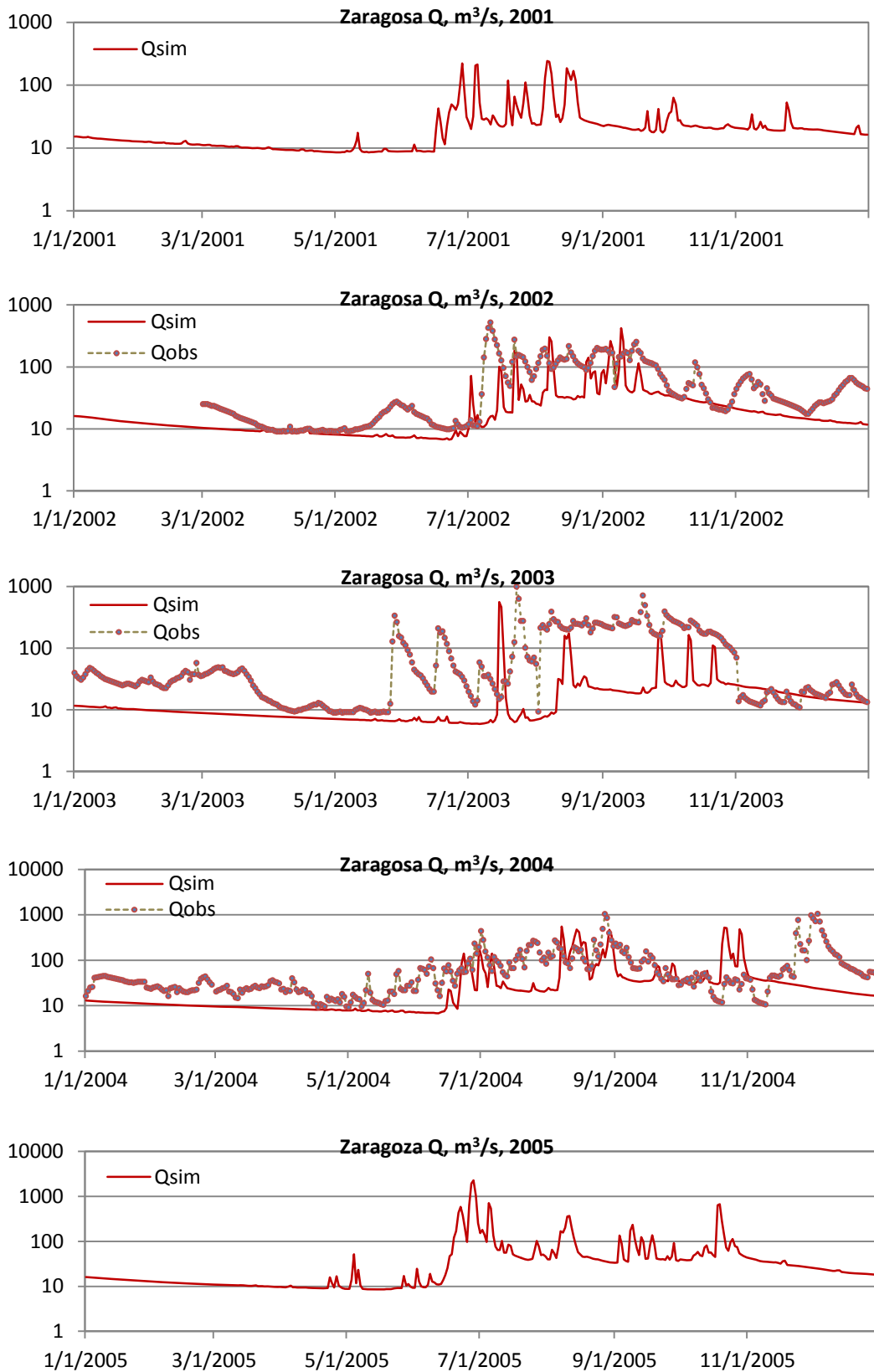
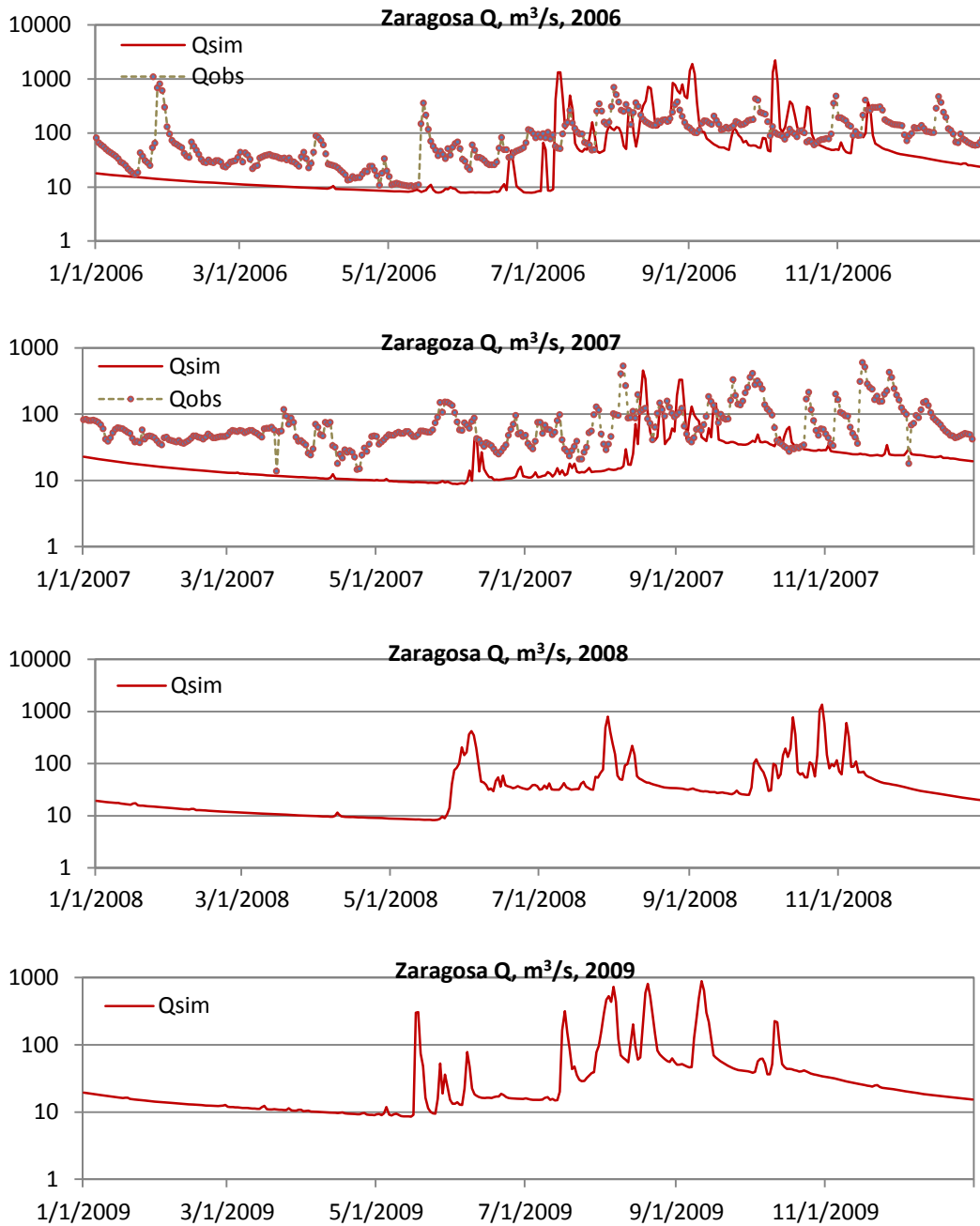
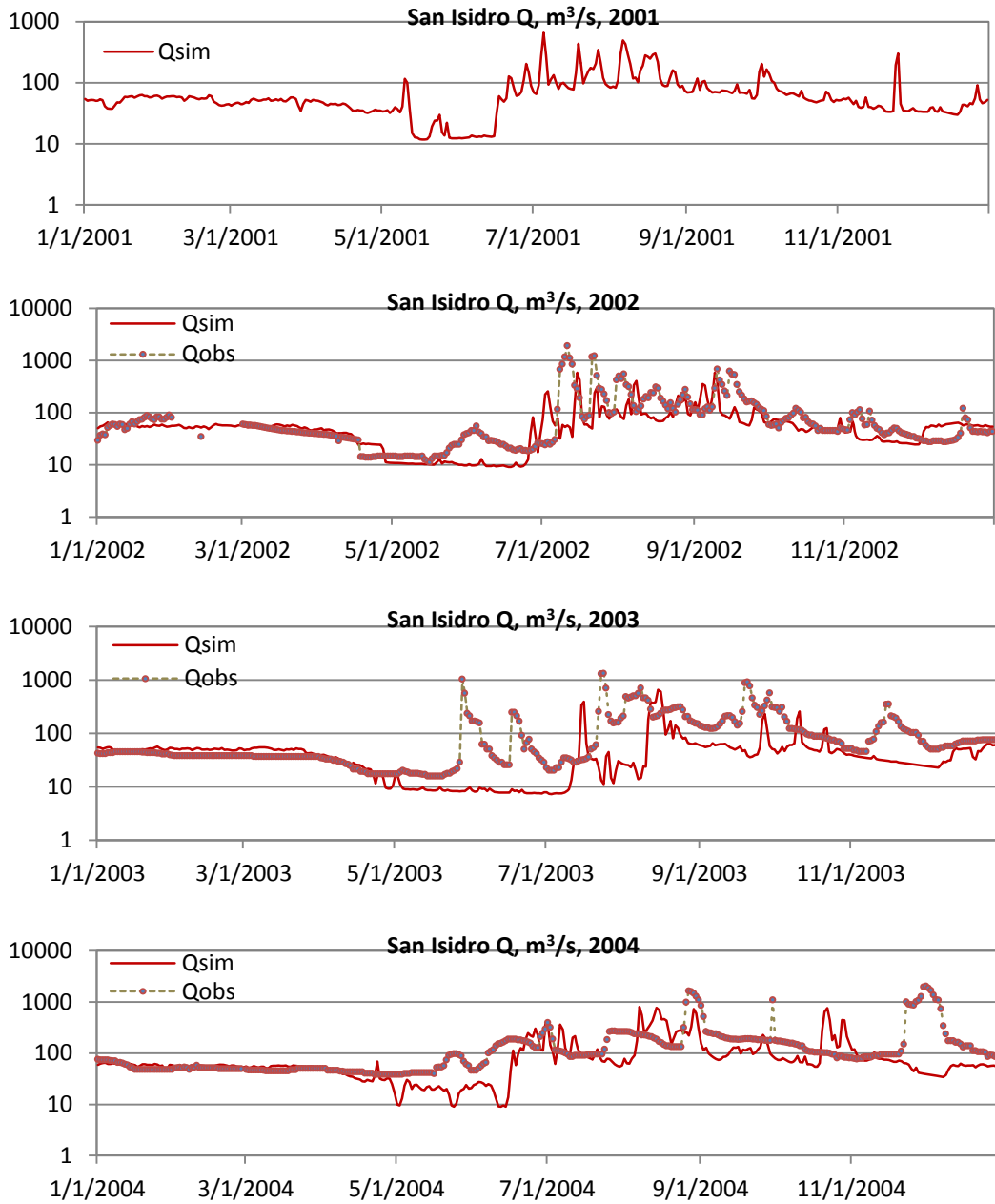


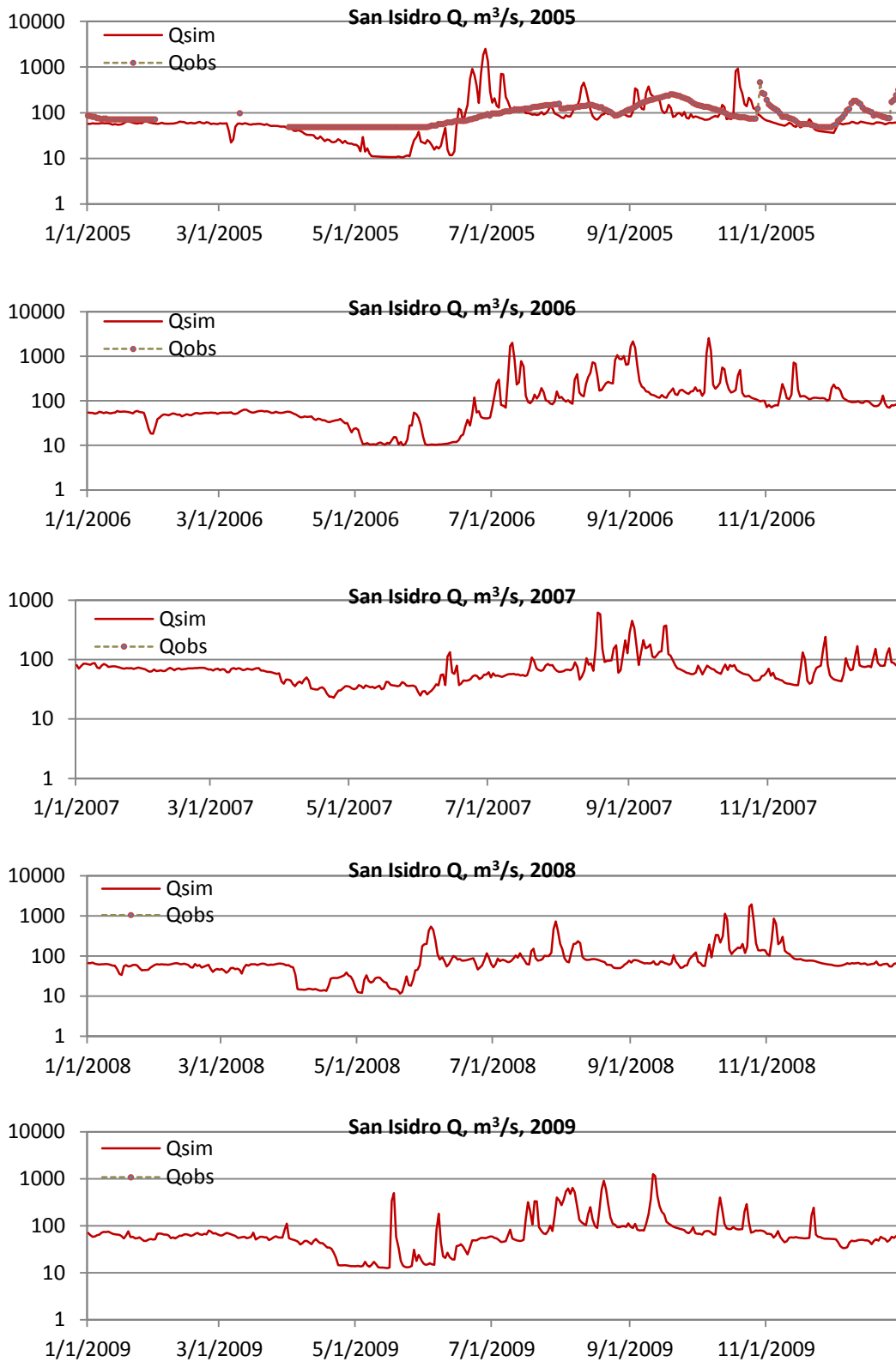
Figure 3.4-14. Validation for Pampanga River Basin (2001-2009):Zaragoza



**Figure 3.4-14.** Validation for Pampanga River Basin (2001-2009):Zaragosa



**Figure 3.4-15.** Validation for Pampanga River Basin (2001-2009): San Isidro



**Figure 3.4-15.** Validation for Pampanga River Basin (2001-2009): San Isidro



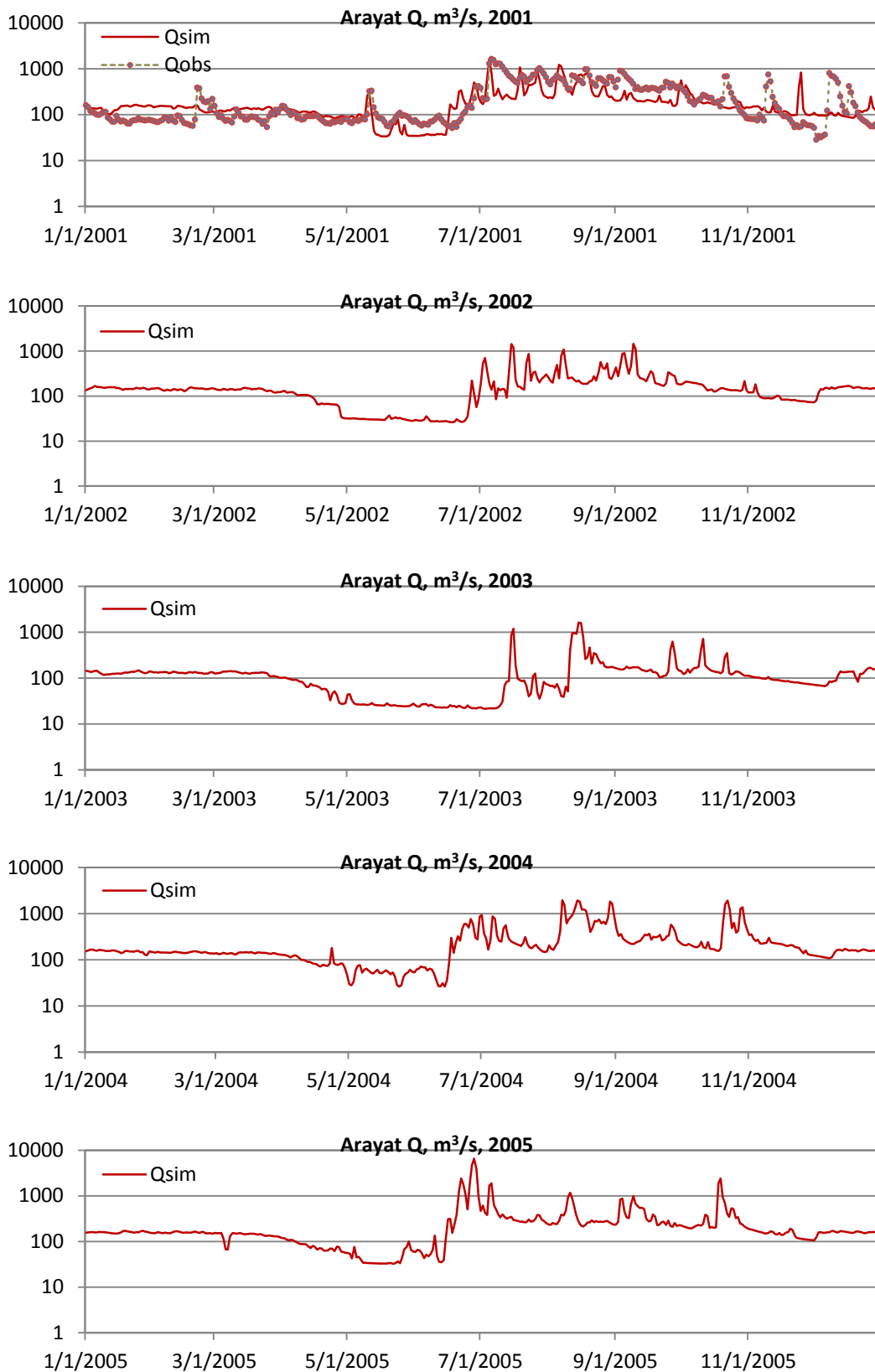


Figure 3.4-16. Validation for Pampanga River Basin (2001-2009): Arayat

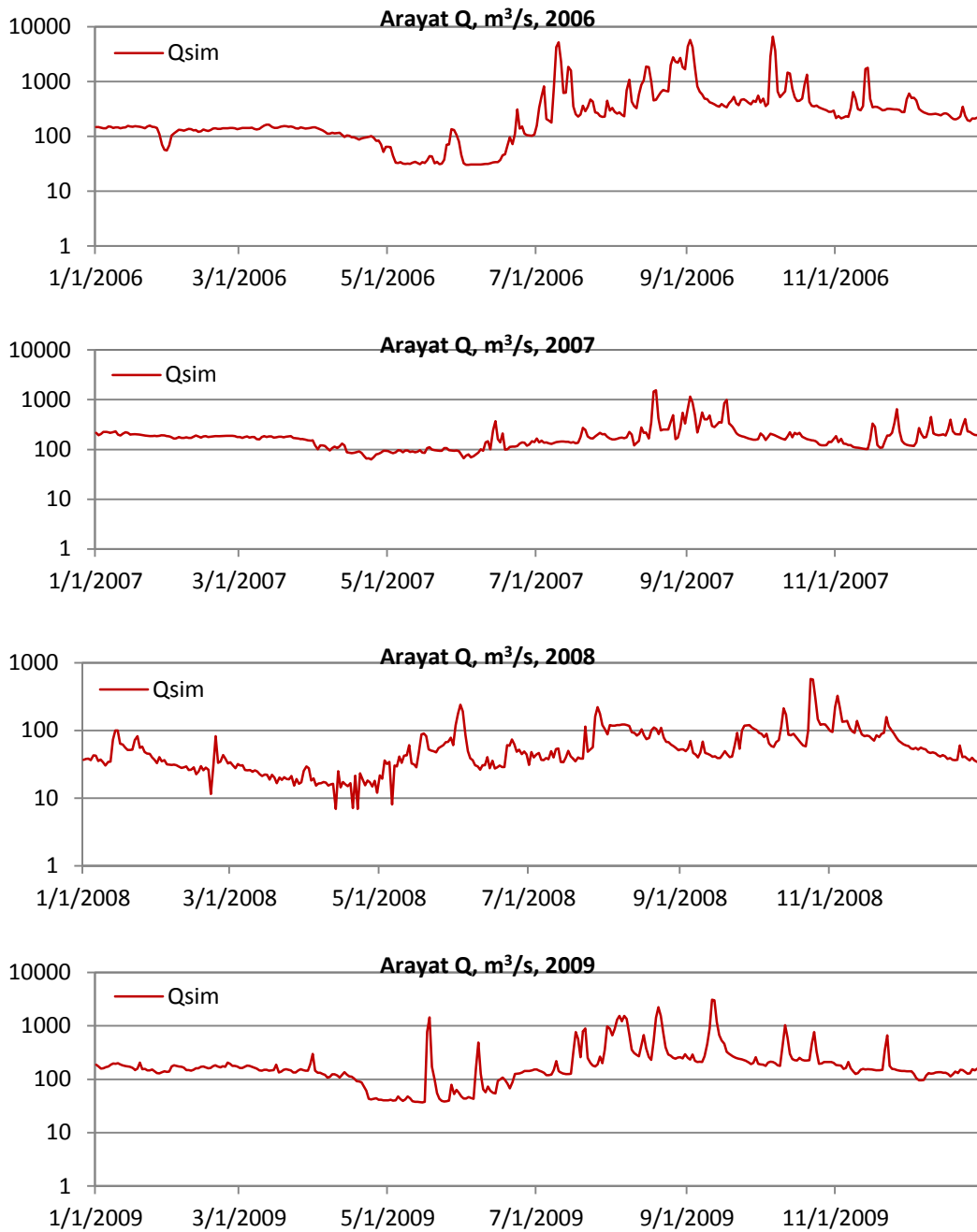


Figure 3.4-16. Validation for Pampanga River Basin (2001-2009): Arayat

### 3.5 Spatial Distribution of Soil Moisture

#### 3.5.1 Introduction to LDAS-UT

The Land Data Assimilation System of The University of Tokyo (LDAS-UT) consists of a land surface model (LSM) used to calculate fluxes and soil moisture, a radiative transfer model (RTM) to estimate microwave brightness temperatures ( $T_b$ ) from surface temperature and soil moisture, and an optimization scheme to search for optimal values of parameters and near-surface soil moisture by minimizing the difference between modeled and observed brightness temperatures.

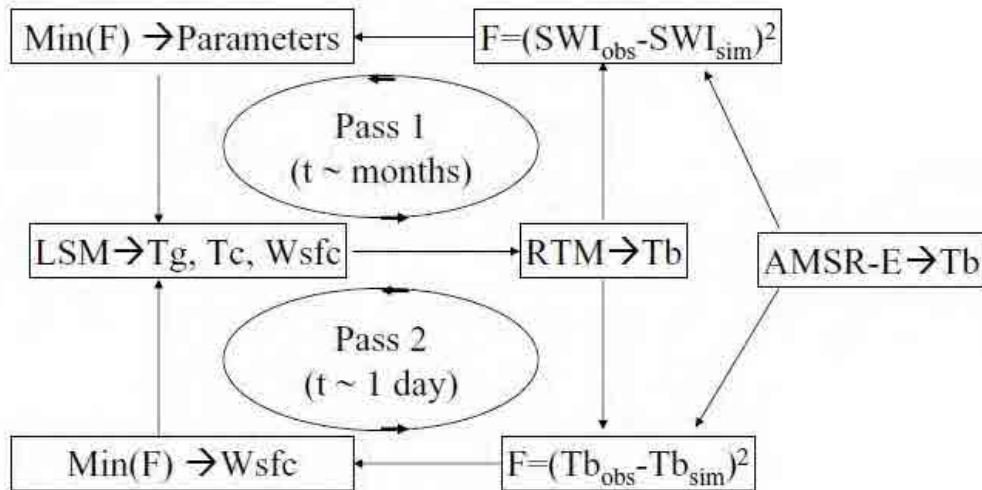


Figure 3.5-1. The Land Data Assimilation System (LDAS-UT).

Figure 3.5-1 shows the LDAS-UT algorithm, which includes a dual-pass assimilation technique. Both passes assimilate observed brightness temperatures of the vertical polarization at a lower frequency (6.9 GHz) and a higher frequency (18.7 GHz). This choice is critical to production of stable and reliable estimates of soil moisture. The vertical polarization is more desirable than the horizontal polarization because it is relatively insensitive to vegetation coverage. Because the lower frequency  $T_b$  is much more sensitive to near-surface soil moisture than the higher frequency, their difference is correlated based on the soil wetness using a soil wetness index (SWI), which is defined

$$\text{by } SWI = 2(T_b^{18.7V} - T_b^{6.9V}) / (T_b^{18.7V} + T_b^{6.9V}). \quad (\text{eq.17})$$

A high SWI value corresponds to a wet surface, and a low value to a dry surface.

Estimating brightness temperatures using RTM requires the input of near-surface soil water content ( $w_1$ ), ground temperature ( $T_g$ ), canopy temperature ( $T_c$ ), vegetation water content (VWC), canopy parameters, surface roughness parameters and soil texture. Simulation of surface variables ( $w_1, T_g, T_c$ ) using the LSM also requires a number of soil and vegetation parameters.

Accordingly, the modeled  $T_b$  is sensitive to several parameters used in the LSM and RTM. In Pass 1, these parameters are obtained by minimizing a cost function that accounts for the difference between modeled and observed long-term brightness temperatures ( $t_{pass1}$ ; scale of two to three months). The cost function includes an observation error term and a background error term. The observation error term is defined by:

$$F_{obs} = \sum_{t=0}^{t_{pass1}} \left[ (T_{b,est}^{6.9V} - T_{b,obs}^{6.9V})^2 + (T_{b,est}^{18.7V} - T_{b,obs}^{18.7V})^2 \right] \quad (\text{eq.18})$$

where the subscript *obs* denotes the observed value and *est* is the modeled value.

In Pass 1, the background error term is not directly accounted for in the cost function; rather, it is realized via adjustment of the near-surface soil water content ( $w_1$ ) at each observation time so that the recalculated SWI value, which depends on  $w_1$ , is close to  $(SWI_{est} + SWI_{obs})/2$ .

Note that this adjustment is implemented after adding the bias term  $(T_{b,est} - T_{b,obs})^2$  into Eq. (18) (see details in **Figure 3.5-1**). In addition, due to the existence of model deficiencies and errors in the forcing data, the simulated soil moisture may become unrealistic without this adjustment, resulting in absence of a correlation between  $T_{b,est}$  and  $T_{b,obs}$  regardless of how the parameter values are tuned. Accordingly, this adjustment is critical in terms of optimizing the parameters.

The optimal parameter values are then transferred into Pass 2 for retrieval of the soil moisture and the surface energy budget by assimilating the brightness temperature into the LSM. Pass 2 only optimizes the near-surface soil moisture, and its assimilation window ( $t_{pass2}$ ; ~ 1 day) is much shorter than that for Pass 1. The cost function for Pass 2 is defined by:

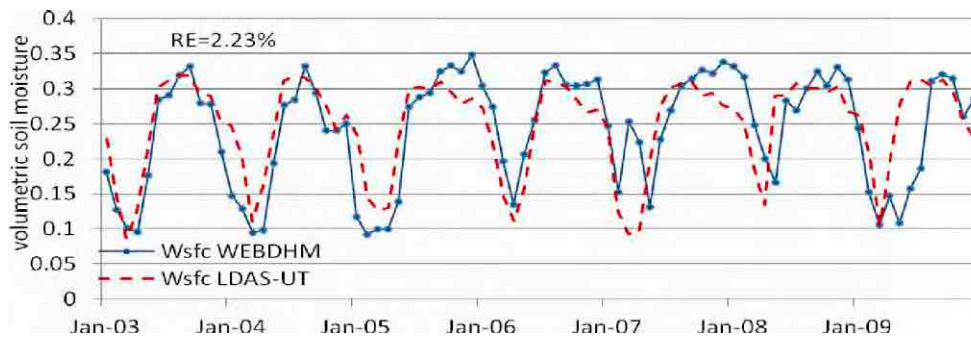
$$F_{obs} = \sum_{t=0}^{t_{pass2}} \left[ (T_{b,est}^{6.9V} - T_{b,obs}^{6.9V})^2 + (T_{b,est}^{18.7V} - T_{b,obs}^{18.7V})^2 \right] + \left[ (T_{b0,bg}^{6.9V} - T_{b0}^{6.9V})^2 + (T_{b0,bg}^{18.7V} - T_{b0}^{18.7V})^2 \right] \quad (\text{eq. 19})$$

where,  $T_{b0,bg}$  and  $T_{b0}$  are the simulated brightness temperature at the initial time of each assimilation cycle using the background value of  $w_{1,0}$  (i.e.,  $w_{1,bg}$ ) and the renewed  $w_{1,0}$  value, respectively. Pass 1 requires just one execution because the optimized parameters only include static model parameters and initial soil water conditions. Accordingly, it can be implemented using

previous data prior to the real-time assimilation of satellite data in Pass 2.

### 3.6 Inter-Comparison of the Soil Moisture Products by WEB-DHM and LDAS-UT

To supplement validation of calibrated WEB-DHM outputs, monthly surface soil moisture outputs of LDAS-UT were compared with surface soil moisture outputs from WEB-DHM. Rainfall assimilation input utilized the monthly GPCP dataset, hence, analysis of the results were compared based on monthly outputs of LDAS-UT and compared with monthly outputs from WEB-DHM. Since LDAS-UT has limitations in assimilating soil moistures in forested areas, sample comparison was done in the Zaragoza station of Pampanga river basin (land use is mostly agriculture or C3 grasslands in this part of the basin). Monthly results of the comparison from 2003-2009 are given in **Figure 3.6-1**.

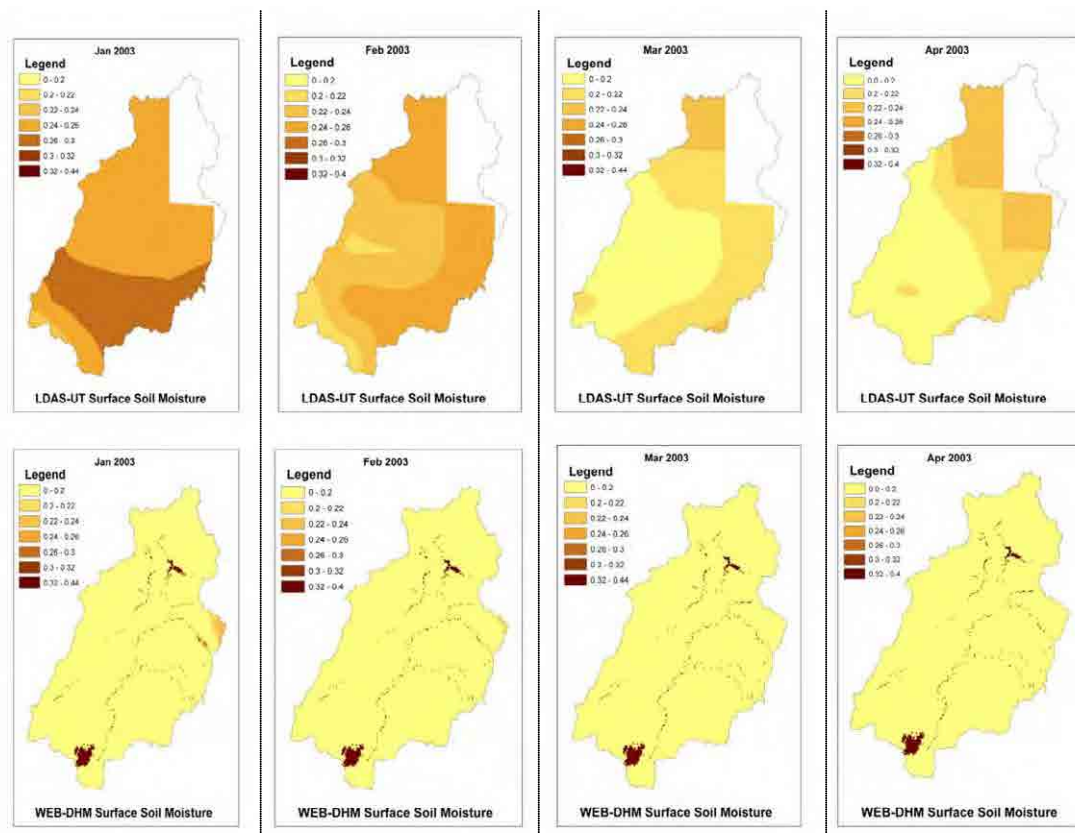


**Figure 3.6-1.** Comparison of surface soil moistures from LDAS-UT and WEBDHM in Zaragoza Station of Pampanga River Basin.

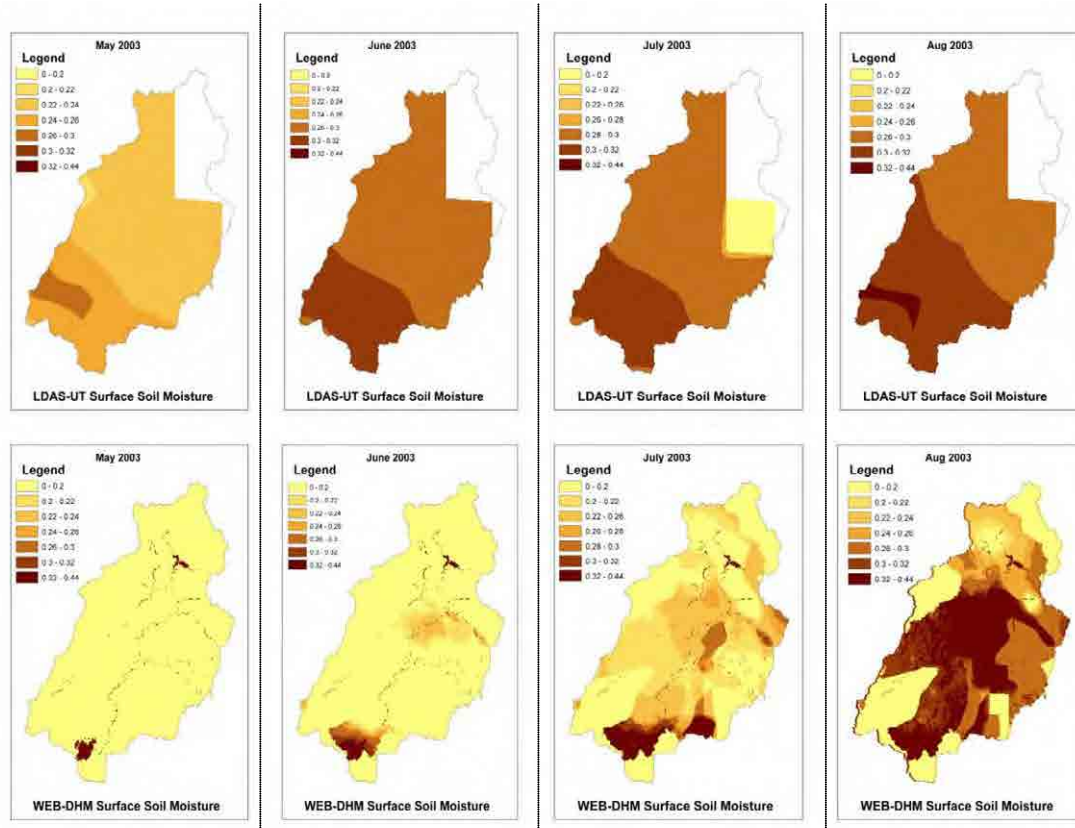
Results showed that the temporal behavior of soil moisture from basin scale hydrological modeling and larger scale estimation using LDAS-UT can be used to estimate large scale soil moisture of the area. Relative error (RE) was found to be 2.23%. Currently there are some differences in the transition between wet and dry season due primarily to: 1.) Coarser resolution grid of LDAS-UT as compared to that of WEB-DHM, 2.) Differences in rainfall input between LDAS-UT (uses Tropical Rainfall Measuring Mission (TRMM) rainfall) and WEB-DHM (uses observed rainfall), and 3.) Scale of comparison between LDAS-UT (grid point) and WEB-DHM (basin average upstream of Zaragoza gauge). However, results show that the estimations of the regional surface soil moistures from LDAS-UT are very similar with those from basin scale hydrological simulations hence, they can be used to verify past basin scale soil moisture trends especially in areas with short vegetation in areas with no observed soil moistures. Further verification of these values should be done when soil moisture information become available in the

future.

Monthly spatial distribution of surface soil moisture in the Pampanga river basin was also compared to check if LDAS-UT and WEB-DHM had similar pattern. January to December spatial distribution in Pampanga river basin for 2003 are given in **Figure 3.6-2**. Note that although seasonality is apparent at the point scale, distribution pattern of soil moisture may vary significantly within the basin. The output of LDAS-UT for soil moisture over the region gives similar outputs as those simulated by WEB-DHM but at a coarser scale ( $0.25^{\circ} \times 0.25^{\circ}$  grid). Color legends are given at 0.01 to 0.02 (0.0001% to 0.0002%) scales. Similar patterns (50% or higher) are evident in the months of March, April, May, August, September, October and December. The differences are as a result of differences in rainfall inputs and courser resolution grids.



**Figure 3.6-2.** January to December 2003 spatial patterns of surface soil moisture in the Pampanga River Basin simulated from WEB-DHM (lower figures) and assimilated from LDAS-UT(upper figures).(cont.)



**Figure 3.6-2.** January to December 2003 spatial patterns of surface soil moisture in the Pampanga River Basin assimilated from LDAS-UT(upper figures) and simulated from WEB-DHM (lower figures). (cont.)